

Utah State University

DigitalCommons@USU

All Graduate Theses and Dissertations

Graduate Studies

12-2008

Evaluation of Arrayed-Field Concentration Measurements and U. S. EPA-Regulatory Models for the Determination of Mixed-Source Particulate Matter Emissions

Derek Jones
Utah State University

Follow this and additional works at: <https://digitalcommons.usu.edu/etd>



Part of the [Environmental Engineering Commons](#)

Recommended Citation

Jones, Derek, "Evaluation of Arrayed-Field Concentration Measurements and U. S. EPA-Regulatory Models for the Determination of Mixed-Source Particulate Matter Emissions" (2008). *All Graduate Theses and Dissertations*. 156.

<https://digitalcommons.usu.edu/etd/156>

This Thesis is brought to you for free and open access by the Graduate Studies at DigitalCommons@USU. It has been accepted for inclusion in All Graduate Theses and Dissertations by an authorized administrator of DigitalCommons@USU. For more information, please contact digitalcommons@usu.edu.



EVALUATION OF ARRAYED-FIELD CONCENTRATION MEASUREMENTS
AND U. S. EPA-REGULATORY MODELS FOR THE DETERMINATION
OF MIXED-SOURCE PARTICULATE MATTER EMISSIONS

by

Derek Jones

A thesis submitted in partial fulfillment
of the requirements for the degree

of

MASTER OF SCIENCE

in

Civil and Environmental Engineering

Approved:

Randal Martin
Major Professor

Laurie McNeill
Committee Member

Larry Hipps
Committee Member

Byron Burnham
Dean of Graduate Studies

UTAH STATE UNIVERSITY
Logan, Utah

2008

ABSTRACT

Evaluation of Arrayed-Field Concentration Measurements and U. S. EPA-Regulatory
Models for the Determination of Mixed-source Particulate Matter Emissions

by

Derek Jones, Master of Science

Utah State University, 2008

Major Professor: Randal Martin
Department: Environmental Engineering

With the continued population growth and the blurring of the urban and rural interface, air quality impacts associated with agricultural particle-producing processes are becoming increasingly important. There is a lack of emission rate data from these source types and no prescribed measurement technique available to the agricultural and regulatory communities. One technique that has shown promise is combining field measurements with inverse modeling. This approach was used herein to examine particulate emissions from an almond harvesting operation, a cotton ginning facility, and comparative emissions from conservation versus conventional tillage practices. EPA-approved models ISCST3 and AERMOD were used with AirMetrics samplers. With error representing the standard deviation for all values, for ISCST3, the almond harvesting operation found PM_{10} emissions for shaking were 3.4 kilograms per hectare; $PM_{2.5}$, PM_{10} , and TSP emissions for sweeping were 0.81 ± 0.76 , 4.8 ± 3.7 , and 7.5 ± 5.1 $kg\ ha^{-1}$, respectively; $PM_{2.5}$, PM_{10} , and TSP emissions for pickup were 1.7 ± 1.5 , $6.1 \pm$

1.9, and $10.3 \pm 3.8 \text{ kg ha}^{-1}$, respectively. Using AERMOD, the almond harvesting operation found PM_{10} emissions for shaking were 4.4 kg ha^{-1} ; $\text{PM}_{2.5}$, PM_{10} , and TSP emissions for sweeping were 1.3 ± 1.5 , 8.3 ± 9.4 , and $27.0 \pm 41.2 \text{ kg ha}^{-1}$, respectively; $\text{PM}_{2.5}$, PM_{10} , and TSP emissions for pickup were 2.7 ± 1.3 , 15.7 ± 14.1 , and $42.3 \pm 20.7 \text{ kg ha}^{-1}$, respectively. $\text{PM}_{2.5}$, PM_{10} , and TSP emissions from the cotton gin were determined to be 1.7 ± 1.4 , 14.3 ± 17.0 , and $27.9 \pm 41.1 \text{ g s}^{-1}$ using ISCST3 and 0.9 ± 0.9 , 10.5 ± 18.8 , and $43.0 \pm 79.9 \text{ g s}^{-1}$ using AERMOD, respectively. ISCST3 emission rates for the combined tillage operations for $\text{PM}_{2.5}$, PM_{10} , and TSP were 0.15 ± 0.24 , 0.44 ± 0.17 , and 1.4 kg acre^{-1} , while AERMOD rates were 0.17 ± 0.27 , 0.66 ± 0.25 , and 2.1 kg acre^{-1} , respectively. ISCST3 emissions for the conventional tillage operations for $\text{PM}_{2.5}$, PM_{10} , and TSP were 0.47 ± 2.1 , 1.1 ± 0.23 , and 3.4 kg acre^{-1} , and the AERMOD rates were 0.18 ± 0.26 , 1.2 ± 0.24 , and 5.1 kg acre^{-1} , respectively.

(91 pages)

CONTENTS

	Page
ABSTRACT.....	ii
LIST OF TABLES.....	vi
LIST OF FIGURES.....	viii
LIST OF FIGURES.....	viii
INTRODUCTION.....	1
Particulate Matter.....	2
Agricultural Particulate Matter.....	5
Objectives.....	6
Literature Review.....	7
Tillage emissions.....	8
Cotton gin emissions.....	9
Almond harvest emissions.....	13
PM emission rate determination techniques.....	14
METHODOLOGY.....	20
Particle Mass Concentration Measurement.....	20
Meteorological Measurements.....	23
Inverse Modeling.....	23
Lidar.....	26
Field Sites Descriptions.....	29
Almond harvest.....	29
Cotton gin.....	33
Tillage.....	36
RESULTS AND DISCUSSION.....	39
Almond Harvest Results.....	39
Almond harvest PM concentration measurements.....	39
Almond harvest emission rates.....	44
Cotton Gin Results.....	56
Tillage Emissions.....	63
Tillage PM concentration measurements.....	63

Tillage emission rates	66
SUMMARY AND CONCLUSIONS	79
Almond Harvest Conclusions	79
Cotton Gin Conclusions.....	82
Tillage Conclusions	85
ENGINEERING SIGNIFICANCE.....	89
FUTURE WORK.....	91
REFERENCES	92
APPENDICES	99
Appendix A: Almond Orchard Field Experiment Notes	100
Appendix B: Cotton Gin Specifications and Emissions Data.....	105
Appendix C: Tillage Instrumentation	107

LIST OF TABLES

Table		Page
1	Yearly PM emissions from several agricultural processes	10
2	Emission factors for the cotton ginning process	12
3	NASS tally of the number of cotton bales ginned from 2004 – 2007	13
4	PM concentrations upwind and downwind of various almond harvesting operations ($\pm 1\sigma$).....	40
5	Fraction of TSP that is PM _{2.5} and PM ₁₀ for each operation upwind and downwind of the orchard and campaign averages upwind and downwind	42
6	Summary table of meteorological inputs used in ISCST3	45
7	Estimated (red) and measured (black) PM concentrations upwind and downwind of various almond harvesting operations ($\pm 1\sigma$)	48
8	Emission rates for each operation in the almond harvesting process, as determined by inverse modeling using ISCST3	49
9	Comparison of modeled and measured concentrations on October 9, 2006 for each sample location, those at 2 m only were modeled with an ISCST3 determined emission rate of $24 \mu\text{g s}^{-1} \text{m}^{-2}$	52
10	Emission rates for each operation in the almond harvesting process, as determined by inverse modeling using AERMOD.....	54
11	Summary table of some meteorological inputs used in modeling.....	57
12	PM concentrations measured at the cotton gin	58
13	Measured-to-modeled concentration ratios for each day at the cotton gin with ISCST3 and AERMOD ($\pm 1\sigma$).....	59

14	Emission rates (g s^{-1}) determined by inverse modeling techniques for the cotton gin, with the emissions data provided by the cotton gin ($\pm 1\sigma$).....	60
15	Average sampler measured PM concentrations ($\pm 1\sigma$) for each operation upwind and downwind of the tillage site	65
16	Fraction of TSP that is $\text{PM}_{2.5}$ and PM_{10} for each operation upwind and downwind of the tillage site, and campaign averages upwind and downwind ($\pm 1\sigma$)	66
17	Summary table of meteorological inputs used in ISCST3	68
18	Estimated (red) and measured (black) PM concentrations upwind and downwind of various tillage operations ($\pm 1\sigma$)	69
19	Emission rates for each operation determined by inverse modeling using ISCST3	74
20	Emission rates for each operation determined by inverse modeling using AERMOD	77
21	Ratio of AERMOD determined emission rates to ISCST3 determined emission rates	81
22	Comparison of ISCST3 and AERMOD determined emission rates	87
23	Exhaust specifications for the cotton gin	105
24	Emissions data for the cotton gin.....	106
25	Summary of instruments located at each site for tillage study of field PA-47	107
26	Summary of instruments located at each site for tillage study of field PA-46	108

LIST OF FIGURES

Figure	Page
1	Sources of agricultural PM.8
2	PM emissions from agricultural tillage operations by state.....10
3	Monthly variability in agricultural tillage emissions by state.....10
4	Estimation of monthly PM ₁₀ emissions for agricultural land preparation.....11
5	A conceptual drawing of the lidar.....28
6	Graphical representation of a staple scan with the lidar.29
7	Layout of the almond orchard with sampler locations.....31
8	Layout of the almond orchard with meteorological tower and lidar locations.31
9	Cotton gin layout with tower and lidar locations indicated33
10	Windrose plot for Five Points, CA from December 6-20 for 2001-2005.....35
11	The highlighted area is field PA-47.....36
12	The highlighted area is field PA-46.....37
13	A lidar scan taken on October 2 at 10:02 showing the PM ₁₀ concentration field in $\mu\text{g m}^{-3}$41
14	Average measured upwind and downwind PM concentrations with the particle size contributions to the total PM for the almond orchard.43
15	Illustration of background determination using OPC data from sample location D9.5.....47
16	ISCST3 modeled results for mock sweeping operations on October 9, 2006 with north winds.....48
17	Emission rates determined by inverse modeling using ISCST3 for each day of the almond harvest study.....50

18	Emission rates for each almond harvest operation determined by inverse modeling using ISCST3 compared with those found by CARB (2003).	51
19	AERMOD modeled results for mock sweeping operations on October 9, 2006 with north winds	53
20	Emission rates determined by inverse modeling using AERMOD for each day of the almond harvest study.	55
21	Emission rates for each almond harvest operation determined by inverse modeling using AERMOD compared with those found by CARB (2003).....	56
22	A comparison of lidar (a) and ISCST3 (b) model derived PM _{2.5} concentrations in $\mu\text{g m}^{-3}$ (using emission rates estimated from AP-42) for a cotton gin on December 11, 2006.	62
23	A comparison of lidar (a) and ISCST3 (b) model derived PM _{2.5} concentrations in $\mu\text{g m}^{-3}$ (using emission rates estimated from AP-42) for a cotton gin on December 14, 2006.....	62
24	Average measured upwind and downwind PM concentrations with the particle size contributions to the total PM for the tillage operations.....	67
25	Edited average measured upwind and downwind PM concentrations with the particle size contributions to the total PM for the tillage operations.....	70
26	ISCST3 modeled results for a disc pass of the conventional tillage operations on October 23, 2008 with light north winds.....	71
27	Emission rates for each operation determined by inverse modeling using ISCST3.	73
28	PM emissions (g m^{-2}) of combined and conventional tillage operations for PM _{2.5} , PM ₁₀ , and TSP determined using ISCST3.	74
29	AERMOD modeled results for a disc pass of the conventional tillage operations on October 23, 2007 with light north winds.....	75

30 Emission rates for each operation determined by inverse modeling using AERMOD.....77

31 PM emissions (g m^{-2}) of combined and conventional tillage operations for $\text{PM}_{2.5}$, PM_{10} , and TSP determined using AERMOD.....78

32 Summary of ISCST3, AERMOD, and CARB (2003) emission rates from the various processed of an almond harvest80

33 Average of the daily emission rates determined by of ISCST3, AERMOD, Emissions Data, and Emission Factors for the cotton gin.84

34 Average emission rates from the cotton gin for December 12 – 14, 2006.....85

35 Comparison of ISCST3, AERMOD emission rates and AP-42 emission estimates for the tillage operations88

INTRODUCTION

Increasing size and geographic concentration of agricultural facilities, along with accompanying urban encroachment, have heightened the scrutiny of agricultural gaseous and particulate emissions in the United States (Capareda et al., 2005). Pressure to meet global food demands has increased production and facility size. Resultantly, the U. S. Environmental Protection Agency (U. S. EPA), in addition to special interest groups and the general public, has become increasingly interested in monitoring and controlling air pollution from agriculture facilities (U. S. EPA, 2006a). Pollutants of concern from agricultural processes include particulate matter (PM) and gaseous species, such as ammonia (NH₃), hydrogen sulfide (H₂S) and methane (CH₄) along with several others (NRC, 2003). The concern for air quality near agricultural facilities spurs the need for reliable methods for quantifying emissions from agriculture facilities (Aneja et al., 2006). Due to the limited number of studies used to make the current emission estimates used by the U. S. EPA, these estimates have been determined to be inadequate (NRC, 2003).

Currently, federal regulation of agricultural air pollutant emissions is limited. The Comprehensive Environmental Response, Compensation and Liability Act (CERCLA) and the Emergency Planning and Community Right-to-Know Act (EPCRA) require any facility to report when the 45.5 kg/d production threshold of hazardous material is exceeded; hazardous waste includes ammonia and hydrogen sulfide, which are commonly emitted from agricultural facilities (NRC, 2003). However, in December 2007 the EPA proposed a rule exempting confined animal feeding operations from reporting emissions of hazardous air pollutants under the provisions of CERCLA. The Clean Air Act (CAA) under the new source performance and other sections limits

emissions of volatile organic compounds (VOC) and PM in certain industries, such as the automobile and petroleum refining industries, but does not include limits for agriculture. The CAA also regulates ambient PM concentrations under the National Ambient Air Quality Standards (NAAQS), but there are no regulations which specifically address the contribution of agricultural PM emissions. Additionally, active enforcement of any regulation is problematic because of the inadequacy of accepted methodologies for accurately measuring emissions and the limited number of studies and information available on source emissions for these types of operations.

Particulate Matter

Small solids and liquid droplets that are suspended in air are known as aerosols or particulate matter (PM). These aerosols are typically considered pollutants because of the effects they have on human health, welfare issues and aesthetics. Aerosols can be primary: released in particulate form directly from a source into the atmosphere; or secondary: formed by a gas-to-particle conversion process (Jacobson, 2002). Particulate pollution comes from a variety of sources both biogenic or natural, such as volcanoes, forest fires and sea spray, and anthropogenic or human caused, such as through the burning of fossil fuels and human induced attrition processes. As an example, various agriculture processes can produce particles small enough to remain suspended in the atmosphere which could then significantly contribute to local and regional air pollutant problems (Colls, 2002).

Particle diameter is of prime concern when assessing the health impacts because different sized particles have different access to the body. The U. S. EPA defines particle size using aerodynamic particle diameters, because particles behave with aerodynamic

characteristics while in the respiratory system. Aerodynamic diameter is the theoretical diameter of a particle in an air stream if it were spherical with a unit-density that would settle at the same rate as the particle in question in still air (Cooper and Alley, 2002). The aerodynamic diameter (d_{aero}) can be related to the physical diameter (d_{phy}) by the following relationship:

$$d_{\text{aero}} = d_{\text{phy}} \sqrt{\rho} \quad (1)$$

where ρ is the density of the particle (Colls, 2002).

Particles with an aerodynamic diameter less than or equal to 2.5 micrometers (μm) are often referred to as $\text{PM}_{2.5}$ or “fine” particles, and particles between 2.5 and 10 μm are typically called the “coarse” fraction. Total suspended particulates (TSP) is a term used to describe all atmospherically suspended aerosols regardless of size, while PM_{10} refers to all PM with an aerodynamic diameter less than or equal to 10 μm , and $\text{PM}_{2.5}$ includes only PM with an aerodynamic diameter less than 2.5 μm .

PM that is deposited deep within the respiratory system poses the greatest health risk; typically these are particles from 0.1 to 2.5 μm . PM_{10} can enter the respiratory (nasal/throat) passages, while $\text{PM}_{2.5}$ can penetrate deep into the lung tissue (Mihelcic, 1999). Exposure to PM can result in a variety of health problems including irritation of airways, coughing, decreased lung function, aggravated asthma, and increased risk of respiratory and cardiovascular disease (Dockery et al., 1989; Pope, 1991; U. S. EPA, 2003b; U. S. EPA, 2006b). PM can also have welfare and environmental effects including a decrease in visibility, environmental damage (such as acidification of water systems and/or changing the nutrient balance of ecosystems) and aesthetic damage (particulates can stain and damage stone and other materials of buildings and

monuments). Fine particles are major contributors to decreased visibility, or haze. Deposition of PM can acidify streams, thus altering the nutrient balance in coastal waters and large river basins, damaging sensitive crops and affecting diversity of ecosystems (U. S. EPA, 2008).

Due to the health and welfare effects associated with particle size, the U. S. EPA has established NAAQS found in Title 40, part 50 of the Code of Federal Regulations (CFR) that establish the maximum allowable ambient concentration for both PM_{2.5} and PM₁₀. The NAAQS for PM_{2.5} is 15 micrograms per cubic meter ($\mu\text{g m}^{-3}$) averaged annually, with a 24-hour concentration standard of $35 \mu\text{g m}^{-3}$. The NAAQS for PM₁₀ is $50 \mu\text{g m}^{-3}$ averaged annually, with a 24 hour concentration standard of $150 \mu\text{g m}^{-3}$ (CFR, 2007).

The U. S. EPA currently recognizes specific point sampler instruments as reference methods for measuring ambient PM concentrations. Reference methods use filter based samplers that incorporate inertial size separation techniques, such as cyclone separators or impaction plates. The NAAQS regulate ambient PM concentrations but do not directly account for source emissions. Federal regulations have been promulgated specifying air pollutant emission limits for a number of industrial source categories, along with the required techniques to quantify the emissions from these typically ducted (stack) point sources (CFR, 2007). A consistent and reliable means for measuring emission rates from large-scale, area-type facilities, such as agricultural operations, is needed. A comprehensive measurement approach is needed to quantify PM emissions from these facilities so that any future regulations will be appropriate, quantifiable, and enforceable.

Agricultural Particulate Matter

Due to urban expansion into agricultural areas and increasing awareness of long-range transport phenomena, the air quality associated with agricultural processes is of increased concern and regulation in the near future is likely. Agricultural sources of PM include a variety of operations, such as confined animal feed operations (CAFOs), field burning, tilling, harvesting and other processing techniques. Agricultural facilities can also contribute to the formation of secondary PM through the production of large quantities of gaseous species, such as ammonia which then may photochemically transfer to the particulate forms ammonium nitrate or ammonium sulfate (Liang et al., 2003; Mount et al., 2002; NRC, 2003; Redwine et al., 2002; U. S. EPA, 2004). In addition to the adverse health and welfare effects of agricultural PM, odorous, non-regulated compounds including ammonia and hydrogen sulfide have been found to bind to PM (Jerez et al., 2005; Bunton et al., 2006), leading to strong odors and a reduction of adjacent residential property values (Palmquist et al., 1997).

Agricultural pollutant sources can include fields while being worked, animal holding facilities, and storage piles. The PM produced by agricultural facilities is often associated with area-type sources and can be difficult to measure due to facility layout, daily and seasonal operational variability, and meteorological conditions (Bingham et al., 2006). These factors make placing discrete samplers in the path of the particulate plumes tricky and unpredictable without utilizing an unreasonably large number of instruments. Additionally, the sources of agricultural emissions are often mobile, daily and/or seasonally varied, can be multiple sources at any given time, and can be spread out over a large area. In contrast, facilities that release all emissions from a single point source,

such as a smoke stack, are much more easily characterized, because the source location is explicitly identified and operations are generally much more temporally consistent.

For these reasons the amount of literature and corresponding data examining agricultural PM emissions are limited. The sources and types of PM depend on the geographic location, time of year, time of day, moisture content of the soil and types of operations of the facility. Due to these complexities, quantifying and characterizing the PM emissions from agricultural facilities using traditional, point sampler methods are problematic (Bingham et al., 2006).

Objectives

The main objective of this study was to estimate primary (direct) agricultural emissions of size-specific particulate emissions, including TSP, PM₁₀, and PM_{2.5} from certain types of agricultural operations. Successful development of the methodologies described within this document could lead to a reliable means for measuring emission rates from a wide range of diffuse area PM sources. The primary technique described herein utilized an array of point samplers to measure the near-source PM concentration fields. Emission rates were then determined using inverse modeling methods described in subsequent sections by incorporating U. S. EPA-approved dispersion models (ISCST3 and AERMOD). The work herein is part of a larger, co-operative project involving the development of lidar technologies to determine particulate flux upwind and downwind of the target areas, deriving areal fluxes via mass balance modeling techniques. Using the two modeling approaches, facility PM emissions were determined for an almond orchard during the various harvest procedures, a cotton gin throughout the complete ginning process, and post-harvest, field tillage processes. The emission rates determined from the

experiments were compared with each other and with those of the California Air Resources Board (CARB) (2003) for the almond harvest and the AP-42 emissions algorithm (U. S. EPA, 1985) for the tillage. Cotton ginning emissions were compared to the emissions calculated using the AP-42 emissions summary document and the emissions data provided for the cotton gin.

Literature Review

Before appropriate regulations can be established and enforced, research must be done to determine typical PM emissions from agricultural facilities. Beyond regulation, this information can also be used for comparisons of management practices in order to reduce and effectively manage agricultural-based air pollution. In 1996, Congress organized the Agricultural Air Quality Task Force (AAQTF) to address issues dealing with air quality. Because Congress learned that many previous studies alleging that agriculture is a source of PM₁₀ were based on erroneous data (USDA-AAQTF, 2007), the AAQTF was charged to ensure that federal policies that related to air pollution are based on sound, peer-reviewed research with consideration given to economic feasibility.

According to E. H. Pechan and Associates (2004) tillage and CAFOs are the largest contributors to agricultural PM in the United States. These operations are responsible for more than 90% of PM emissions from agricultural sources. Other sources of agricultural PM include cotton ginning, crop burning, and crop transport. Figure 1 shows a variety of agricultural practices and the percent each contributes to the total agricultural PM emissions based on data from the National Emissions Inventory (NEI) (U. S. EPA, 2002).

The U. S. EPA developed the Compilation of Air Pollutant Emission Factors (AP-42) in 1985 to provide a means for estimating emissions from various sources (U. S. EPA, 1985). PM emission factors from various agricultural processes are included in this document, which can allow for emission calculations for a number of these processes. Table 1 provides information about yearly PM emissions from agricultural operations which produce substantial amounts of PM emissions. Table 1 includes PM emission estimates from the Central States Regional Air Planning Association (CENRAP) region, including 9 states (listed in Figure 2 and Figure 3), for tillage and CAFOs. The yearly emission estimates for California are also provided in Table 1. Nationwide emission estimates are also presented in Table 1 for cotton ginning and almond harvesting.

Tillage emissions

Tillage is a combination of practices that prepare land for the planting of crops. There can be a number of processes depending on the soil composition and the crop to be planted. Some tillage processes may include chiseling (turning over and mixing the soil)

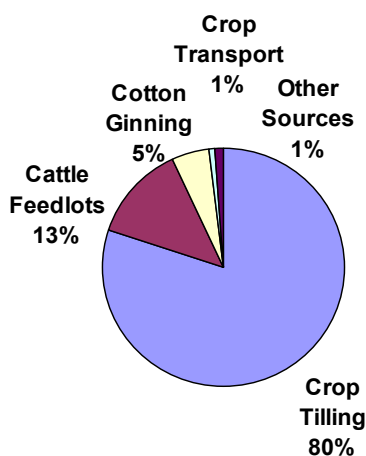


Figure 1. Sources of agricultural PM (U. S. EPA, 2002).

discing (breaking up large pieces of soil) and planing (further breaking up of the soil and preparing rows for planting). The tillage emission estimates of PM_{10} and $PM_{2.5}$ determined using AP-42 by Penfold et al. (2002) for the CENRAP region given in Table 1 are shown for each of the included states in Figure 2. Mechanical operations, such as tillage processes, will generally produce larger particles (Jacobson, 2002). Figure 2 supports this, as $PM_{2.5}$ comprises only 20% of the PM_{10} . Total agricultural tillage PM_{10} emissions for the CENRAP region, see Table 1, are estimated at 1.4 million tons year⁻¹, with $PM_{2.5}$ emissions contributing nearly 270,000 tons to this total. These numbers are 25% to 30% lower than the predicted 2002 NEI (Penfold et al., 2002). Additionally, Penfold et al. (2002) found that there is high monthly variability in tillage emissions, as shown in Figure 3.

The state of California has initiated numerous studies to improve crop specific emission rates and compiled this information with crop calendars and acreage data to estimate PM_{10} emissions from agricultural land preparation, which would include tillage and harvest activities. Figure 4 shows statewide PM_{10} emissions for agricultural land preparation activities by month, showing the monthly variability of agricultural tillage. The monthly values shown in Figure 4 can be summed to show total PM_{10} emissions of 34,000 tons year⁻¹ for California tillage processes using AP-42 emission estimate techniques, as compiled previously in Table 1 (Gaffney and Yu, 2003).

Cotton gin emissions

Cotton gins are considered agricultural operations, not general industry (Wakelyn, Thompson, and Norman, 2005). They are, however, subject to state regulations for PM and must obtain operating permits from state air pollution regulatory agencies (SAPRAs).

Table 1. Yearly PM emissions from several agricultural processes

Operation	PM _{2.5}	PM ₁₀	TSP	reference
	tons year ⁻¹	tons year ⁻¹	tons year ⁻¹	
Tillage	300,000	1,400,000	-	Penfold et al., 2002 ^A
CAFOs	7,700	51,000	-	Penfold et al., 2002 ^A
California Tillage	-	34,000	-	Gaffney and Yu, 2003 ^B
Cotton Ginning	-	7,600 - 11,000	22,000 - 29,000	U.S. EPA, 1985; NASS, 2008 ^C
Almond Harvesting	-	12,000	-	Goodrich et al., 2007 ^C

^A emission estimates for the CENRAP region

^B emission estimates for California

^C U. S. emission estimates

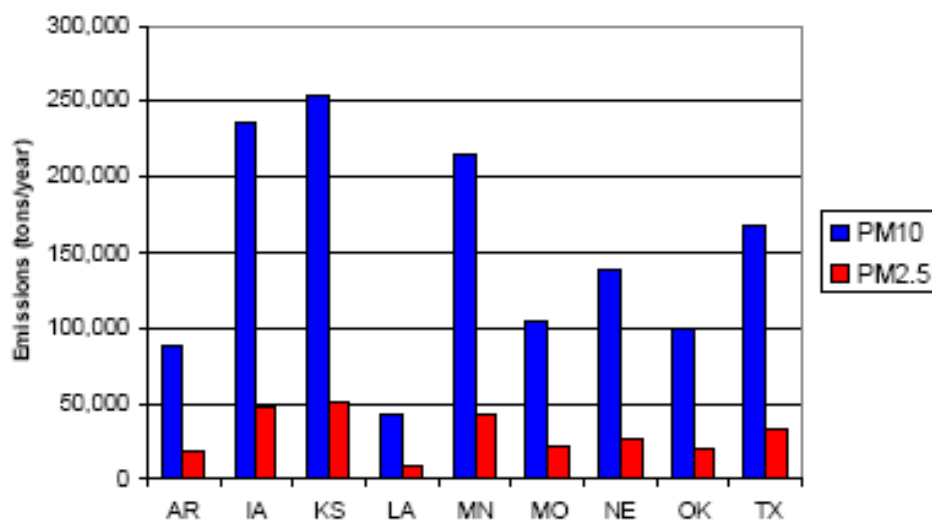


Figure 2. PM emissions from agricultural tillage operations by state (Penfold et al., 2002).

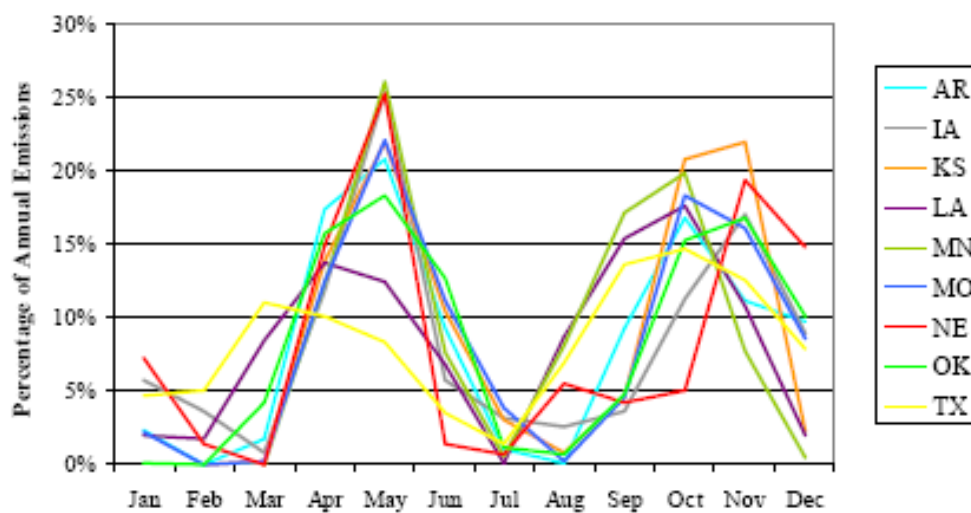


Figure 3. Monthly variability in agricultural tillage emissions by state (Penfold et al., 2002).

AP-42 contains a PM emission factor for cotton gins; however, due to the absence of sampling data, many SAPRAs use the ISCST3 dispersion model to back calculate an allowable emission rate for regulatory permitting purposes (Wanjura et al., 2005).

Typically, SAPRAs will run the model varying the emission rate until the NAAQS are exceeded for criteria pollutants $PM_{2.5}$ and PM_{10} at the downwind facility border, then establish acceptable emission rates for the pollutants based on these data (Buser et al., 2001).

Data indicate that PM_{10} comprises 37 percent of the total PM emitted from the cotton ginning process (U. S. EPA, 1985). After the cotton is picked, fibers and lint need to be separated from the seeds and seedpods. Flat circular saw blades separate the lint from the seeds which may be recovered and sold to cottonseed buyers. The gin also removes any impurities and moisture in the cotton by feeding it into the gin using suction. PM is emitted during various phases of the ginning process, during the lint cleaning,

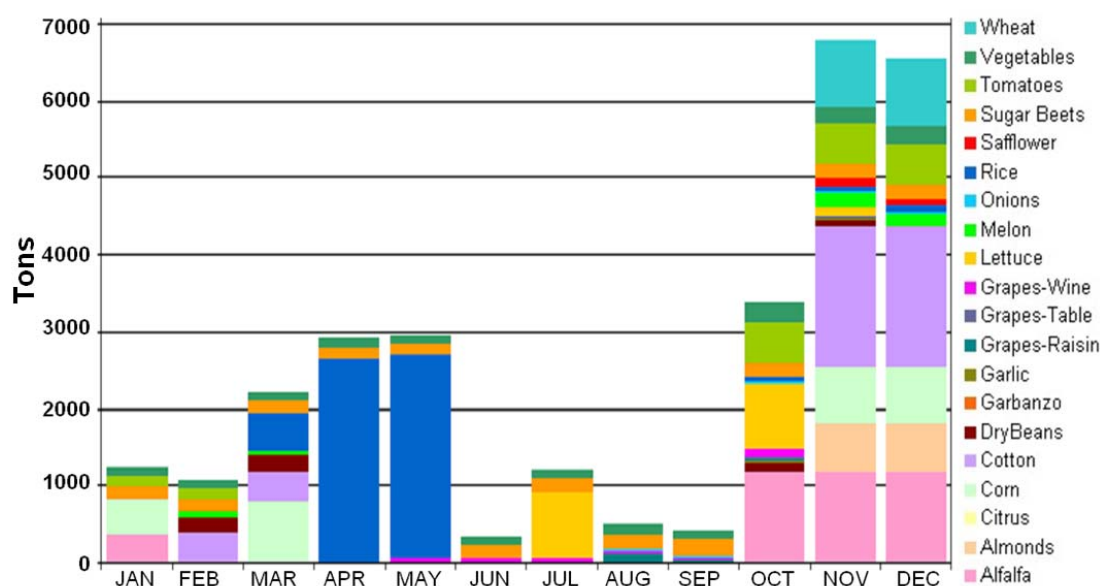


Figure 4. Estimation of monthly PM_{10} emissions for agricultural land preparation (Gaffney and Yu, 2003).

drying, bailing, loading and unloading, and exhaust from mote (dust) and master fans.

Simple, mechanical pollution control devices are typically used to reduce PM emissions from ginning operations. These can include cyclones, fine screens and perforated metal drums. Table 2 presents current emission factors for cotton gins with various operations and configurations. Total gin emission factors are also given for different gin configurations (U.S. EPA, 1985).

In Table 3, the National Agricultural Statistics Service (NASS) presents the number of bales ginned, by state, for the years 2004 to 2007. A typical bale of cotton weighs 500 lbs. With the information given in Table 3 and the emission factors provided in Table 2, total PM and PM₁₀ emissions from cotton gins throughout the listed states can be estimated at 19,000 – 31,000 tons year⁻¹ for total PM and 6,400 – 12,000 tons year⁻¹ for PM₁₀.

Table 2. Emission factors for the cotton ginning process (U. S. EPA, 1985)

Source	Total PM, lb/bale	PM ₁₀ , lb/bale
Unloading fan	0.29	0.12
No. 1 dryer and cleaner	0.36	0.12
No. 2 dryer and cleaner	0.24	0.093
No. 3 dryer and cleaner	0.095	0.033
Overflow fan	0.071	0.026
Lint cleaners with high efficiency cyclones	0.58	0.24
Lint cleaners with screened drums or cages	1.1	-
Cyclone robber system	0.18	0.052
Mote fan	0.28	0.13
Mote trash fan	0.077	0.021
Battery condenser with high efficiency cyclones	0.039	0.014
Battery condenser with screened drums or cage	0.17	-
Master trash fan	0.54	0.074
Cotton gin total No. 1 ^A	2.4	0.82
Cotton gin total No. 2 ^B	3.1	1.2

^A with high-efficiency cyclones on all exhaust streams

^B with screened drums or cages on lint cleaners and battery condensers, and high-efficiency cyclones on all other exhaust streams

Almond harvest emissions

Almond harvesting consists of shaking the almonds loose from the trees, sweeping them into rows where they are allowed to dry, and then using mechanical pickers to gather the row contents and load them into special trailers for transport. About 25% of the material in the rows is orchard debris: leaves, grass, twigs, pebbles and soil (U. S. EPA, 1985). Emissions from almond harvesting operations can be greatly varied as there are many varieties of harvesting equipment and different types of almond facilities (Lundquist, 1993). Almond harvesting can run from 2 to 4 months, usually beginning in August. Of the different steps in the harvesting process, pickup machines are believed to be responsible for the majority of the PM emissions. Pickup machines typically emit four times the PM₁₀ that sweeping emits and 40 times the dust that the shaking process emits (Ludwig, 2007). Flocchini et al. (2005) performed a study similar

Table 3. NASS tally of the number of cotton bales ginned from 2004 – 2007 (NASS, 2008)

State	Running Bales Ginned			
	2004	2005	2006	2007
AL	769,300	802,000	633,250	387,550
AZ	534,600	462,000	391,850	370,800
AR	2,006,500	2,098,650	2,410,000	1,809,400
CA	2,059,750	1,401,250	1,180,450	1,183,750
FL	91,700	111,200	139,650	101,700
GA	1,711,700	1,976,450	2,075,450	1,546,300
KS	18,300	70,400	78,400	40,600
LA	888,200	1,105,650	1,255,500	695,900
MS	2,263,700	2,089,000	2,029,000	1,271,150
MO	806,800	864,400	966,600	785,550
NM	55,050	60,350	46,800	46,700
NC	1,304,050	1,310,950	1,234,700	763,100
OK	219,950	267,500	165,900	264,850
SC	356,000	372,300	369,800	148,050
TN	947,150	1,082,400	1,265,750	586,600
TX	4,751,600	5,871,450	4,828,600	5,617,750
VA	140,400	161,600	140,150	95,900
U.S. total	18,924,750	20,107,550	19,211,850	15,715,650

to the project proposed herein (a lidar was also used) for the Almond Board of California, but, to date the results are not available. Researchers have measured relative PM emissions from different setup configurations of the machines used in the almond harvesting process (Goodrich et al., 2007). As a result of these findings, some recommendations are available that have been shown to reduce PM₁₀ emissions; these include setting sweeper heads at optimal heights, reducing the number of blower passes during the sweeping process, using wire tines on sweeper heads, reducing the speed of pickup machines, lowering separator fan speed and maintaining a clean orchard floor (Ludwig, 2007). A reduction in the number of blower passes, from 3 to 1, was found to give a 50% reduction in emissions. The reduction of blower passes also left a significant amount, 4.5 kg ha⁻¹, of almond meats in the field (Goodrich et al., 2007).

The California Air Resources Board (CARB) determined almond PM₁₀ emissions, based on measurements taken from 1994 to 1998, for shaking, sweeping and pickup to be 0.415, 4.15 and 41.2 kg ha⁻¹, respectively, giving 45.8 kg ha⁻¹ total PM₁₀ emissions for the almond harvesting process (CARB, 2003). These account for significant amounts of emissions, 12,000 tons year⁻¹ of PM₁₀, when applied to the total area of almond production (Goodrich et al., 2007).

PM emission rate determination techniques

In addition to providing a means for estimating emissions from various sources the AP-42 emission estimates also enable states to prepare State Implementation Plans (SIPs) aimed at reducing PM emissions. These PM emission factors provide formulas for estimating agriculture emissions. Chapter 9.1 of the AP-42 addresses agricultural tillage and estimates emissions using Equation 2:

$$E = k(5.38)s^{0.6} \quad (2)$$

where E are the emissions in units of kg ha⁻¹, k is a particle size multiplier, and s is the silt content of the surface soil. For PM_{2.5} k = 0.042, for PM₁₀ k = 0.21, and for TSP k = 1 (U. S. EPA, 1985).

Most of the studies used to develop the AP-42 emission factor document for agricultural emissions used the exposure profiling measurement technique. Exposure profiling, typically used to measure line sources, involves measuring the passage of pollutant immediately downwind of the source. Measurements are made directly and simultaneously by multipoint sampling over the cross section of the open dust source plume. This method is currently recognized by the U. S. EPA as the most appropriate for anthropogenic dust sources (U. S. EPA, 2002). This method is designed to isolate a single emission source, without shielding it from ambient conditions such as wind. Due to the limited number of exposure profiling studies and geographic variability, the emission factors for agricultural PM are still deemed to be inadequate (Capareda et al., 2005; Gaffney and Yu, 2003; U. S. EPA, 2003a).

In 2002, a dust emission inventory was prepared by Sonoma Technology, Inc. (STI) for CENRAP using the U. S. EPA emission factor approach and, for comparison, a bottom-up approach. For the bottom-up approach, development of the dust emission inventory for tillage and CAFOs incorporated county-level data on key variables affecting emissions including soil moisture content, amount of mechanical and animal activity, silt content of soil, and other factors. The study showed the bottom-up method derived emissions of PM_{2.5} were 295,000 tons year⁻¹; which was 20% lower than the

estimates determined using the traditional top-down (AP-42 emission factor) approach (Penfold et al., 2002).

A 1996 study compared particulates generated using five different tillage systems and found that number and type of operations influenced PM emissions; the measured emissions were half those predicted by the AP-42 emission factors (Coates, 1996). A PM₁₀ emission inventory was prepared for the San Joaquin Valley (CA) in 2003 using process specific emission rates. Data were gathered on the total acreage for each type of crop and the type of activities required to produce that crop. Emission factors developed by Gaffney and Yu (2003) were then used to calculate an emission inventory. Using this approach decreased the PM₁₀ emission estimates for land preparation by nearly 60%, from 34,000 (see Table 1) to 13,000 tons year⁻¹, while the emission estimates for harvesting increased by nearly 75% from 7,600 to 13,300 tons year⁻¹ (Gaffney and Yu, 2003).

With known emission rates and characterization of the atmosphere, dispersion models are often used to predict concentrations of various gases and PM. The U. S. EPA has approved a number of dispersion models for use in regulatory applications. These are listed in Appendix W of 40 CFR Part 51 (U. S. EPA, 1998); included are the Industrial Source Complex Short-Term Model, version 3 (ISCST3) and the American Meteorological Society/Environmental Protection Agency Regulatory Model (AERMOD), which as of November 2005 is recommended for all regulatory applications (U. S. EPA, 1995; U. S. EPA, 2005). Models are designed for estimating pollutant concentration levels surrounding sources. Models are useful because they can give reasonable predictions of impacts future facilities may have on air quality. They are an

economical and feasible alternative to extensive measurement programs. Modeling is the only practical approach for isolating the effects of one of many sources, and although modeling may not be totally accurate, it is precise, and therefore, reproducible (Cooper and Alley, 2002). For these reasons, regulation has become increasingly dependent on dispersion modeling for predicting boundary and off-property pollutant concentrations. When modeled pollutant concentrations exceed U. S. EPA or state approved ambient limits the source is required to present solutions that will decrease pollution to acceptable levels (Buser et al., 2001).

Due to the difficulties in reliably assessing agricultural emission rates described earlier, emission rates for many agricultural processes are not available making the typical modeling approach explained previously not viable (NRC, 2003). One accepted approach for determining agricultural emission rates is to use “inverse modeling,” or to back-calculate emission rates using dispersion models in combination with field concentration measurements (Parnell et al., 1994; NRC, 2003). Inverse modeling requires point samplers be used to measure PM concentrations near facilities, coupled with meteorological measurements to characterize the dispersion characteristics of the atmosphere. With this approach, PM concentrations can be measured in relatively few locations and compared with modeled results to determine an emission rate that would produce the measured concentrations at each location.

Inverse modeling has been used in research to determine emission factors from different types of sources including agricultural facilities (Faulkner et al., 2007; Parnell et al., 1993; Parnell et al., 1994; Venkatram, 1999). Studies have also been performed to test validity of inverse modeling (Haupt, Young, and Allen, 2006) with encouraging

results. ISCST3 has been recommended for modeling agricultural feedlot emissions (Earth Tech, 2001; Parnell et al., 1994). ISCST3 is also the model most commonly used to predict PM concentrations from agricultural low-level point sources (Wanjura et al., 2005). ISCST3 is known to have deficiencies for very stable or calm atmospheric conditions, and it is also unable to sufficiently account for the effects of small-scale terrain features and vegetation (Bunton et al., 2006). Gaussian plume modifications, such as empirical corrections and estimated dispersion coefficients from experimental data, have been investigated in field laboratory experiments as a means to provide better representation of agricultural sources (Gassman and Bouzaher, 1995; Keddie, 1980; Rege and Tock, 1996).

The AAQTF has recently addressed the possibility of over sampling PM_{10} when using the federal reference methods (FRM) in agricultural settings. The FRMs are gravimetric sampling methods with inertial particle size separators. PM_{10} measured in urban environments is typically smaller than coarse PM emitted in rural environments and the inherent errors associated with aerodynamic separation could bias samples from larger size fractionations. This bias could result in unequal regulation between urban and agricultural industries (Buser, 2004; Buser et al., 2001; Capareda et al., 2005). The U. S. EPA has not fully acknowledged this concern, but it could possibly affect emission rate results obtained by gravimetric inertial samplers and by inverse modeling.

An emerging technology, light detection and ranging (lidar) technology uses lasers to map and characterize (giving spatially-resolved size distributions and concentrations) aerosols within the boundary layers (Menut et al., 1999). Recently, scanning lidar systems have been developed for mapping and characterizing aerosol

plumes near the ground (Cooper et al., 2003; Kovalev and Eichinger, 2004). PM concentrations and emission rates from agricultural processes have been estimated with lidar (Bingham et al., 2006; Holmen, Eichinger, and Flocchini, 1998; Holmen et al., 2001a; Holmen et al., 2001b; Wilkerson et al., 2006; Zavyalov et al., 2006). Lidar technology is unique because of its capability to give spatial and temporal resolution, as compared with the gravimetric sampler methods which give a time averaged mass concentration at a particular point. However, a lidar will give only volumetric, not mass concentrations. In order to determine the commonly accepted mass emission rates, a lidar must be used in conjunction with gravimetric samplers to determine estimates of particulate density. Lidar concentration fields can then be used with mass balance or dispersion models to derive relevant emission rates.

METHODOLOGY

Within the scope of this project three different agricultural operations were studied: an almond harvest, a cotton ginning process, and a comparison between a variety of tillage practices. Field measurements were made near Dunnigan, California at an almond orchard from September 26 to October 11, 2006. Measurements of the cotton ginning process were made at a cotton gin near Lemoore, California from December 11 to December 14, 2006. Finally, from October 19 to 29, 2007, measurements were made near Los Banos, California of differing crop tillage processes.

Samplers located upwind of the facilities measured background concentrations of PM, while the samplers located downwind measured background plus facility produced PM. The facility-derived pollutant concentrations were calculated by subtracting the background concentration from the downwind concentrations.

Particle Mass Concentration Measurement

At each site, portable AirMetrics MiniVol PM₁/PM_{2.5}/PM₁₀/TSP samplers were used to determine the point-specific mass concentrations. The placement of the MiniVols was site dependent and they were placed at ground level (~2 m) or hung on either 10 meter (m) or 15 m towers. They were generally placed in an array around the suspected source area, with samplers more concentrated in the suspected upwind and downwind locations.

The MiniVols can be programmed to operate for a desired time period and consist of a size-segregating sample inlet (an impactor), a 47 millimeter (mm) filter cartridge, and a pump. The sample inlet can be equipped with different impactor heads, which

separate particles using inertial impaction based on the impactor's jet diameter, the jet-to-plate spacing and the particle's aerodynamic diameter. The MiniVols operate at five liters per minute (L min^{-1}) and collect the size-segregated particulate matter on 47 mm Teflon filters that were pre-weighed and pre-conditioned at Utah State University's (USU) Utah Water Research Laboratory (UWRL). The conditioning steps consisted of storage in a room temperature dessicator for a minimum of 24 hours before any weights were taken and then successive weights were obtained with a minimum of one day between each weighing. After the filters had been used in the MiniVols they were returned to the UWRL for post-test conditioning and a final weight determination. Filter weights were measured in milligrams (mg) to three decimal places (i.e. 1 microgram (μg)) using a Mettler Type MT5 balance (Mettler Instrument Corp.). The final filter weights reported were the average of three consecutive weights which were within $\pm 2.5 \mu\text{g}$ of the mean, which translates to a minimum system method detection limit (MDL) of $0.36 \mu\text{g m}^{-3}$ based on a 24 hr average sampling time. Once the final filter weight was measured, the mass of PM collected was found by taking the difference in pre- and post-weights; then, using the air flow and run time, a mass concentration was determined.

MetOne 9722 optical particle counters (OPC) were typically collocated with the MiniVol particle samplers. The OPCs provide near-realtime (20 – 60 second averaging) size distribution and particle count information, which can be used to estimate the duration and intensity of an impact by any particulate plume. The OPCs operate by passing sample air through a right angle light scatter detector. The OPC pulls 2 L min^{-1} sheath air to protect the system's optics and a sample air flow rate of 1 L min^{-1} . The instrument counts particles and calculates their size using scattered light. A particle in

the sample volume will scatter light from the laser diode, while a 60 steradian solid angle elliptical mirror, located at a right angle to the laser beam, then collects the scattered light. The collected light is converted to a voltage pulse with an amplitude that is based on the scattered light intensity. The pulse is then categorized using size discriminators and counted as a particle in one of eight size bins from $> 0.3 \mu\text{m}$ to $> 10 \mu\text{m}$. The OPC outputs the number of particles in the sample that fall within each bin for a set time interval. From this information, an optical size distribution can be found.

The OPC can also provide a volume concentration by assuming a radius (the geometric mean of the bin cutoff radii) for each bin and then finding the particle volume (assuming spherical particles). This gives the volume for each particle in the bin and can be multiplied by the number of particles in the bin to obtain a sample volume, or a total volume of all the particles in that bin. This can be divided by the sample volumetric flow to get a concentration of the volume of PM per volume of air. If a particle density is known, a mass concentration can then be found by multiplying the volume concentration by the density. If the density is unknown, then it can be estimated by comparing the mass concentration measured by the MiniVols with the volume concentration measured by the OPCs. An effective density can then be found by the following:

$$\rho_{particle} = \frac{C_{mass}}{C_{volume}} \quad (3)$$

where $\rho_{particle}$ is the effective particle density, with typical units (g cm^{-3}), and C_{mass} is the mass concentration (g m^{-3}) and C_{volume} is the volume concentration ($\text{cm}^3 \text{m}^{-3}$).

Meteorological Measurements

Characterization of the atmosphere is essential during the studies, and a host of meteorological measurements were required to effectively model the on-site transport and dilution of the emitted PM. Davis Weather Station Vantage Pro Plus systems were used to collect time-averaged meteorological variables such as wind speed, wind direction, ambient air temperature, relative humidity, barometric pressure, and incident solar radiation (insolation). In addition to the Davis Weather Station, cup anemometers and HOBO® temperature sensors were placed at various elevations on the towers to measure the vertical wind speed and temperature profile up to 15 m. A tethered balloon system was also used to obtain wind and temperature profile data above the tower heights. Temperature profiles, as well as insolation and wind speed, were used to determine stability class. Campbell Scientific CSAT3 3D sonic anemometers were mounted on towers to determine turbulence information such as the friction velocity (u^*), fluxes of sensible and latent heat and the Bowen ratio, and the Monin Obukhov length. A Garmin etrex Vista global positioning satellite system (GPS) documented the spatial coordinates of buildings, towers, samplers and other significant structures.

Inverse Modeling

In order to determine emission rates using the facility-derived pollutant concentrations, inverse modeling requires an initial seed emission rate, which can be obtained from literature, from locally collected meteorological data, facility layout, and location and extent of pollutant sources and receptors. The U. S. EPA approved Gaussian plume models ISCST3 and AERMOD were used in this study and results from each were

compared to quantify the similarities and differences between the two models. Both of these models assume steady-state conditions, continuous emissions, conservation of mass and a Gaussian distribution of vertical and crosswind pollutant concentrations (Cooper and Alley, 2002). The general Gaussian plume equation uses the Pasquill-Gifford horizontal and vertical plume spread parameters, σ_y and σ_z , to account for downwind plume dispersion as shown in Equation 4.

$$C_{10} = \frac{Q}{2u\pi\sigma_y\sigma_z} \exp\left(-\frac{1}{2} \frac{y^2}{\sigma_y^2}\right) \left\{ \exp\left(-\frac{1}{2} \frac{(z-H)^2}{\sigma_z^2}\right) + \exp\left(-\frac{1}{2} \frac{(z+H)^2}{\sigma_z^2}\right) \right\} \quad (4)$$

C_{10} is the 10 minute average concentration ($\mu\text{g m}^{-3}$) at a given downwind receptor location, Q is the pollutant emission rate ($\mu\text{g s}^{-1}$), u is the average wind speed at release or stack height (m s^{-1}), y is the horizontal distance of the chosen receptor from the centerline of the plume (m), z is the height of the receptor above ground level (m) and H is the effective release or stack height (m), which includes estimates of plume rise due to buoyancy and/or momentum (Cooper and Alley, 2002).

ISCST3 assumes a Gaussian distribution of pollutants in the y - and z -directions based on time averaged meteorological data. It uses stability classes to address pollution dispersion due to atmospheric mixing. Stability classes are typically determined by a combination of vertical temperature lapse rates and incoming solar radiation or methods using vertical or horizontal wind variance (Turner, 1970). Stability classes indicate the level of atmospheric mixing and thus dispersion of pollutants. For example, Class A stability is considered highly unstable which promotes dispersion of pollutants. Class A stability is categorized as having a dT/dz less than $-19 \text{ }^\circ\text{C km}^{-1}$ or strong insolation (solar

altitude greater than 60°) and wind speed less than 2.8 m s^{-1} . Class G stability is considered highly stable, hindering dispersion, and is categorized as having a dT/dz greater than $40 \text{ }^\circ\text{C km}^{-1}$ or weak or no insolation (solar altitude less than 15°) and wind speed less than 1.8 m s^{-1} . AERMOD requires more detailed meteorological and surface characteristic information to calculate a spectrum of continuous dispersion functions. Because of the additional input requirements for AERMOD and the lack of an established database for these inputs many regulatory agencies continue to use ISCST3; for this reason both models were used in this study.

AERMOD uses continuous functions for atmospheric stability determinations, and based on stability determines the appropriate distribution, a Gaussian distribution for stable atmospheric conditions, and a non-Gaussian distribution for unstable, or turbulent conditions. AERMET, an AERMOD meteorological data preprocessor, derives boundary layer parameters such as friction velocity, Monin-Obukhov length, convective velocity scale, temperature scale and surface heat flux based on the measurements of typical meteorological parameters. AERMET can also provide AERMOD with temperature, wind direction and speed at multiple heights. AERMOD uses these data to calculate concentrations accounting for change in dispersion rates with height. AERMOD is better at accounting for terrain features and building downwash phenomena than ISCST3 (Paine et al., 1998). The interface used to run the models was the commercially available ISC-AERMOD View packaged by Lakes Environmental, Inc.

ISCST3 and AERMOD were the models selected for this study based on the objective of determining agricultural emission rates using EPA approved regulatory models. Another approach used in similar studies was the application of backward

Lagrangian stochastic (bLS) models. Studies have compared the Gaussian-based models to the bLS; Galvin et al. (2006) found that the two modeling approaches gave similar results, while Price et al. (2004) found the bLS models produced emission results an order of magnitude higher than the Gaussian-based models.

To run the models used in this study, on-site meteorological data and hourly cloud ceiling heights (retrieved from the U.S. National Oceanic and Atmospheric Association (NOAA) website for unedited surface weather observations) were compiled and formatted to run the models. Concentrations modeled using E_{seed} were compared to the facility-derived concentrations (those measured by the samplers minus the upwind background) at each sampler location. The ratios of measured concentrations ($C_{measured}$) to the modeled concentrations ($C_{modeled}$) at each receptor location were gathered and averaged. This average ratio was multiplied by the seed emission rate (E_{seed}) to give the emission rate corresponding to the measured concentrations ($E_{estimated}$) as shown in Equation 5.

$$E_{estimated} = E_{seed} \left(\frac{C_{observed}}{C_{modeled}} \right) \quad (5)$$

Lidar

The study described herein was a supporting study to a much larger investigation involving developing lidar emissions measurement technology. Although the lidar measurements are not within the scope of the objectives presented herein, the AGLITE lidar system is briefly described, as the results of this study will ultimately be compared to those from the lidar measurements. The AGLITE system was developed for

agricultural PM measurement by USU's Space Dynamics Laboratory. Lidar is an acronym for light detection and ranging and the system used in conjunction with the described studies uses a coaxial 10 kilohertz (KHz) micropulsed Neodymium-Doped Yttrium-Aluminum-Garnet (NdYAG) laser that radiates at three wavelengths: 355 nanometers (nm), 532 nm, and 1064 nm. The spatial resolution of the lidar is 6 m and it can make up to 10 measurements per second. The laser power is adjustable to allow for eye safe operation over its scanning range, from 500 m to 15 km. A digital camera is mounted to the system for additional safety monitoring and alignment enhancement. The lidar system is installed in a trailer for mobility purposes. A turret controls the azimuth and elevation of the laser beam, which allows the lidar to scan an area of several hundred square meters in less than a minute. The high temporal and spatial resolution of the lidar allows for correlation of lidar-derived concentrations with specific on-site activities and events. The beam is sent out and ambient particles scatter the light; some of the scattered light returns to the lidar. This return signal is collected with a 12-inch telescope where the photons are then counted (see Figure 5).

The lidar data can then be processed to give particulate volume concentrations and, with a known or estimated density, a mass concentration field with temporal and spatial resolution. The lidar typically begins a campaign by "staring," or sending a motionless beam, near an OPC/MiniVol cluster in order to obtain a particle density calibration. Stares are performed periodically throughout a study for continual instrument calibration. In order to find facility emissions, the lidar typically performs "staple scans" as shown in Figure 6. A staple consists of a vertical scan upwind of the facility, a horizontal scan over the facility and one or several vertical scans downwind of

the facility. This gives a background PM concentration (the upwind scan) and a background plus facility-derived concentration (the downwind scan). This creates a box around the facility in order to capture and measure all facility emissions. The scans can be averaged and compared to the modeled results at corresponding elevations.

A mass balance can then be used to calculate the flux through the box using the following mass balance equation:

$$Q_{in} C_{in} = Q_{out} C_{out} + \left(\frac{dC}{dt} \right) V \quad (6)$$

where Q is the flow in $\text{m}^3 \text{min}^{-1}$, C is the concentration in $\mu\text{g m}^{-3}$ and V is the volume of the box in m^3 , assuming steady-state conditions. An additional assumption which must be made is that pollutant is not reactive or settling within the box.

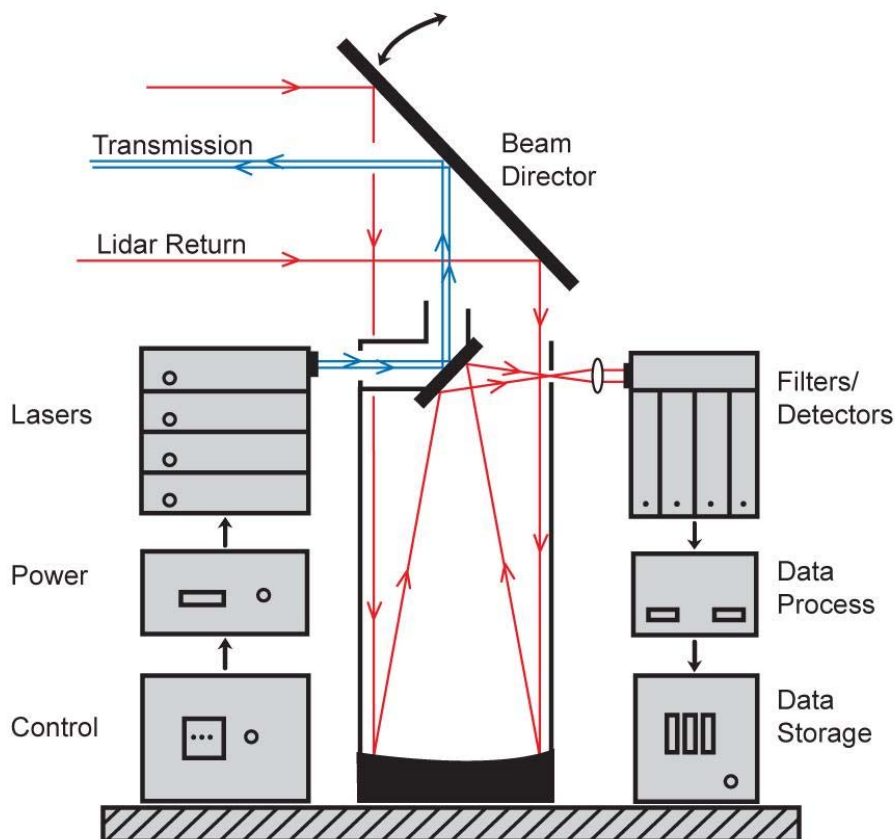


Figure 5. A conceptual drawing of the lidar.

Field Sites Descriptions

Almond harvest

Field measurements during various harvest operations were made near Dunnigan, California at an almond orchard from September 26 to October 11, 2006. The orchard was divided into three sections and consisted of approximately 3850 almond trees, including a number of different varieties. There were 113 rows aligned in a parallel north-south orientation. Section 1 included the 60 rows on the east side of the orchard, section 2 included the next 20 rows and the final 33 rows on the west side composed section 3. The rows in section 1 were 229 m long with 6.3 m between rows. Sections 2 and 3 were 226 m long with 6.1 m spacing between the rows. The orchard was approximately 700 m in total (east-west) length. The orchard was bordered by a paved road to the north and gravel roads to the east and west, and a dirt road to the south. A residential home was located just north of the orchard, and to the south was an open field with some slight elevational changes in terrain. The surrounding areas were occupied by other almond orchards. For modeling purposes each row was divided into an east and

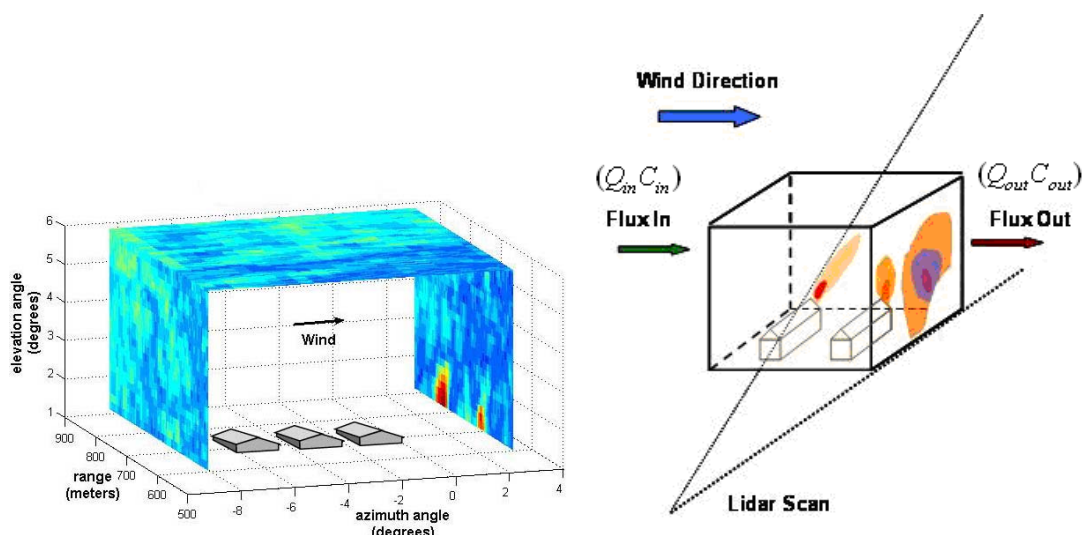


Figure 6. Graphical representation of a staple scan with the lidar.

west half (roughly the areas shaded by the trees' canopies). These were then modeled as area sources and could be "turned on" or "turned off" by assigning a seed emission rate or not, depending on orchard operations. Figure 7 shows the orchard, with an overlay of the source areas and sampler/receptor locations used in the modeling.

Historical wind direction data from the California Irrigation Management Information System (CIMIS) station near Woodland, CA showed a W – SW prevailing wind (CIMIS, 2008) for the given time of year. Sampler locations were designated both north and south of the orchard due to wind direction variability while on site; these locations are also shown on Figure 7. There were OPCs placed at two heights (2 m and 9 m) for some of the sample locations, and at only 2 m for other locations used during a sample run, along with a set of MiniVol samplers also at each height. Specific sampler locations varied daily with wind conditions and orchard operations.

The sample locations north of the orchard were numbered from west to east. A presumed upwind tower U1 was fitted with samplers and designed to give background concentration measurements. Preliminary site visits showed a frequent northern component to the wind and from this the south end of the orchard was designated as downwind, hence the 'D' notation. Similarly, the sampler locations south of the orchard were numbered from west to east. For southerly winds, the SA1 (South Asparagus 1, named for the small, adjacent asparagus crop) tower was set up to measure background concentrations.

Figure 8 shows the various locations of the supporting meteorological towers and the lidar depending on wind direction. The north and south meteorological towers were each equipped with five collocated cup anemometers and HOBO® temperature sensors at

the following heights: 1.60 m, 2.57 m, 4.19 m, 6.45 m, and 9.09 m. The sonic tower was equipped with three sonic anemometers at 2 m, 5 m and 10 m heights. The Davis Weather Station was located on the air quality trailer at an elevation of 5 m.

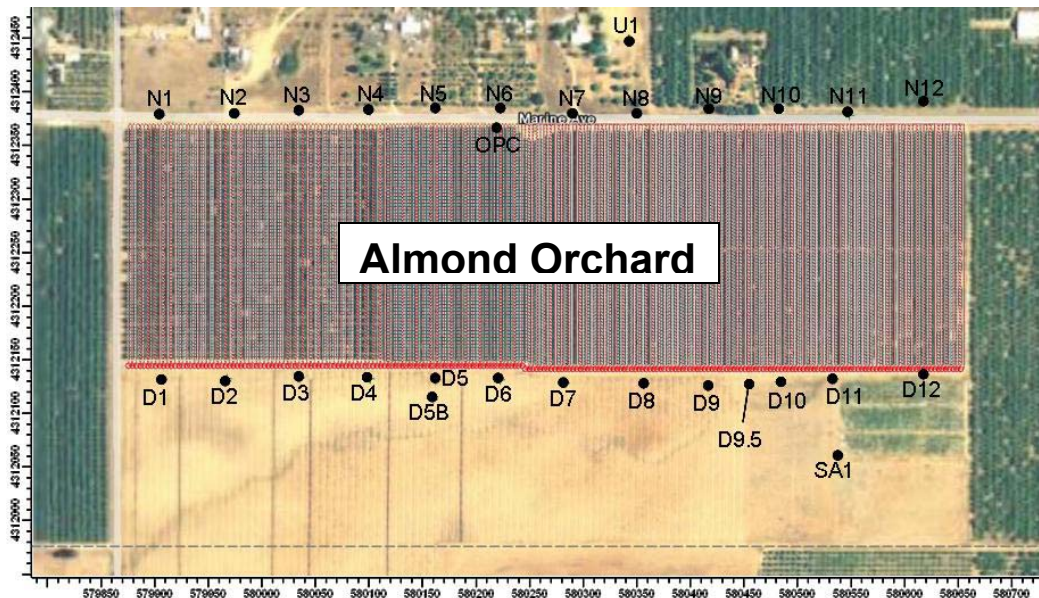


Figure 7. Layout of the almond orchard with sampler locations. The axes are in units of meters and represent UTM coordinates in NAD27.

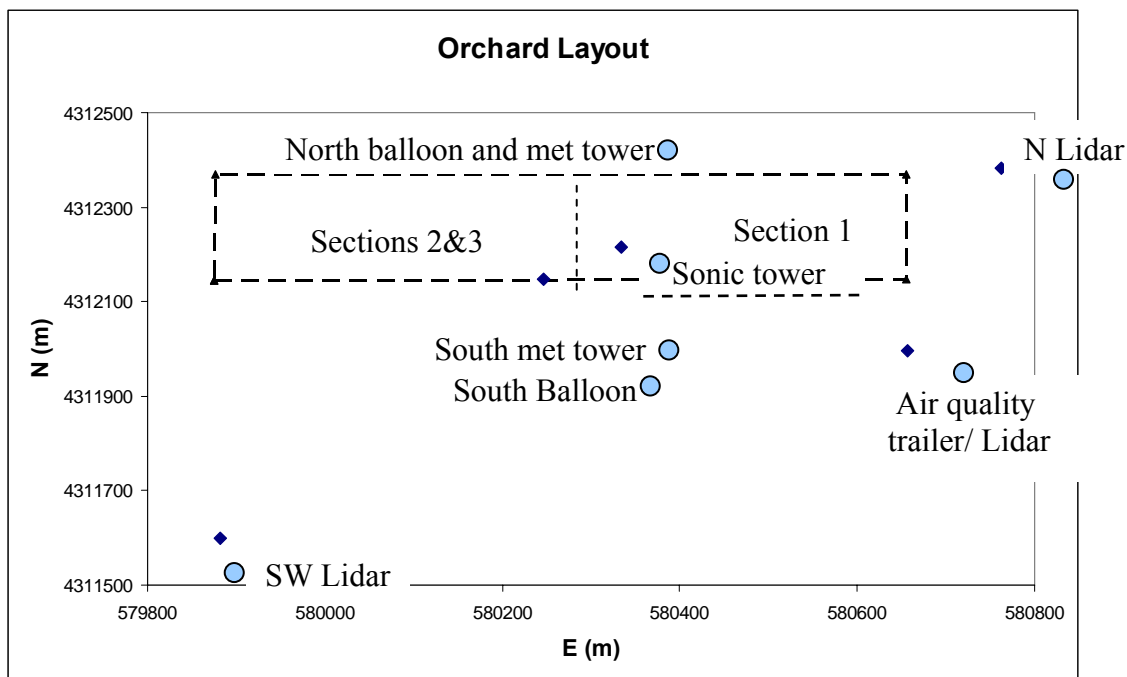


Figure 8. Layout of the almond orchard with meteorological tower and lidar locations. The axes represent UTM coordinates in NAD27.

The almond harvesting processes consists of three separate processes: shaking, sweeping and harvesting. The model of shaker used in this study was an Orchard Rite “The Bullet” Sideshaker. The sweeper was a 20-year old Weiss McNair Model HS30, and the harvester was a power take-off (PTO) driven 2006 Flory Model LD 80.

Shaking of the Carmel and Monterey variety trees began on September 26, 2006. The shaker moved from west to east in a serpentine manner shaking one tree at a time. On September 30, Section 1 was swept, and on October 1, Sections 2 and 3 were swept. Section 1 was harvested on October 2, 2006. Unfortunately, the winds did not follow the predicted patterns and producer harvest activities could not be delayed; therefore, mock sweepings were performed (typical sweeping equipment was used, but almonds weren't present in the orchard having been previously collected) in Section 1 on October 3rd and 11th, and in Sections 2 and 3 on October 9th. On the 10th of October, Sections 2 and 3 were harvested. Rows where operations took place were noted in order to properly quantify emissions and run the air quality dispersion models; more detailed notes are found in Appendix A. As previously mentioned, during the modeling runs rows where operations took place were “turned on” by assigning a seed emission rate in units of $\mu\text{g m}^{-2} \text{s}^{-1}$; for rows in which multiple (n) passes were made the seed emission rate was multiplied by n, the number of passes in that row. The terrain surrounding the orchard is relatively flat with no downwind buildings, so terrain and building features were not used in modeling. Meteorological data were compiled as needed from the on-site meteorological equipment for each model. Due to the limited amount of research available for almond harvest emission rates a “seed” emission rate of $50 \mu\text{g s}^{-1} \text{m}^{-2}$ was

determined using tillage emission rate calculations with Equation 2 for soil with a silt content of 50% and a 2 hour sample run.

Cotton gin

Measurements of cotton gin emissions were made near Lemoore, California from December 11 to December 14, 2006. The cotton gin layout is shown in Figure 9. The cotton gin produced approximately 20 bales of cotton per hour, with each bale weighing nearly 220 kg. The gin processing facility itself was approximately 30 m wide and 67 m long. Thirty seven meters south of the gin was a seed barn which was 40 m wide by 124 m long with open sides and a pitched roof. The cotton gin was equipped with 42 cyclones of varying height and diameter designed to reduce the PM emissions from the

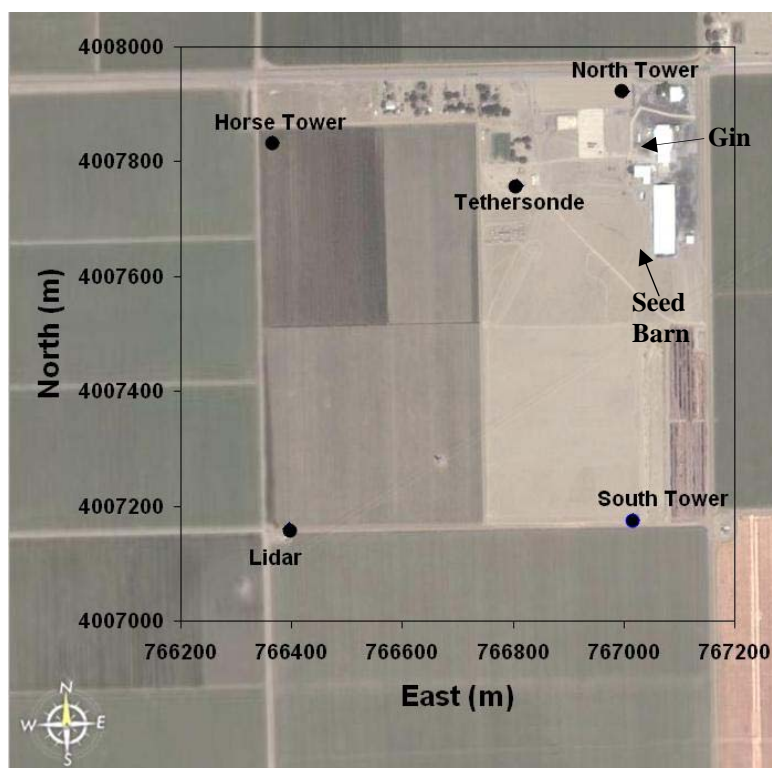


Figure 9. Cotton gin layout with tower and lidar locations indicated. The axes are in units of meters and represent UTM coordinates in NAD27.

various parts of the processes. Four cyclones were located on the west side of the gin with the remainder on the north end of the east side. There were a few other outbuildings including a maintenance shed on the west between the gin and seed barn and an office building to the north of the gin. The facility had dirt roads and little vegetation on the premises.

Historical weather data were gathered from the Five Points CIMIS station (CIMIS, 2008), which is within 17 miles to the north of the gin. The windrose, Figure 10, shows a major southeast wind component for the first part of December, however there is also a significant amount of wind out of the northeast. Based on these data, the tower and lidar locations were determined as shown in Figure 9.

The north tower was equipped with five cup anemometers at the following heights: 2.5 m, 3.8 m, 6.0 m, 8.9 m, and 14.3 m with a wind vane at 13.7 m. A Davis

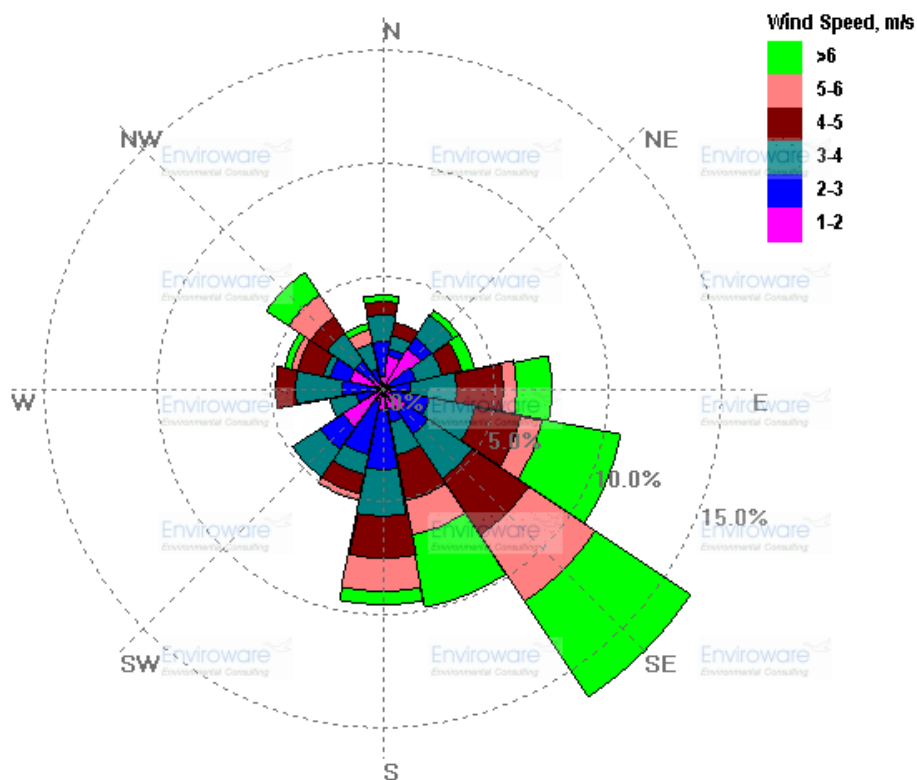


Figure 10. Windrose plot for Five Points, CA from December 6-20 for 2001-2005.

Weather Station was attached to the north tower at an elevation of 14.9 m. Four MiniVol samplers were placed at an elevation of 13.4 m with each configured for a different size fractionation (TSP, PM₁₀, PM_{2.5} and PM₁), while two MiniVol samplers, a PM₁₀ and a PM_{2.5}, were placed at 7.9 m. OPCs were mounted to the tower to match the MiniVol locations, one at 13.5 m and one at 8.4 m. The south tower was equipped with five cup anemometers at the following heights: 2.5 m, 4.1 m, 6.3 m, 9.7 m, and 15.2 m with a wind vane at 13.7 m. As with the north tower, four MiniVol samplers with different size-fractionation were placed at an elevation of 13.4 m and three MiniVol samplers, two PM₁₀ samplers (for replicate analysis) and a PM_{2.5} sampler, were placed at 7.7 m. OPCs were mounted to the tower to match the MiniVol locations, one at 13.3 m and one at 8.4 m. The “horse” tower was equipped with one OPC mounted at 8.2 m (the name refers to the identification of the OPC fixed to that tower). The tethered balloon was operated to the west of the gin so as not to interfere with the other measurements or gin operations. The lidar was located in the southwest corner in order to scan perpendicular to the expected wind direction. Another Davis Weather Station was located on the air quality trailer (next to the lidar trailer) at an elevation of 5 m.

Emission factors estimate the amount of PM₁₀ and TSP emitted from cyclones for various operations in the cotton ginning process (refer to Table 2). For modeling purposes, the emission factors, given in lbs bale⁻¹, were converted to g s⁻¹, assuming 4 months of operation each year and 22 hours of operation daily, and assigned to cyclones (modeled as point sources). Owing to the lack of any nearby topographical changes, no terrain features were used; however, the surrounding buildings were incorporated into the

model. $PM_{2.5}$ emissions data for the gin were procured from the California Air Resources Board (CARB). A $PM_{2.5}$ emission rate (E_{seed}) for modeling was determined by assuming four months of operation per year at 22 hours per day and evenly dividing the $PM_{2.5}$ emissions data for the gin among the 42 cyclones. Appendix B also contains information on the number of cyclones, size, and exit velocity.

Tillage

Measurements of tillage emissions were made near Los Banos, California from October 19 to October 29, 2007. Tillage emissions were measured on two fields: PA-47 highlighted in Figure 11 and PA-46 highlighted in Figure 12. Conventionally, land preparation by tillage is a multi-step procedure involving multiple disc passes, a chisel pass and a land plane pass. The conventional or traditional tillage operation measured in



Figure 11. The highlighted area is field PA-47. Combined tillage operations were measured here.

this study required five operations: disc 1 on October 23, chisel on October 25, disc 2 on October 26, disc 3 on October 27 and a land plane pass on October 29. Combined tillage methods were also studied in order to compare PM emissions. The combined tillage operations included a chisel pass, performed on October 19, and a pass with an optimizer on October 20. The optimizer incorporated all disc passes and land plane passes in a single pass. After the optimizer, the ground was ready for planting and irrigation.

Conventional tillage operations were performed on PA-46, while a combined tillage operation using an optimizer was performed on PA-47 to allow comparative emissions from the different tillage operations. PA-46 is approximately 0.22 km², and PA-47 is approximately 0.19 km². Cotton was grown, harvested and chopped prior to the land preparation operations studied in this campaign. The fields were bordered by dirt



Figure 12. The highlighted area is field PA-46. Conventional tillage operations were measured here.

roads. The surrounding areas were active agricultural fields also consisting of chopped cotton.

The sampling layout was determined based on historical weather data gathered from the Los Banos CIMIS station (CIMIS, 2008) which is located within one mile of the tillage site. The station showed a predominant north to northwest wind, with some early morning winds from the east. Thus, the lidar, tower and sampling locations shown in Figure 11 and Figure 12 were selected. Sampler locations were designated both north and south of the tillage site to characterize both the background PM and the tillage plume as shown in Figure 11 and Figure 12. An upwind tower U1 was fitted with samplers and designed to give background concentration measurements. Other sampler locations were labeled based on their orientation to the tillage site. For complete instrumentation at each location see Appendix C.

The lead tractor was equipped with a global positioning system (GPS) to define the area of each operation. The area was then defined and modeled as an area source with both ISCST3 and AERMOD dispersion models. The terrain surrounding the tillage site was flat with no surrounding buildings, so terrain and building features were not used in modeling.

RESULTS AND DISCUSSION

Almond Harvest Results

The average temperature and barometric pressure at the almond orchard from September 26 to October 11, 2006 were 18.6°C and 100.6 kPa, respectively. The wind direction was variable over the course of the study. The average wind speed during the study was 1.4 m s⁻¹. Due to the variability of the wind, several different sampling configurations were conceived, and before each run samplers were arrayed to best suit atmospheric conditions. Figure 8 gives the orchard layout with lidar locations and meteorological tower locations and Figure 7 shows the layout of the almond orchard with the sampler locations.

Almond harvest PM concentration measurements

An array of AirMetrics MiniVol samplers were positioned to characterize the background/upwind and the downwind PM concentrations for each run. The average measured PM concentrations upwind and downwind for the almond orchard are provided in Table 4. The upwind concentrations were measured by separate MiniVols for each particle size and for the campaign averaged $32.2 \pm 12.0 \mu\text{g m}^{-3}$, $160.6 \pm 155.0 \mu\text{g m}^{-3}$ and $258.6 \pm 194.1 \mu\text{g m}^{-3}$ for PM_{2.5}, PM₁₀ and TSP, respectively. The uncertainty represents the standard deviation. Upwind PM_{2.5}, PM₁₀ and TSP concentrations ranged from 18.3 to 55.6 $\mu\text{g m}^{-3}$, 36.9 to 465.7 $\mu\text{g m}^{-3}$, and 81.1 to 603.3 $\mu\text{g m}^{-3}$, respectively, over the course of the campaign. Downwind concentrations averaged $31.8 \pm 15.9 \mu\text{g m}^{-3}$, $114.5 \pm 78.5 \mu\text{g m}^{-3}$ and $368.8 \pm 412.9 \mu\text{g m}^{-3}$; and ranged from 17.8 to 77.0 $\mu\text{g m}^{-3}$, 25.2 to 535.9 $\mu\text{g m}^{-3}$ and 129.0 to 1829.3 $\mu\text{g m}^{-3}$ for PM_{2.5}, PM₁₀ and TSP, respectively.

Average downwind concentrations of PM_{2.5}, PM₁₀, and TSP were 107%, 92%, and 140%, respectively, of those upwind.

Theoretically, the downwind samplers should always measure higher concentrations than the upwind, with the largest differences correlating with operations producing the most PM. However, for some of the observed operations, the average upwind concentrations as measured by the filter-based systems were higher than those measured downwind. This may be explained by sampler locations not having sufficient stand off distance from the operations or the background location being impacted by nearby sources, such as traffic on dirt roads or adjacent PM producing operations.

On October 2 and again on October 9, an orchard upwind of the study site was actively harvesting almonds, with sweeping and pickup operations. The plumes created

Table 4. PM concentrations upwind and downwind of various almond harvesting operations ($\pm 1\sigma$)

Date		PM _{2.5} μg m ⁻³	PM ₁₀ μg m ⁻³	TSP μg m ⁻³	Orchard Operation
9/26/2006	Upwind	-	47.1	-	Shaking
	Downwind	-	125.2 ± 24.1	-	
10/1/2006	Upwind	55.6	377.5	603.3	Sweeping
	Downwind	22.8 ± 3.0	114.0 ± 50.1	234.2 ± 125.9	
10/2/2006 AM	Upwind	36.6	-	458.0	Pickup
	Downwind	53.2 ± 23.8	173.0 ± 98.8	485.9 ± 147.9	
10/2/2006 PM	Upwind	-	-	-	Pickup
	Downwind	27.6 ± 0.3	157.6 ± 174.1	994.6 ± 1180.1	
10/3/2006	Upwind	35.1	63.6	-	Mock Sweeping
	Downwind	41.4 ± 7.0	104.3 ± 25.7	328.1 ± 79.2	
10/9/2006	Upwind	27.4	42.2	81.1	Mock Sweeping
	Downwind	38.0 ± 26.0	86.3 ± 46.9	142.3 ± 18.8	
10/10/2006 AM	Upwind	18.3	184.2	151.6	Pickup
	Downwind	25.9 ± 7.8	80.0 ± 16.7	482.2	
10/10/2006 PM	Upwind	27.1	36.9	206.7	Pickup
	Downwind	25.4 ± 4.4	57.0 ± 8.8	208.1 ± 19.8	
10/11/2006	Upwind	25.4	372.4	149.4	Mock Sweeping
	Downwind	18.8 ± 1.2	52.4 ± 12.1	152.3 ± 13.2	

by these operations were visibly much larger vertically and horizontally than those produced by the operations at the study site. This was supported by lidar data (Figure 13) which depicts plumes generated by pick up operations in the orchard of this study (at a distance of 550 to 800 m from the lidar) and a plume generated by operations at a neighboring orchard (~1200 m). Not only was the plume from the neighboring orchard larger both vertically and horizontally, but the concentrations associated with the neighbor's plume were nearly an order of magnitude higher than those measured at the study orchard. Sample contamination can also be verified by inspecting the OPC data.

Due to the nature of time-averaged sampling, even a single exposure at these potentially high concentrations can significantly bias the final measured concentrations.

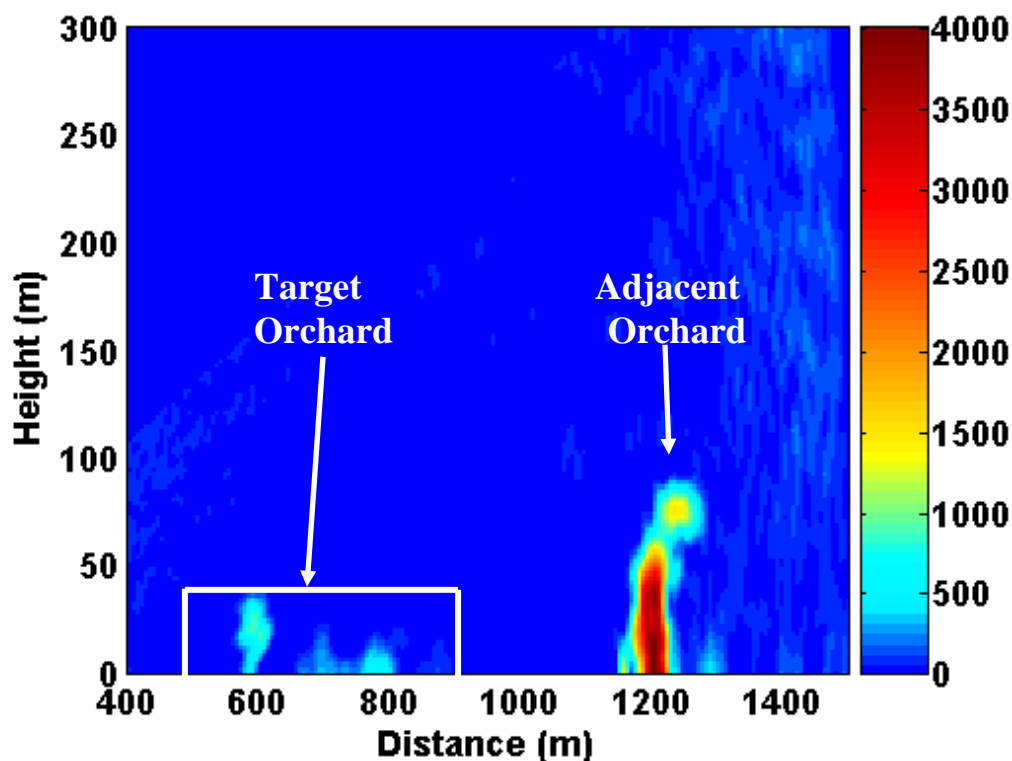


Figure 13. A lidar scan taken on October 2 at 10:02 showing the PM₁₀ concentration field in $\mu\text{g m}^{-3}$. The almond orchard of interest in this study was located at a distance of 550 to 800 m from the lidar. The large, highly-concentrated plume 1200 m from the lidar was generated by a neighboring harvest.

Results on days with neighboring operations are, therefore, likely, unreliable unless “clean” backgrounds can be determined. The OPC data can be used to estimate “clean” background concentrations. A method for estimating “clean” background concentrations for these scenarios will be discussed in the subsequent inverse modeling results section.

The mass fraction of each PM size with respect to the measured TSP values for both upwind and downwind samplers for each operation are presented in Table 5 and shown in Figure 14. On average, upwind TSP was comprised of 16% PM_{2.5} and 44% PM₁₀ with the remaining TSP mass being contributed by particles larger than 10 μm. Similarly, average downwind TSP was comprised of 12% PM_{2.5} and 34% PM₁₀. Overall, PM_{2.5} comprised 13% of TSP and PM₁₀ comprised 34% of TSP for the almond orchard experiment. The TSP compositions along with mass concentrations are shown graphically in Figure 14.

On September 26 (the shaking operation) only PM₁₀ was measured, so size fraction data were not available. Furthermore, on other dates without size fraction information, shown in Table 5 as no data (-), upwind samples were likely contaminated

Table 5. Fraction of TSP that is PM_{2.5} and PM₁₀ for each operation upwind and downwind of the orchard and campaign averages upwind and downwind

Date	Upwind		Downwind		Orchard Operation
	PM _{2.5} /TSP	PM ₁₀ /TSP	PM _{2.5} /TSP	PM ₁₀ /TSP	
9/26/2006	-	-	-	-	Shaking
10/1/2006	0.09	0.63	0.10	0.49	Sweeping
10/2/2006 AM	0.08	-	0.11	0.36	Pickup
10/2/2006 PM	-	-	0.03	0.16	Pickup
10/3/2006	-	-	0.13	0.32	Mock Sweeping
10/9/2006	0.34	0.52	0.27	0.61	Mock Sweeping
10/10/2006 AM	0.12	-	0.05	0.17	Pickup
10/10/2006 PM	0.13	0.18	0.12	0.27	Pickup
10/11/2006	0.17	-	0.12	0.34	Mock Sweeping
	Average Upwind		Average Downwind		
	0.16	0.44	0.12	0.34	

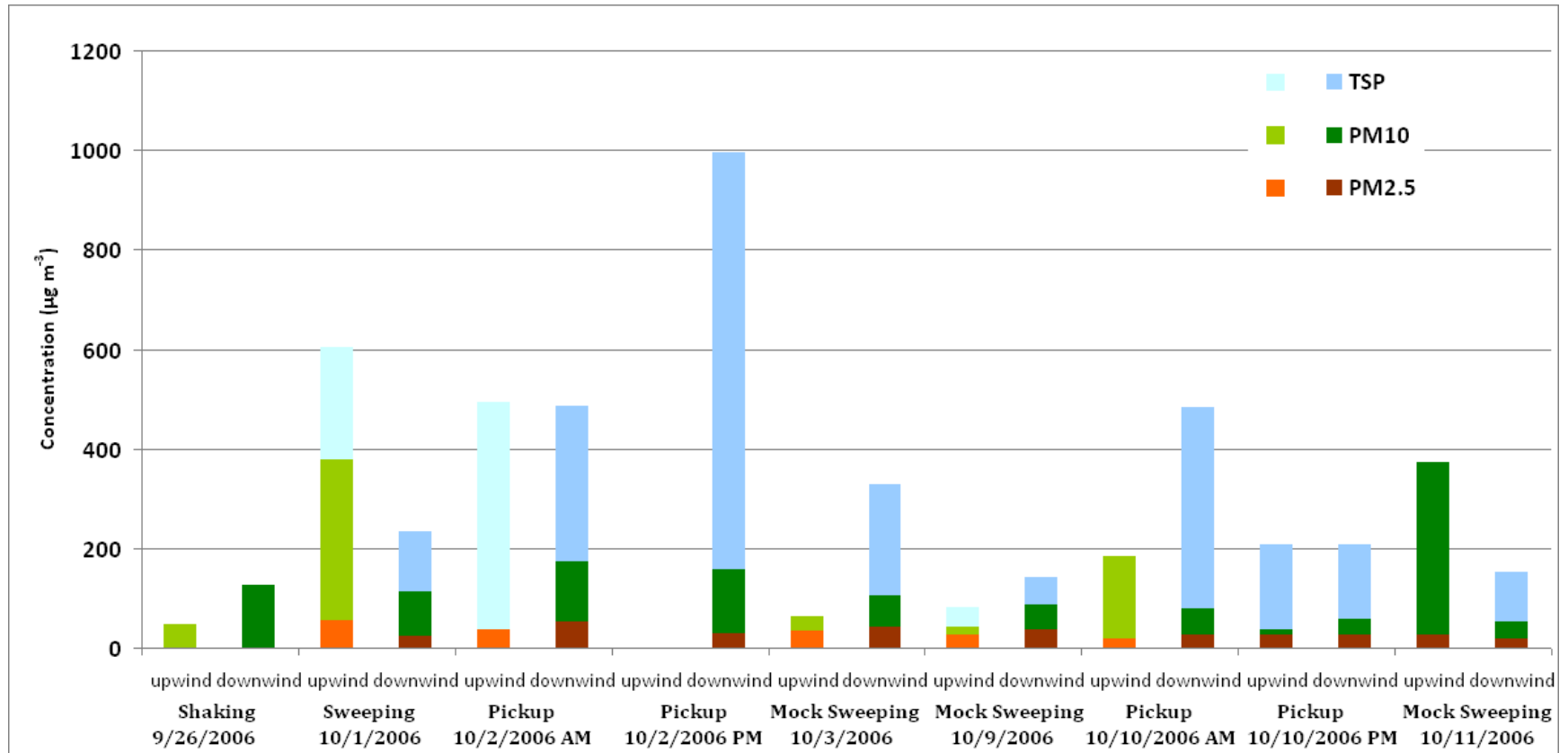


Figure 14. Average measured upwind and downwind PM concentrations with the particle size contributions to the total PM for the almond orchard.

(from nearby operations) or unreliable (larger concentrations for smaller sizes likely due to operator error). Figure 14 shows no upwind PM_{10} for the October 2 AM pickup operation; this is because the upwind sampler did not run. For the October 2 PM pickup run, the upwind samplers were apparently contaminated and, therefore, not reliable, so no data are shown in Figure 14. On October 3, 10 AM, and 11, the upwind TSP samples were also likely contaminated and, therefore, not used in subsequent calculations.

PM produced by almond harvest operations tends toward larger diameter particles (U. S. EPA, 1985); this being the case concentrations of $PM_{2.5}$ should not vary greatly between the upwind and downwind sampling locations, whereas concentrations of PM_{10} and TSP should be more variable, as was seen in this study. The almond harvest campaign averaged $PM_{2.5}$ downwind concentrations were 107% of those measured upwind; however, many of the upwind and downwind concentrations are within the standard deviation of the mean. The average downwind concentrations of TSP are 140% larger than those upwind. The greater average is likely heavily influenced by the October 2 pickup operation for which there is no upwind data for comparison. A comparison of sample events where there are both upwind and downwind data found that the TSP concentrations are not significantly greater downwind. Downwind PM_{10} concentrations were 102% of those upwind. A potential reason for no significant change in PM_{10} concentrations upwind and downwind is likely high background concentrations of PM_{10} due to operations at neighboring orchards.

Almond harvest emission rates

ISCST3 and AERMOD models were run according to notes in Appendix A. Rows where operations occurred were modeled as area sources. As previously

mentioned, the terrain of interest (sampler locations) surrounding the orchard was flat with no buildings, so terrain and building effects were not of concern in modeling.

Meteorological data, shown in Table 6, were obtained from on-site measurements as needed/available for each model. Insolation data for October 3 were missing due to equipment malfunction. ISCST3 used the stability classes, assigned hourly, to determine atmospheric dispersion. A “seed” emission rate of $50 \mu\text{g s}^{-1} \text{m}^{-2}$ was used for modeling. This often produced modeled concentrations slightly higher than those measured.

The modeled concentrations represent facility produced pollutant. Thus, to compare the modeled concentrations to those determined from the sampler data, the measured background PM concentration needed to be subtracted from the measured downwind concentration results. Ideally, the background PM concentration for each operation was measured by an upwind tower distanced from the operations so as not to be affected by varying wind direction or turbulent eddies created by the operations themselves. For some operations during this campaign, however, background levels could not readily be established in this manner due to higher measured concentrations at upwind locations compared to those at the downwind locations. This is likely a result of contaminated samples.

Table 6. Summary table of meteorological inputs used in ISCST3

Date	Wind Speed m s^{-1}	Wind Direction degrees	Temp $^{\circ}\text{C}$	Humidity %	Insolation W m^{-2}	Pressure kPa	Stability Class	Operation
9/26/2006	3.9	337	23.7	24	422	100.7	C, D	Shaking
10/1/2006	2.4	73	16.7	63	496	100.6	B, C	Sweeping
10/2/2006 AM	1.3	149	16.0	64	249	100.8	E, B	Pickup
10/2/2006 PM	2.5	78	18.8	50	427	100.8	C	Pickup
10/3/2006	3.0	268	20.3	49	-	100.3	D	Mock Sweeping
10/9/2006	5.1	360	28.1	21	532	100.1	C, D	Mock Sweeping
10/10/2006 AM	9.5	344	19.8	24	504	100.4	D	Pickup
10/10/2006 PM	8.8	360	24.0	20	609	100.3	D	Pickup
10/11/2006	4.0	359	25.5	22	613	100.5	C	Mock Sweeping

In these instances, OPC data were used to establish background PM concentrations. For operations on October 2, October 10, and October 11 background samples measured higher PM concentrations than those measured downwind, making the apparent emission rates of PM negative. The OPC time series data were examined for sample periods of interest and an OPC background concentration (OPC_{back}) was found by taking an average of the OPC measured concentrations with any plume events omitted, as shown in Figure 15. A ratio of OPC_{back} and the average OPC measured concentration for the sample period (OPC_{ave}) could then be used to scale the collocated MiniVol concentration (C_{ave}), which would represent the period average PM concentration, to provide a background mass concentration (C_{back}), according to Equation 7. An average of C_{back} values for feasible locations (feasibility was based on ability to separate plume events) could then be used as a background PM concentration in determining facility produced concentrations.

$$C_{back} = C_{ave} \left(\frac{OPC_{back}}{OPC_{ave}} \right) \quad (7)$$

Figure 15 shows a time series of TSP volume concentrations measured with an OPC at tower D9.5 for the October 2 afternoon pickup operation contaminated by a plume event just before 12:30. Including this plume event, the average TSP volume concentration for the pickup operation was $4.83 \times 10^{-5} \text{ cm}^3 \text{ m}^{-3}$. With this plume event omitted the period average volume concentration was $1.45 \times 10^{-5} \text{ cm}^3 \text{ m}^{-3}$. A ratio of these was then multiplied by the measured, filter-based (MiniVol) mass concentration ($159.8 \text{ } \mu\text{g m}^{-3}$), as per Equation 7, to find a background mass concentration of $48.1 \text{ } \mu\text{g m}^{-3}$ for the indicated sampling period. Background PM concentrations were estimated in this manner for October 1, October 2, October 10, and October 11 as shown in Table 7.

ISCST3 modeled concentrations ranged from 0.0 to $441 \mu\text{g m}^{-3}$, with the highest concentrations typically modeled at a height of 2 m on the downwind edge of the orchard. Figure 16 shows an example of ISCST3 modeled concentrations for a mock sweeping sample run on October 9, 2006 with 5.1 m s^{-1} north winds. Emission rates were determined using Equation 5. The average observed-to-modeled concentration ratios calculated for $\text{PM}_{2.5}$, PM_{10} , and TSP were found to be 0.38 ± 0.78 , 1.20 ± 0.97 , and 2.24 ± 1.61 , respectively. Multiplying the average ratio for each operation by the original “seed” emission rate yielded the emission rates found in Table 8. $\text{PM}_{2.5}$ emission rates ranged from 1.8 to $34.9 \mu\text{g s}^{-1} \text{ m}^{-2}$, PM_{10} emission rates ranged from 5.5 to $93.5 \mu\text{g s}^{-1} \text{ m}^{-2}$ and TSP emission rates ranged from 14.6 to $150.8 \mu\text{g s}^{-1} \text{ m}^{-2}$, with pickup operations generally having the highest emission rates.

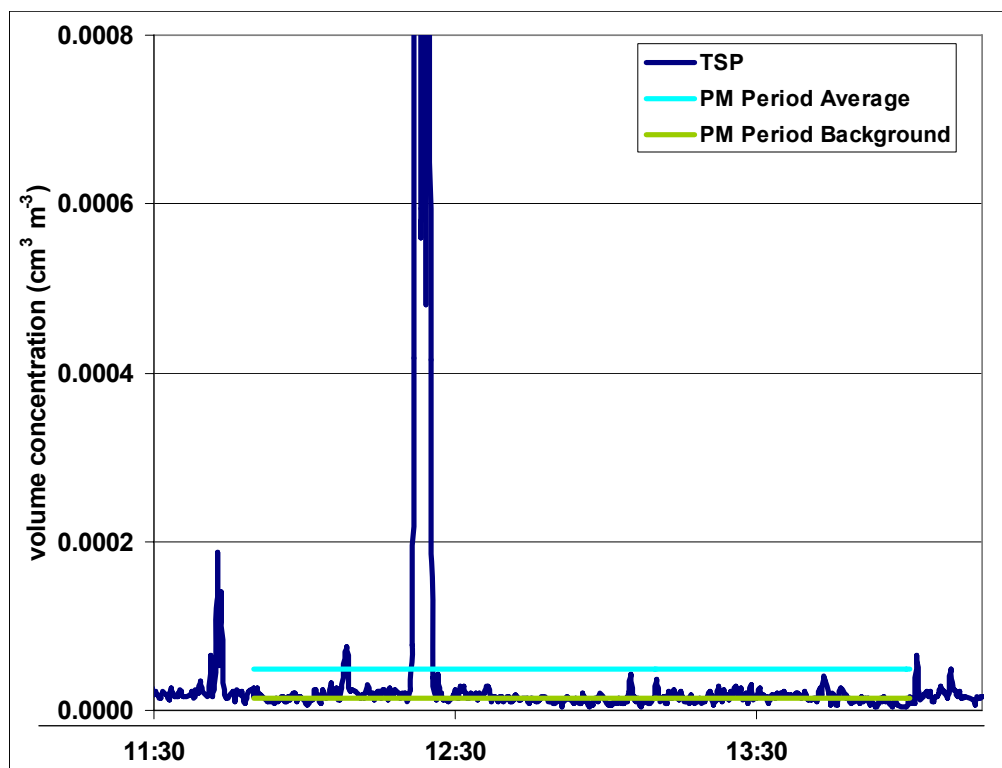


Figure 15. Illustration of background determination using OPC data from sample location D9.5.

Table 7. Estimated (red) and measured (black) PM concentrations upwind and downwind of various almond harvesting operations ($\pm 1\sigma$)

Date		PM _{2.5} $\mu\text{g m}^{-3}$	PM ₁₀ $\mu\text{g m}^{-3}$	TSP $\mu\text{g m}^{-3}$	Orchard Operation
9/26/2006	Upwind	-	47.1	-	Shaking
	Downwind	-	125.2 \pm 24.1	-	
10/1/2006	Upwind	19.6	25.2	145.2	Sweeping
	Downwind	22.8 \pm 3.0	114.0 \pm 50.1	234.2 \pm 125.9	
10/2/2006 AM	Upwind	26.3	42.5	70.0	Pickup
	Downwind	53.2 \pm 23.8	173.0 \pm 98.8	485.9 \pm 147.9	
10/2/2006 PM	Upwind	22.3	27.1	48.1	Pickup
	Downwind	27.6 \pm 0.3	157.6 \pm 174.1	994.6 \pm 1180.1	
10/3/2006	Upwind	-	63.6	-	Mock Sweeping
	Downwind	41.4 \pm 7.0	104.3 \pm 25.7	328.1 \pm 79.2	
10/9/2006	Upwind	27.4	42.2	81.1	Mock Sweeping
	Downwind	38.0 \pm 26.0	86.3 \pm 46.9	142.3 \pm 18.8	
10/10/2006 AM	Upwind	18.3	37.1	151.6	Pickup
	Downwind	25.9 \pm 7.8	80.0 \pm 16.7	482.2	
10/10/2006 PM	Upwind	14.3	22.8	63.1	Pickup
	Downwind	25.4 \pm 4.4	57.0 \pm 8.8	208.1 \pm 19.8	
10/11/2006	Upwind	12.4	25.8	66.3	Mock Sweeping
	Downwind	18.8 \pm 1.2	52.4 \pm 12.1	152.3 \pm 13.2	

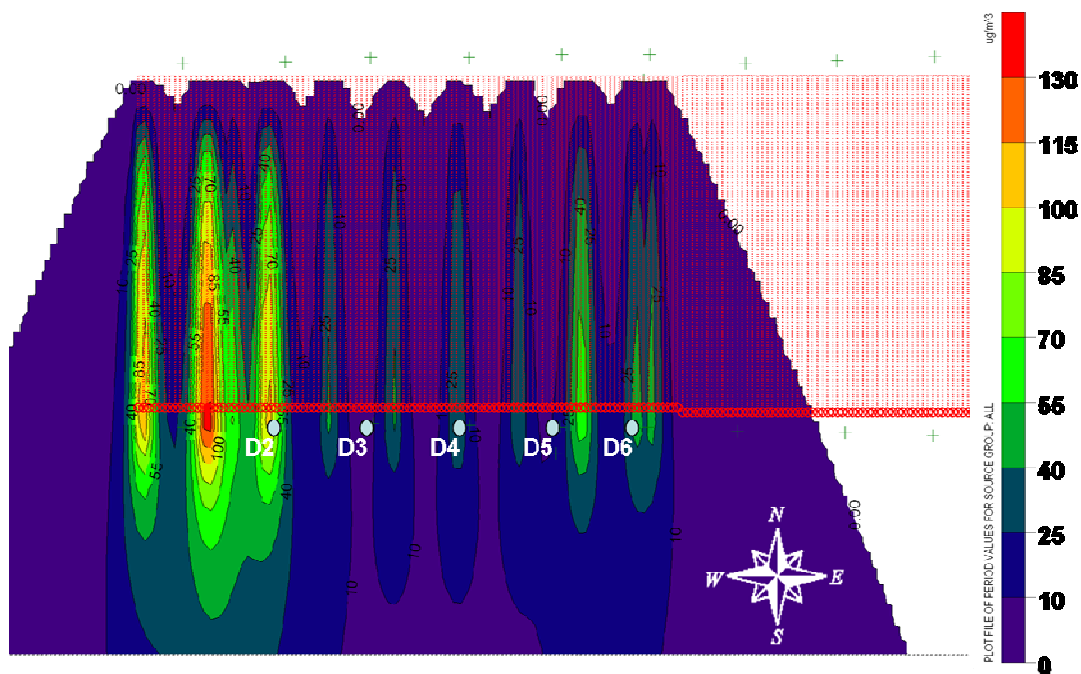


Figure 16. ISCST3 modeled results for mock sweeping operations on October 9, 2006 with north winds. Sampler locations are denoted.

Emission rates for shaking were not determined for PM_{2.5} and TSP because no sampler data were taken for these sizes. For the October 3 mock sweeping operation, emission rates could not be determined for PM_{2.5} and TSP because there were few available MiniVol samplers configured for these size ranges and the wind was consistently out of the east, with this combination the ISCST3 plume missed the sample locations for these sizes. An emission rate for PM₁₀, however, was successfully determined due to the additional number of PM₁₀ samplers which were able to capture the process plume.

Figure 17 shows emission rates from each sample run after normalizing the data presented in Table 8 by the time of each operation and converting the units from $\mu\text{g m}^{-2}$ to kg ha^{-1} . Figure 17 shows a spike in TSP emissions for the pickup run on the morning of October 10th. This is due to the low measured upwind concentration of TSP and the high TSP concentrations measured downwind.

To compare emission rates by operation, individual emission rates were then grouped by operation and averaged. The emission rates determined for each operation are

Table 8. Emission rates for each operation in the almond harvesting process, as determined by inverse modeling using ISCST3

Date	Operation	PM _{2.5} $\mu\text{g s}^{-1} \text{m}^{-2}$	PM ₁₀ $\mu\text{g s}^{-1} \text{m}^{-2}$	TSP $\mu\text{g s}^{-1} \text{m}^{-2}$
9/26/2006	shaking	-	42	-
10/1/2006	sweeping	2.4	48	63
10/2/2006 am	pickup	4.6	24	38
10/2/2006 pm	pickup	7.2	93	146
10/3/2006	mock sweeping	-	82	-
10/9/2006	mock sweeping	21	39	100
10/10/2006 am	pickup	35	67	431
10/10/2006 pm	pickup	20	68	151
10/11/2006	mock sweeping	1.8	5.5	15

shown in Figure 18. The PM₁₀ emission rate for shaking operations was determined to be 3.39 kg ha⁻¹. The emission rates of PM_{2.5}, PM₁₀, and TSP for sweeping operations were 0.81, 4.76 and 7.53 kg ha⁻¹, respectively. The emission rates of PM_{2.5}, PM₁₀, and TSP for pickup operations were 1.73, 6.14 and 19.7 kg ha⁻¹, respectively. Based on these results, the observed almond harvest produced 14.3 kg of PM₁₀, 24% of these emissions occurred during shaking, 33% occurred during sweeping and 43% occurred during pickup. The PM_{2.5} emissions from pickup operations were slightly greater than twice those from sweeping, and the TSP emissions from pickup operations were 2.6 times those from sweeping. The pickup operations produced the most emissions. These results were also compared to the emission rates given by CARB (2003). As seen in Figure 18, CARB provided PM₁₀ emission rates of 0.415 kg ha⁻¹ for shaking, 4.15 kg ha⁻¹ for sweeping and 41.2 kg ha⁻¹ for pickup. Due to the variability of orchard soil type, ground cover, and large variability in harvesting equipment these results are not implausible.

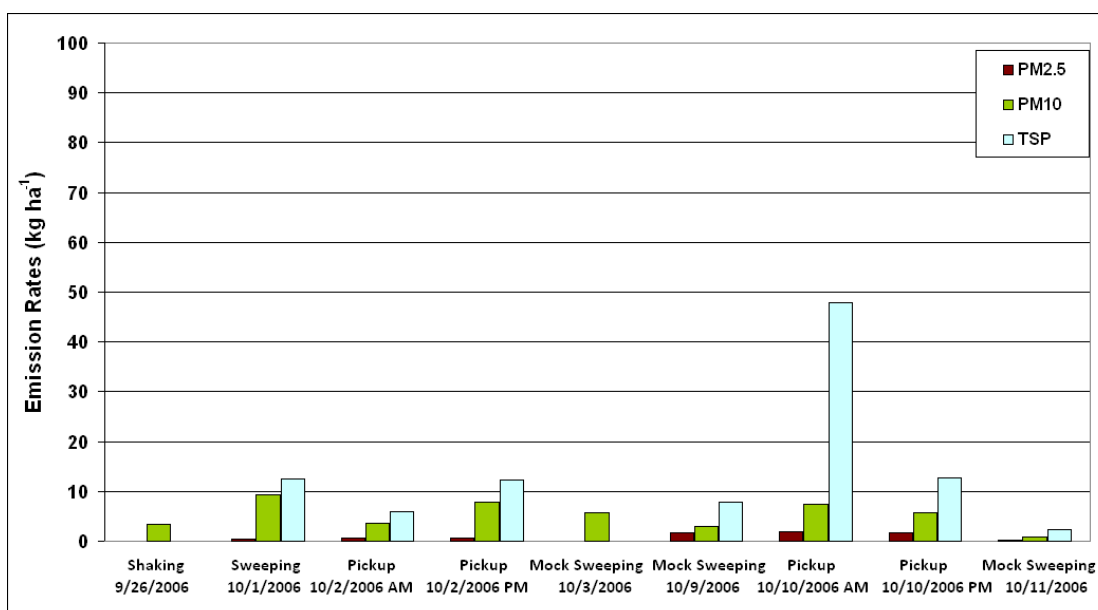


Figure 17. Emission rates determined by inverse modeling using ISCST3 for each day of the almond harvest study.

Using the determined emission rates, a comparison of the measured and modeled concentrations can provide insight to modeled dispersion discrepancies which may be investigated further. Table 9 shows a comparison of the modeled and measured PM₁₀ concentrations for the October 9th sample run after an emission rate was determined using ISC-based inverse modeling. There is relatively good correlation between the modeled and measured PM₁₀ concentrations at the 2 m height as shown in Table 9, which seemingly indicates that the model provided a reasonable approximation of the concentrations near the ground-level point samplers during the mock sweeping on October 9th. Using only 2 m heights the ISCST3 determined emission rate was 24 $\mu\text{g s}^{-1} \text{m}^{-2}$; when including the single elevated sampler located at 9 m, the overall average emission rate changes to 39 $\mu\text{g s}^{-1} \text{m}^{-2}$ and the observed concentration became more than

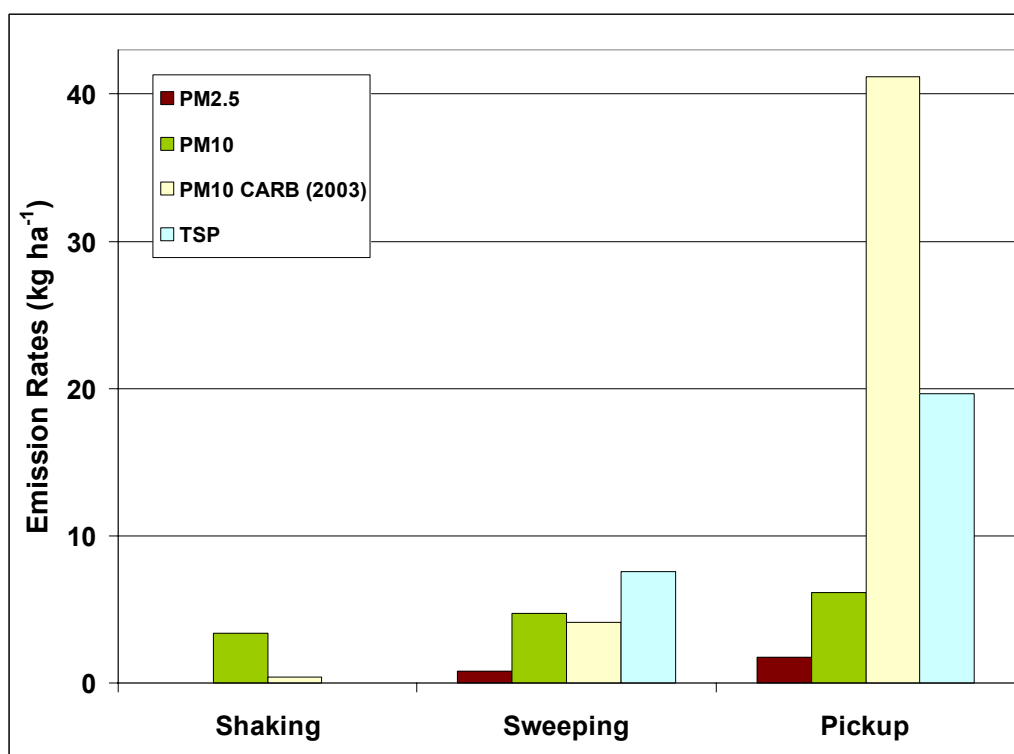


Figure 18. Emission rates for each almond harvest operation determined by inverse modeling using ISCST3 compared with those found by CARB (2003).

twice the modeled concentration at 9 m as shown in Table 9. ISCST3, with assigned stability classes of C and D, predicted concentrations much lower than those measured as elevation increased as evidenced by the given uncertainty. This implies that perhaps for non-bouyant, ground level area sources ISCST3 does not predict vertical dispersion well. Similar results were found by Martin, Moore, and Doshi (2008).

PM concentrations modeled using AERMOD ranged from 0.0 to 661 $\mu\text{g m}^{-3}$. As with ISCST3, the higher concentrations were typically modeled at lower heights downwind of the orchard. An example of AERMOD modeled concentrations for the mock sweeping sample run on October 9, 2006 with 5.1 m s^{-1} north winds is shown in Figure 19. A comparison of Figure 16 and Figure 19 shows that the concentration contours produced by the two models are quite similar, although the absolute concentrations predicted by AERMOD are about 15% lower than those predicted by ISCST3 for the October 9 mock sweeping test run.

The measured-to-modeled ratios for all in-plume locations averaged 0.54 ± 0.71 , 4.4 ± 10.1 , and 5.9 ± 4.0 for $\text{PM}_{2.5}$, PM_{10} , and TSP, respectively. As explained earlier,

Table 9. Comparison of modeled and measured concentrations on October 9, 2006 for each sample location, those at 2 m only were modeled with an ISCST3 determined emission rate of $24 \mu\text{g s}^{-1} \text{m}^{-2}$, while when including all sample locations the model was run with an emission rate of $39 \mu\text{g s}^{-1} \text{m}^{-2}$

Location	PM ₁₀ Concentration in $\mu\text{g m}^{-3}$			Measured-to-modeled ratio	
	Modeled at 24 $\mu\text{g m}^{-2} \text{s}^{-1}$	Modeled at 39 $\mu\text{g m}^{-2} \text{s}^{-1}$	Measured	2 m	all heights
D2 (2 m)	96.9	134.7	139.9	1.44	1.04
D3 (2 m)	9.1	12.7	3.6	0.4	0.28
D4 (2 m)	16.9	23.5	14.2	0.86	0.62
D5 (2 m)	15.7	21.8	23.1	1.47	1.06
D5 (9 m)	-	9.9	23.8	-	2.4
D6 (2 m)	42.8	59.5	35.6	0.83	0.6
Average Ratio				1.0 \pm 0.4	1.0 \pm 0.7

multiplying the average ratio for each operation by the original “seed” emission rate yielded the emission rates found in Table 10. $PM_{2.5}$ emission rates ranged from 1.2 to 38 $\mu\text{g s}^{-1} \text{ m}^{-2}$, PM_{10} emission rates ranged from 10 to 123 $\mu\text{g s}^{-1} \text{ m}^{-2}$, and TSP emission rates ranged from 29 to 563 $\mu\text{g s}^{-1} \text{ m}^{-2}$.

As with ISCST3, AERMOD emission rates for shaking could not be determined for $PM_{2.5}$ and TSP because no sampler data were taken for these sizes. Additionally, the emission rates for the October 2nd PM pickup and the October 3rd mock sweeping operation were omitted because samplers were not impacted by the AERMOD modeled process plume due to easterly winds during these sample runs.

The data presented in Table 10 was then normalized by the time of each operation and the units were converted from $\mu\text{g m}^{-2}$ to kg ha^{-1} . Figure 20 shows the resultant

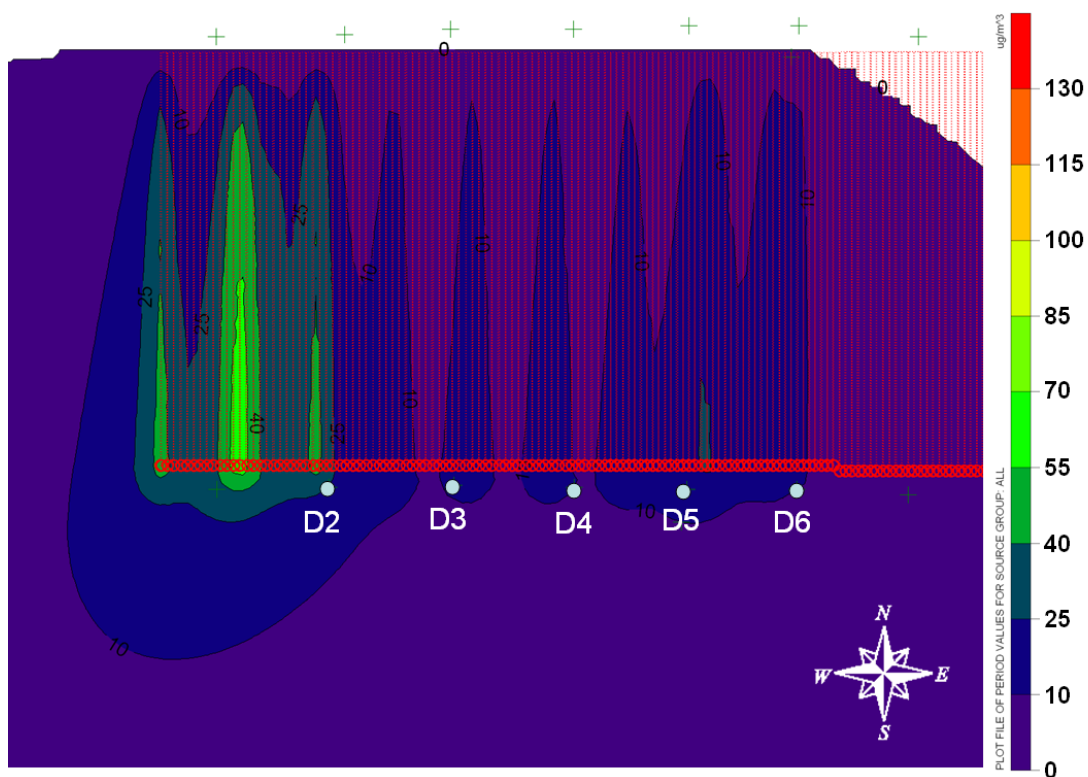


Figure 19. AERMOD modeled results for mock sweeping operations on October 9, 2006 with north winds. Sampler locations are denoted.

emission rates from each sample run. As seen in Figure 20 there is a spike in TSP emissions for the pickup run on the morning of October 10th. This is due to the low measured upwind concentration of TSP and the high TSP concentrations measured downwind.

For comparison, the AERMOD emission rates were grouped and averaged as were the ISCST3 rates. The emission rates determined for each operation are shown in Figure 21. The PM₁₀ emission rate for shaking was found to be 4.38 kg ha⁻¹. The emission rates of PM_{2.5}, PM₁₀, and TSP for sweeping operations were 0.51, 3.68 and 6.41 kg ha⁻¹, respectively. The emission rates of PM_{2.5}, PM₁₀, and TSP for pickup operations were 2.66, 8.81 and 37.2 kg ha⁻¹, respectively. Resultantly, the almond harvest produced 16.9 kg ha⁻¹ of PM₁₀, with 26% of these emissions occurring during shaking, 22% occurring during sweeping and the final 52% occurring during pickup. The PM_{2.5} emissions from pickup operations were 5 times those from sweeping, and the TSP emissions from pickup operations were 5.8 times those from sweeping. The pickup operations produced the most emissions. As with ISCST3, these results were compared to the emission rates determined by CARB (2003) in Figure 21. Again, the differences in

Table 10 . Emission rates for each operation in the almond harvesting process, as determined by inverse modeling using AERMOD

Date	Operation	PM _{2.5} µg s ⁻¹ m ⁻²	PM ₁₀ µg s ⁻¹ m ⁻²	TSP µg s ⁻¹ m ⁻²
9/26/2006	shaking	-	54	-
10/1/2006	sweeping	1.2	26	33
10/2/2006 am	pickup	6.7	33	139
10/2/2006 pm	pickup	-	-	-
10/3/2006	mock sweeping	-	-	-
10/9/2006	mock sweeping	11	56	104
10/10/2006 am	pickup	38	99	563
10/10/2006 pm	pickup	32	123	333
10/11/2006	mock sweeping	2.8	10	29

emissions between the two studies are not implausible due to the variability associated with geography, ground cover, and processing equipment.

When examining AERMOD for PM₁₀ on October 9th, using only the samplers at the 2 m height the determined emission rate was 45 $\mu\text{g s}^{-1} \text{m}^{-2}$, however, including the sampler located at 9 m the emission rate changes to 56 $\mu\text{g s}^{-1} \text{m}^{-2}$ and the measured concentration is only slightly higher at 1.1 times the modeled concentration at 9 m, whereas with ISCST3 the measured concentration was 2.4 times the modeled concentration at that elevation. AERMOD, with a more sophisticated and continuous characterization of the atmosphere, predicted concentrations more similar to those measured than ISCST3 at higher elevations. Apparently, AERMOD is better at predicting the vertical dispersion of non-buoyant, ground level area sources than ISCST3. This was expected, as AERMOD is designed to more accurately characterize the atmosphere.

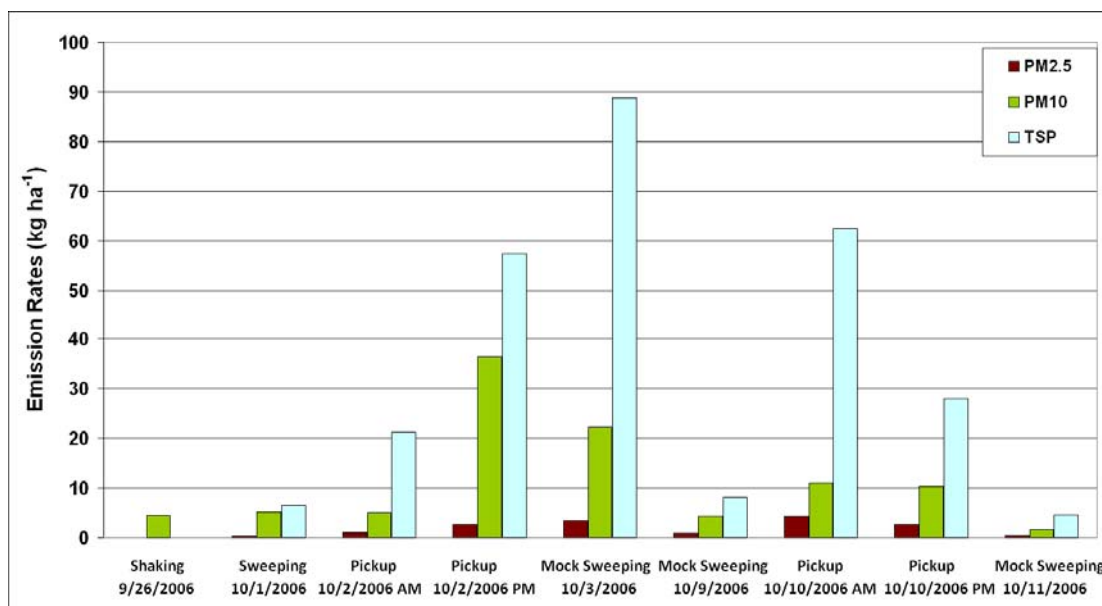


Figure 20. Emission rates determined by inverse modeling using AERMOD for each day of the almond harvest study.

Cotton Gin Results

Measurements of cotton gin emissions were made near Lemoore, California from December 11 to December 14, 2006. The average temperature and barometric pressure during the study were 10.2 °C and 101.99 kPa, respectively. Daily meteorological data are provided in Table 11. The wind direction was variable from day to day and the average wind speed during the study was 2.0 m s⁻¹. Model set up data such as cyclone height, size and exit velocity can be found in Appendix B. Unfortunately, due to equipment failure insolation was not measured by any on-site instruments during this study. Insolation data used as an AERMOD input were taken from the CIMIS station

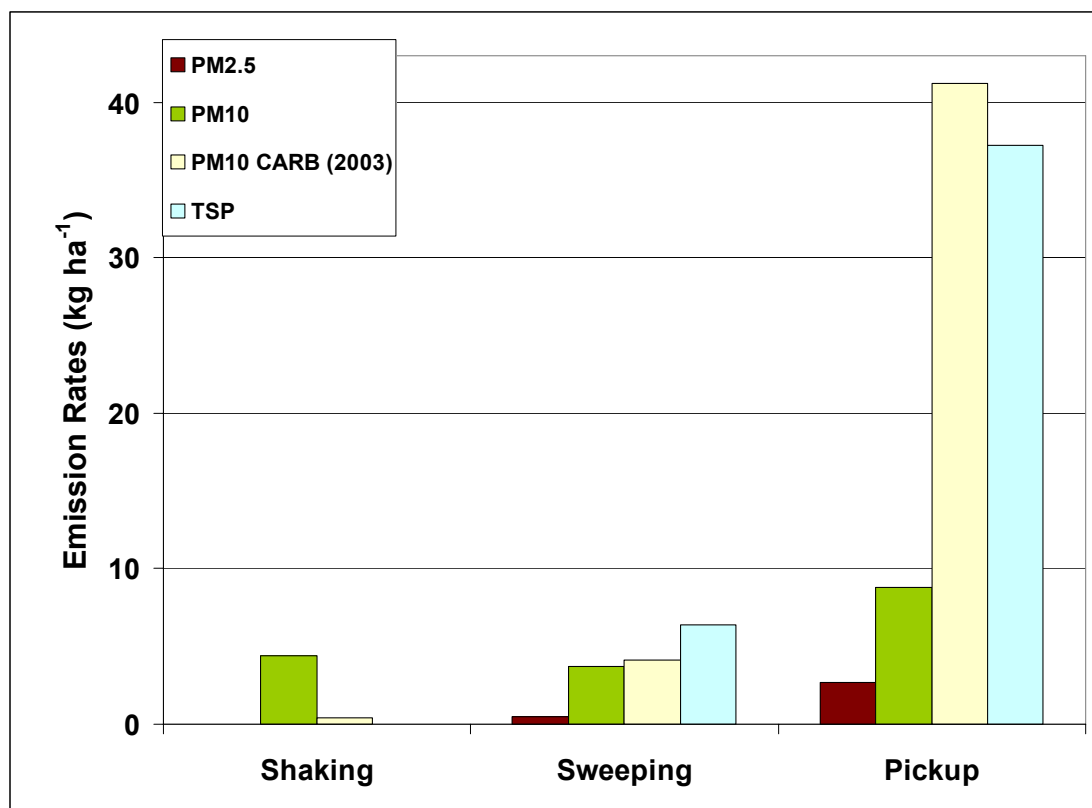


Figure 21. Emission rates for each almond harvest operation determined by inverse modeling using AERMOD compared with those found by CARB (2003).

number 15 located in Stratford, CA which is 10 miles south of Lemoore, CA.

During the study, the average measured PM_{2.5}, PM₁₀, and TSP concentrations were 34.5, 41.9, and 73.3 $\mu\text{g m}^{-3}$, respectively. PM_{2.5} concentrations ranged from 7.9 to 59.8 $\mu\text{g m}^{-3}$, PM₁₀ concentrations ranged from 9.4 to 76.3 $\mu\text{g m}^{-3}$, and TSP concentrations ranged from 16.5 to 110.4 $\mu\text{g m}^{-3}$. As shown in Table 12, December 11, 2006 had the lowest measured PM concentrations and December 14, 2006 had the highest. The high concentrations on the 14th are likely a result of visible plumes resulting from waste material being removed from the cyclones, transported and dumped to temporary storage rows immediately southwest of the seed barn.

In this study, the emission factors for cotton ginning (U. S. EPA, 1985), presented in Table 2, were used as seed emission rate inputs for PM₁₀ and TSP. Emissions data, obtained from CARB Facility Details (see Appendix B), provided a PM_{2.5} emission rate of 2.6 tons year⁻¹. A fan discharge piping summary, obtained from the gin, provided model input such as flow rates, diameters, exit velocities, and number of cyclones in each bank of cyclones in addition to providing a production rate of 20 bales hour⁻¹ (see Appendix B). Processes were assigned to banks of cyclones based on number and grouping of cyclones as that information was not provided by the gin. The emission factors, given in lbs bale⁻¹, and the PM_{2.5} emissions data, given in tons year⁻¹, were

Table 11. Summary table of some meteorological inputs used in modeling

Date	Wind Speed m s ⁻¹	Wind Direction degrees	Temp °C	Humidity %	Insolation W m ⁻²	Pressure kPa	Stability Class
12/11/2006	1.7	140	7.1	91	213	102.3	B, C, D
12/12/2006	2.3	140	10.2	87	219	102.1	C, D
12/13/2006	1.9	118	12.6	81	368	102.1	B, C
12/14/2006	1.3	41	14.6	77	226	101.6	C, B

converted to units of g s^{-1} using the assumption that the gin operates 22 hours daily for 4 months of the year.

Models were run with this input data and example concentration fields are shown in Figure 22b and Figure 23b. These modeled concentrations were then compared with the measured filter-based concentrations as a verification of the emission factors and emissions data, these results are shown in Table 13. The ISCST3 measured-to-modeled ratio ($\pm 1\sigma$) for all days of $\text{PM}_{2.5}$, PM_{10} , and TSP averaged 5.8 ± 5.5 , 1.1 ± 1.3 , and 2.1 ± 2.8 , respectively, while the AERMOD measured-to-modeled ratios of $\text{PM}_{2.5}$, PM_{10} , and TSP for this study averaged 4.5 ± 4.4 , 0.78 ± 1.4 , and 1.1 ± 2.0 , respectively.

While the sample locations were chosen using historical meteorological data to be impacted by the pollutant plume, the sample locations (shown in Figure 22 and Figure 23 as white dots) were not significantly impacted by the pollutant plumes. ISCST3 and

Table 12. PM concentrations measured at the cotton gin

		South Tower		North Tower	
		2 m	9 m	2 m	9 m
		$\mu\text{g m}^{-3}$	$\mu\text{g m}^{-3}$	$\mu\text{g m}^{-3}$	$\mu\text{g m}^{-3}$
11-Dec-06	$\text{PM}_{2.5}$	8.3	7.9	13.7	41.3
	PM_{10}	12.4	9.4	35.5	17.3
	TSP	-	16.5	-	94.4
12-Dec-06	$\text{PM}_{2.5}$	28.9	27.4	59.8	51.8
	PM_{10}	32.5	35.6	52.7	29.8
	TSP	-	59.6	-	83.9
13-Dec-06	$\text{PM}_{2.5}$	30.7	29.2	33.6	34.5
	PM_{10}	31.1	76.3	64.7	53.7
	TSP	-	44.1	-	110.4
14-Dec-06	$\text{PM}_{2.5}$	52.5	-	51.9	46.0
	PM_{10}	-	55.9	65.4	56.2
	TSP	-	71.9	-	105.5

AERMOD both modeled low concentrations, particularly for PM_{2.5} (typically less than 3 µg m⁻³) at the sample sites. Resultantly, the measured-to-modeled ratios varied greatly as seen in Table 13. A ratio of 1.0 would signify that the cotton gin is operating at the specified (for PM_{2.5}) or emission factor (for PM₁₀ and TSP). A ratio of less than 1.0 signifies that the cotton gin is operating below the specified/estimated limit, while a number greater than 1.0 signifies the gin is operating above.

As seen in Table 13, on December 11, all ratios are greater than one; for all other dates the PM₁₀, and TSP ratios are less than one, and the averages for PM₁₀ and TSP are all less than one indicating that the gin is seemingly operating below the specified or estimated (using AP-42) emission rates. In general, the measured-to-modeled PM_{2.5} ratios were larger than 1.0. This could signify that the cotton gin emissions data is not accurate, but there are other likely reasons for this ratio, such as the sample locations were not impacted by the bulk of the plume or the assumptions made about the cotton gin's production or operation schedule were inaccurate. CARB provided emissions data in the Facility Details document (see Appendix B) for PM_{2.5}, PM₁₀, and TSP as 2.6 tons year⁻¹, 9.2 tons year⁻¹, and 18.7 tons year⁻¹, respectively, thus by assuming 22 hour days with 4 months of operation per year the gin emissions for PM_{2.5}, PM₁₀, and TSP are

Table 13. Measured-to-modeled concentration ratios for each day at the cotton gin with ISCST3 and AERMOD ($\pm 1\sigma$)

Date	Measured-to-Modeled Ratio					
	PM _{2.5}		PM ₁₀		TSP	
	ISCST3	AERMOD	ISCST3	AERMOD	ISCST3	AERMOD
12/11/2006	1.04	7.82	3.01	2.94	2.29	4.17
12/12/2006	11.81	8.81	0.51	0.08	0.14	0.02
12/13/2006	1.26	0.58	0.20	0.02	0.13	0.07
12/14/2006	8.95	0.91	0.62	0.08	6.01	0.15
Average	5.8 ± 5.5	4.5 ± 4.4	1.1 ± 1.3	0.78 ± 1.4	2.1 ± 2.8	1.1 ± 2.0

0.24 g s⁻¹, 0.86 g s⁻¹, and 1.8 g s⁻¹, respectively. Using the inverse modeling approach described in this manuscript, emission rates were also determined to compare with these emissions data, the results are shown in Table 14. The average emission rates determined using ISCST3 ($\pm 1\sigma$) for PM_{2.5}, PM₁₀, and TSP were 1.7 \pm 1.4 g s⁻¹, 14.3 \pm 17.0 g s⁻¹, and 27.9 \pm 41.1 g s⁻¹, respectively, and those determined using AERMOD were 0.9 \pm 0.9 g s⁻¹, 10.5 \pm 18.8 g s⁻¹, and 43.0 \pm 79.9 g s⁻¹, respectively.

The average modeled emission rates in Table 14 are at least an order of magnitude greater than the emissions data provided by the cotton gin for PM₁₀ and TSP and nearly an order of magnitude for PM_{2.5}. Emission rates calculated for December 11 were much higher than the emissions data for all size fractions of both models and for PM₁₀, and TSP the determined emission rates on this date are typically an order of magnitude greater than the emission rates determined on the following dates. The emission rates determined using AP-42 emission factors (for PM₁₀ and TSP) were both exceeded on December 11 according to both the ISCST3 and AERMOD. While the measured concentrations were nearly 40% lower on the 11th, the modeled concentrations were an order of magnitude lower for PM₁₀ and TSP on this date, causing the measured-to-

Table 14. Emission rates (g s⁻¹) determined by inverse modeling techniques for the cotton gin, with the emissions data provided by the cotton gin ($\pm 1\sigma$)

Date	PM _{2.5}		PM ₁₀		TSP	
	ISCST3 g s ⁻¹	AERMOD g s ⁻¹	ISCST3 g s ⁻¹	AERMOD g s ⁻¹	ISCST3 g s ⁻¹	AERMOD g s ⁻¹
12/11/2006	0.51	0.80	39.54	38.60	89.38	162.90
12/12/2006	2.88	2.15	6.63	1.06	5.42	0.66
12/13/2006	0.31	0.14	2.65	1.16	5.16	2.77
12/14/2006	2.91	0.30	8.19	1.02	11.71	5.74
Average	1.7 \pm 1.4	0.9 \pm 0.9	14.3 \pm 17.0	10.5 \pm 18.8	27.9 \pm 41.1	43.0 \pm 79.9
Emissions Data	0.24		0.86		1.76	
Emission Factor	-		13.1		39.0	

modeled ratio to be an order of magnitude larger as shown in Table 13. Low modeled concentrations were likely due to meteorological conditions. In Figure 22 both the model and the lidar show the bulk of the pollutant plume missing the sampler locations which is not ideal and can be problematic when taking a ratio of the measured-to-modeled concentrations. Besides the problematic wind direction, the wind speeds were light, there was little insolation, and the atmosphere was relatively stable, with these conditions there would be little dispersion carrying pollutant to the sample locations making these emission rate determinations possibly unreliable. The $PM_{2.5}$ emission rates determined via the inverse modeling approach were all higher than the plant provided emissions data except for the emission rate determined using AERMOD on December 13. Again, this could be a result of problems with the emissions data, or the plume not directly impacting the sample locations.

Figure 22a shows a lidar derived concentration field for the sample run on December 11, 2006. The concentration field was generated by averaging PM concentrations measured by scanning horizontally with the lidar during the sample period. The model uses hourly averaged meteorological data, while the lidar data represents average concentrations collected on time scales of tens of seconds; this would explain some of the differences in detail observed between a and b in Figure 22 and Figure 23; however, the overall patterns in the two figures are very similar. It should be noted that the ISCST3 model (Figure 22b and Figure 23b), does not include background PM, whereas the lidar concentration field (Figure 22a and Figure 23a) implicitly includes both the source and background PM. There was an east wind changing to south during the sample period shown in Figure 22, while for the sample period shown in Figure 23

the winds were predominantly out of the northeast. A visual comparison of the plume patterns on different days, shown in Figure 22 and Figure 23, shows remarkable agreement between the model and results measured using lidar technology. It should also be noted that the point samplers on the towers (shown in Figure 22 and Figure 23 as white dots) were missed by the bulk of the pollutant plumes. This illustrates the limited nature of point sampling and the advantages of lidar technology for PM measurement.

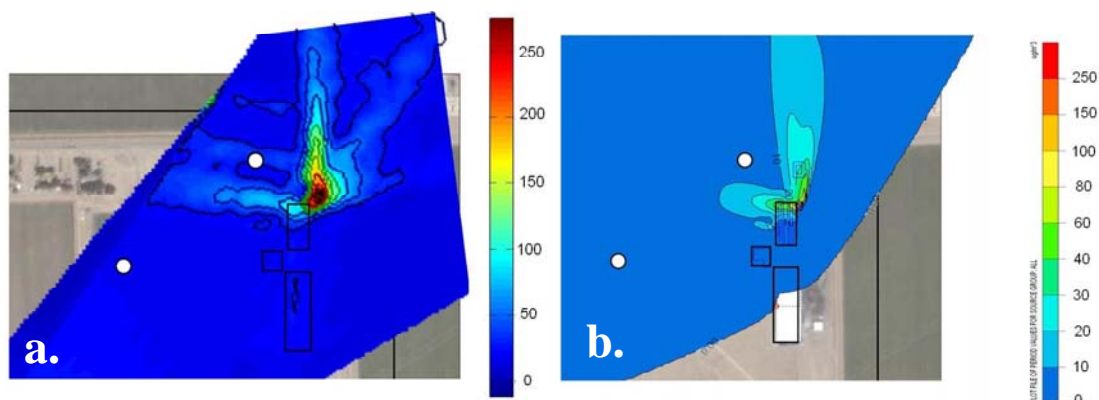


Figure 22. A comparison of lidar (a) and ISCST3 (b) model derived $PM_{2.5}$ concentrations in $\mu\text{g m}^{-3}$ (using emission rates estimated from AP-42) for a cotton gin on December 11, 2006. The model does not include the background aerosol. The white dots are the wind and sampler tower locations.

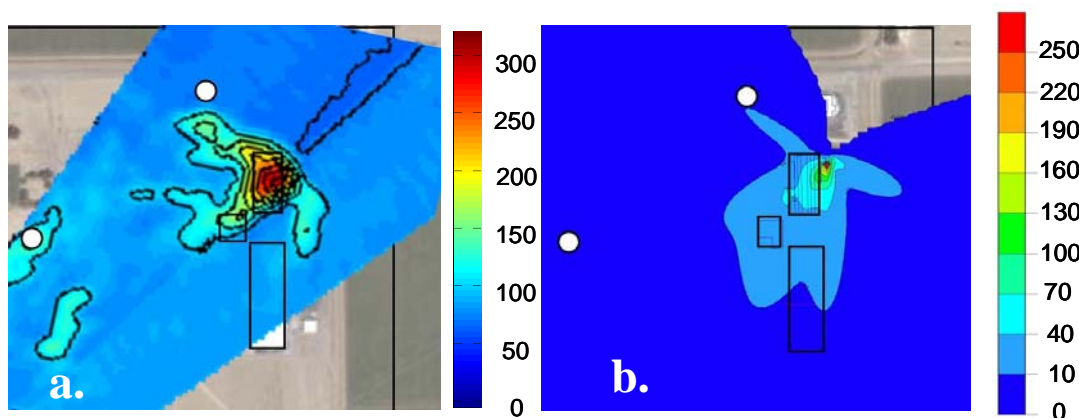


Figure 23. A comparison of lidar (a) and ISCST3 (b) model derived $PM_{2.5}$ concentrations in $\mu\text{g m}^{-3}$ (using emission rates estimated from AP-42) for a cotton gin on December 14, 2006. The model does not include the background aerosol. The white dots are the wind and sampler tower locations.

Based on an understanding of meteorology and local historical data, the best guess point sampler locations were determined. To best quantify and characterize the emitted pollutants samplers need to be in the plume, but due to the complexities of the atmosphere this can be difficult to predict. So while the point samplers were missed by the bulk of the pollutant plume, the lidar was able to adequately quantify the source pollutant distribution.

Tillage Emissions

Measurements of tillage emissions were made near Los Banos, California from October 19 to October 29, 2007. The average temperature and barometric pressure during the study were 23.3 °C and 100.99 kPa, respectively. The wind was predominantly from the north with average wind speeds of 2.3 m s⁻¹.

Tillage PM concentration measurements

An array of AirMetrics MiniVol samplers were positioned to characterize the downwind PM concentrations as well as the background/upwind PM concentrations at the Los Banos tillage site. Observed overall PM_{2.5} concentrations ranged from 5.8 to 52.9 µg m⁻³, PM₁₀ concentrations ranged from 16.3 to 165.3 µg m⁻³, and TSP concentrations ranged from 60.5 to 203.3 µg m⁻³. For each run, samplers that were determined to be upwind or crosswind from the source (tillage site) were treated as local background concentrations and subtracted from the operation-impacted sampler concentrations for emission rate determination using the previously described inverse modeling techniques.

Average upwind/background and downwind/operation-impacted concentrations by operation are shown in Table 15. Background concentrations of PM_{2.5}, PM₁₀ and TSP averaged $28.6 \pm 9.0 \mu\text{g m}^{-3}$, $45.0 \pm 13.3 \mu\text{g m}^{-3}$ and $95.9 \pm 33.4 \mu\text{g m}^{-3}$ and ranged from 18.0 to 41.0 $\mu\text{g m}^{-3}$, 29.8 to 70.5 $\mu\text{g m}^{-3}$ and 60.5 to 157.2 $\mu\text{g m}^{-3}$, respectively.

Uncertainties are represented as the standard deviation. With only one TSP sampler located upwind and one located downwind there is no uncertainty associated with this size fractionation. Concentrations downwind of operations averaged $26.6 \pm 9.9 \mu\text{g m}^{-3}$, $59.0 \pm 9.3 \mu\text{g m}^{-3}$ and $131.9 \pm 58.9 \mu\text{g m}^{-3}$ for PM_{2.5}, PM₁₀ and TSP, respectively, and ranged from 12.3 to 41.4 $\mu\text{g m}^{-3}$ for PM_{2.5}, from 50.0 to 74.8 $\mu\text{g m}^{-3}$ for PM₁₀ and from 62.4 to 203.3 $\mu\text{g m}^{-3}$ for TSP. On average, downwind concentrations of PM_{2.5}, PM₁₀ and TSP were 93%, 131% and 137%, respectively, of those upwind.

As was previously discussed with the almond harvest data, the downwind samplers, theoretically, should always measure higher concentrations than the upwind samplers, with the largest differences correlating with operations producing the most PM. As can be seen in Figure 24, for some operations the average upwind concentrations were higher than those measured downwind. This could be explained by sampler locations not having sufficient stand off distance from the operations or the background location being impacted by nearby sources, such as traffic on dirt roads or other nearby tillage operations. It was observed that at relatively low wind speeds, a tractor passing a sampler location would cause noticeable turbulence; which, in turn, could cause plumes of PM to hit the upwind samplers, if they were not located at a sufficient distance from the operations, regardless of wind direction. Due to the nature of time-averaged sampling, even a single exposure at these potentially high concentrations could

significantly bias the final measured concentrations. As previously discussed, this phenomenon can be verified by inspecting the collocated OPC data. This will be further discussed in the following section.

The mass fraction of each PM size with respect to the measured TSP values for both upwind and downwind samplers for each operation are presented in Table 16 and shown graphically in Figure 24. Upwind TSP was comprised of 35% PM_{2.5} and 57% PM₁₀. Downwind TSP was comprised of 24% PM_{2.5} and 52% PM₁₀. The TSP fractionations along with the relative mass concentrations are shown in Figure 24.

PM produced by agricultural tillage operations tends toward larger diameter particles. According to the U. S. EPA (1985), TSP emissions from agricultural tillage should be typically 21% PM₁₀ and 4.2% PM_{2.5}. This being the case concentrations of PM_{2.5} should not vary greatly between the upwind and downwind sampling locations,

Table 15. Average sampler measured PM concentrations ($\pm 1\sigma$) for each operation upwind and downwind of the tillage site

Date		PM _{2.5} ($\mu\text{g}/\text{m}^3$)	PM ₁₀ ($\mu\text{g}/\text{m}^3$)	TSP ($\mu\text{g}/\text{m}^3$)	Tillage Operation
10/19/2007	Upwind	34.2 \pm 7.4	43.9 \pm 6.7	157.2	Chisel
	Downwind	29.9 \pm 7.0	67.5 \pm 23.9	122.5	
10/20/2007	Upwind	19.0 \pm 5.0	29.8 \pm 2.9	87.0	Optimizer
	Downwind	29.4 \pm 10.8	57.9 \pm 41.3	174.1	
10/23/2007	Upwind	18.0 \pm 1.8	41.4 \pm 4.8	60.5	Disc 1
	Downwind	12.3 \pm 3.1	59.7 \pm 10.8	203.3	
10/25/2007	Upwind	41.0 \pm 10.2	70.5 \pm 17.8	123.6	Chisel
	Downwind	41.4 \pm 6.0	74.8 \pm 25.6	196.0	
10/26/2007	Upwind	28.3 \pm 5.1	39.2 \pm 4.1	84.0	Disc 2
	Downwind	24.6 \pm 4.4	50.0 \pm 20.8	80.5	
10/27/2007	Upwind	23.2 \pm 2.8	37.2 \pm 14.6	70.2	Disc 3
	Downwind	16.5 \pm 5.9	50.7 \pm 26.1	84.3	
10/29/2007	Upwind	36.5 \pm 4.7	53.2 \pm 7.2	89.1	Land Plane
	Downwind	32.3 \pm 6.8	52.3 \pm 13.0	62.4	

whereas concentrations of PM₁₀ and TSP should be more variable, as seen in this study. The campaign averaged PM_{2.5} downwind concentrations are 93% of those measured upwind, as previously mentioned, however many of the upwind and downwind concentrations are within the standard deviation of the mean. The average downwind concentrations of PM₁₀ and TSP are generally significantly larger, 131% and 137%, respectively, of those upwind. A comparison of the upwind to the downwind concentrations in Figure 24 illustrates this.

Tillage emission rates

Using GPS devices located in the lead tractor, the tillage area for each operation was defined and modeled as an area source with both ISCST3 and AERMOD dispersion models. The terrain surrounding the tillage site was flat with no surrounding buildings, so terrain and building features were not used in modeling. On-site meteorological data, shown in Table 17, were compiled as needed/available for each model. As previously

Table 16. Fraction of TSP that is PM_{2.5} and PM₁₀ for each operation upwind and downwind of the tillage site, and campaign averages upwind and downwind ($\pm 1\sigma$)

Date	Upwind		Downwind		Operation
	PM _{2.5} /TSP	PM ₁₀ /TSP	PM _{2.5} /TSP	PM ₁₀ /TSP	
10/19/2007	0.50 ± 0.11	0.64 ± 0.10	0.24 ± 0.06	0.55 ± 0.20	Chisel
10/20/2007	0.21 ± 0.04	0.34 ± 0.03	0.17 ± 0.06	0.33 ± 0.24	Optimizer
10/23/2007	0.28 ± 0.01	0.68 ± 0.08	0.06 ± 0.02	0.29 ± 0.5	Disc 1
10/25/2007	0.31 ± 0.07	0.57 ± 0.14	0.21 ± 0.03	0.38 ± 0.13	Chisel
10/26/2007	0.32 ± 0.07	0.47 ± 0.05	0.31 ± 0.06	0.62 ± 0.26	Disc 2
10/27/2007	0.31 ± 0.04	0.53 ± 0.21	0.20 ± 0.07	0.60 ± 0.31	Disc 3
10/29/2007	0.50 ± 0.07	0.76 ± 0.10	0.52 ± 0.11	0.84 ± 0.21	Land Plane
	Average Upwind		Average Downwind		
	0.35 ± 0.12	0.57 ± 0.17	0.24 ± 0.15	0.52 ± 0.27	

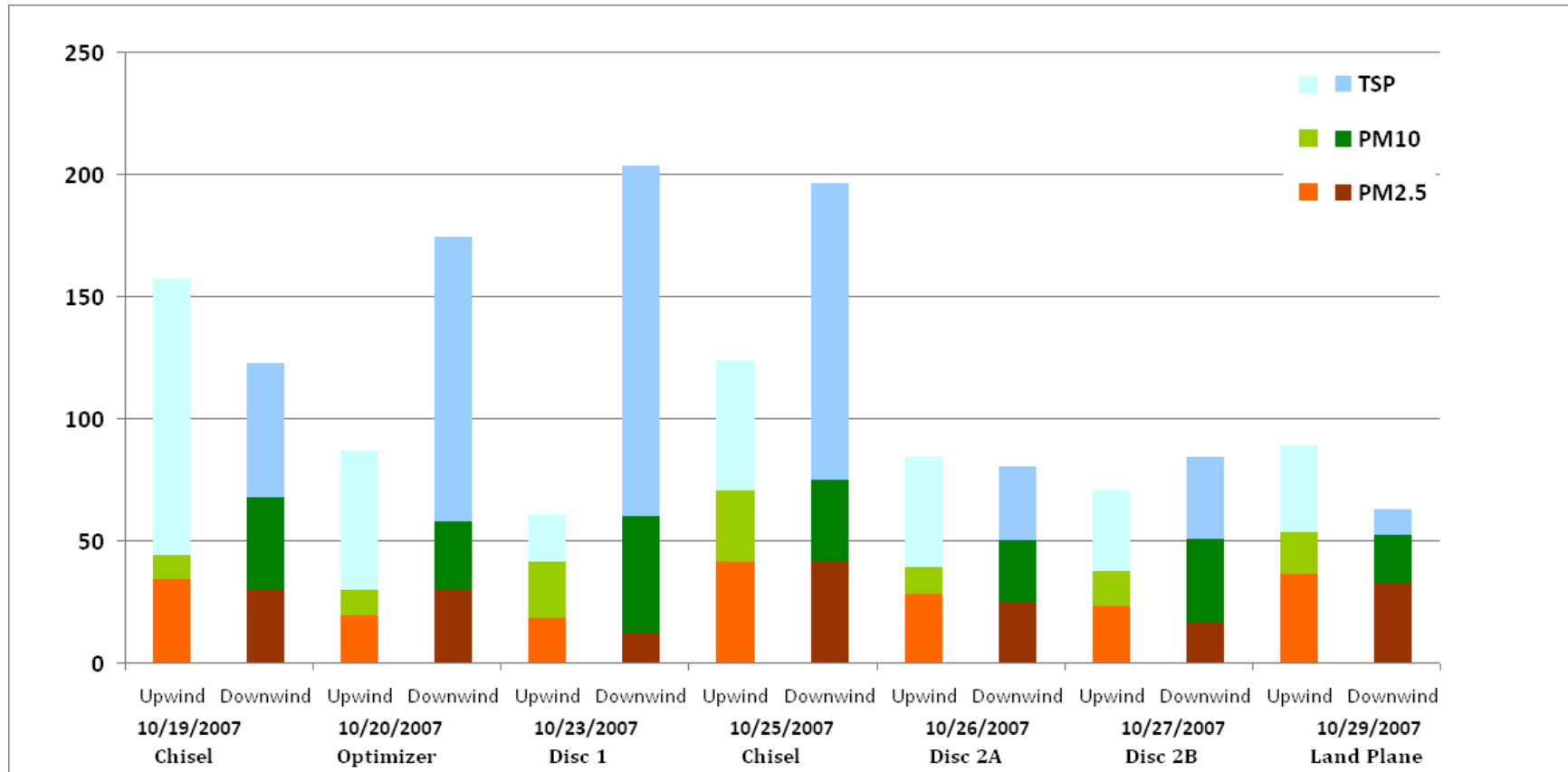


Figure 24. Average measured upwind and downwind PM concentrations with the particle size contributions to the total PM for the tillage operations.

mentioned a stability class was assigned for each hour of operations. The seed emission rate of $50 \mu\text{g s}^{-1} \text{m}^{-2}$ was calculated using Equation 2 for TSP, assuming soil with 50% silt content and a sample run time of 2 hours. This often produced modeled concentrations higher than those measured, but they were generally within an order of magnitude.

Facility-produced pollutant was determined by subtracting the upwind PM concentration (background) from the downwind PM concentration. For some operations during this campaign, however, reliable background levels could not be established in this manner due to higher measured concentrations at background locations than downwind locations. This was likely a result of contaminated samples. Again, OPC data were used to establish background PM concentrations, as described earlier, for the optimizer chisel pass, disc pass 1, disc pass 2B, and the land plane operations because background samples had higher concentrations than those measured downwind, making emission rates of PM negative. The concentrations, estimated (red) and measured (black) are presented in Table 18, and then shown in Figure 25.

ISCST3 modeled concentrations ranged from 0.0 to $663 \mu\text{g m}^{-3}$, with the highest concentrations typically modeled at a height of 2 m on the southern edge of the tillage sites, although this varied slightly with shifting wind directions. Figure 26 shows an

Table 17. Summary table of meteorological inputs used in ISCST3

Date	Wind Speed m s^{-1}	Wind Direction degrees	Temp $^{\circ}\text{C}$	Humidity %	Insolation W m^{-2}	Pressure kPa	Stability Class	Operation
10/19/2007	1.1	76	20.6	56	556	101.1	B, A	Chisel
10/20/2007	6.7	305	16.6	54	485	101.3	D	Optimizer
10/23/2007	1.6	316	26.1	24	457	101.5	B, A	Disc 1
10/25/2007	1.5	2	27.3	30	395	100.4	A, B	Chisel
10/26/2007	2.9	302	22.0	38	506	100.4	B	Disc 2A
10/27/2007	3.1	30	22.7	36	508	101.1	B, A	Disc 2B
10/29/2007	1.7	49	23.5	50	525	101.1	A, B	Land Plane

example of ISCST3 modeled concentrations for a disc pass as part of the conventional tillage operations with 1.6 m s^{-1} north winds.

Emission rates were determined using Equation 5. The ratios of measured and modeled concentrations at the southern edge of the tillage site were very similar; however, at other locations, depending on wind direction, the modeled concentrations dropped off much more quickly than the measured concentration values, resulting in very large measured-to-modeled concentration ratios. The overall measured-to-modeled ratios using all sampling locations were -18 ± 360 ; $6,300 \pm 49,000$; and 24 ± 51 for $\text{PM}_{2.5}$, PM_{10} , and TSP, respectively. These ratios can easily be very large and inconsistent near the borders of the PM plume because here the model is predicting very small

Table 18. Estimated (red) and measured (black) PM concentrations upwind and downwind of various tillage operations ($\pm 1\sigma$)

Date		PM _{2.5} ($\mu\text{g m}^{-3}$)	PM ₁₀ ($\mu\text{g m}^{-3}$)	TSP ($\mu\text{g m}^{-3}$)	Tillage Operation
10/19/2007	Upwind	28.0 \pm 0.40	38.5 \pm 2.7	68.9	Chisel
	Downwind	25.7 \pm 1.8	65.1 \pm 11.3	122.5	
10/20/2007	Upwind	17.9 \pm 1.8	28.0 \pm 2.1	87.0	Optimizer
	Downwind	27.8 \pm 5.3	41.9 \pm 6.4	174.1	
10/23/2007	Upwind	15.5 \pm 0.8	40.0 \pm 3.0	60.5	Disc 1
	Downwind	11.7 \pm 1.2	62.9 \pm 3.0	203.3	
10/25/2007	Upwind	38.6 \pm 3.5	70.5 \pm 10.0	123.6	Chisel
	Downwind	41.4 \pm 2.1	78.2 \pm 7.9	196.0	
10/26/2007	Upwind	24.3 \pm 2.0	39.2 \pm 2.3	84.0	Disc 2
	Downwind	26.7 \pm 2.0	54.7 \pm 7.4	-	
10/27/2007	Upwind	15.6 \pm 2.2	37.2 \pm 7.1	70.2	Disc 3
	Downwind	20.4 \pm 2.6	62.2 \pm 9.6	84.3	
10/29/2007	Upwind	32.8 \pm 2.3	49.1 \pm 2.0	70.0	Land Plane
	Downwind	32.1 \pm 1.7	60.7 \pm 3.9	62.4	

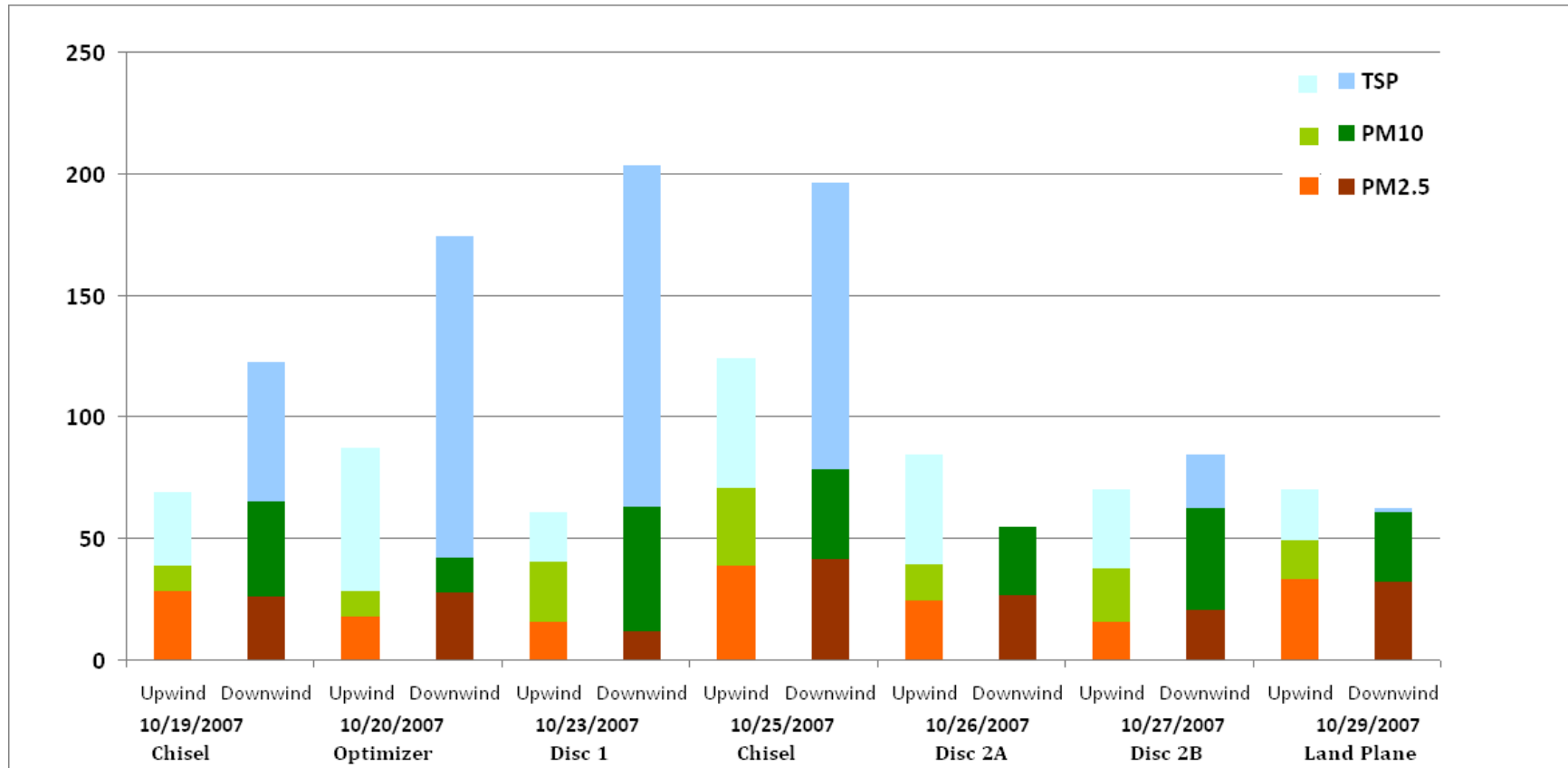


Figure 25. Edited average measured upwind and downwind PM concentrations with the particle size contributions to the total PM for the tillage operations.

concentrations. For example, during the ISCST3 run for the October 27 Disc 2B the model predicted a very low concentration of $0.0014 \mu\text{g m}^{-3}$ at sample location U2 while the observed concentration was $5.3 \mu\text{g m}^{-3}$. This would give a measured-to-modeled ratio of approximately 3,604. This large ratio will significantly affect the average emission rate.

Arya (1998) suggests that the plume edge be defined as 10 percent of the maximum modeled concentration or 2.15σ . Defining the edges of the plume in this manner and using only the ratios calculated for the in-plume locations, the average ratios for measured-to-modeled $\text{PM}_{2.5}$, PM_{10} , and TSP concentrations were found to be 0.035 ± 0.067 , 0.096 ± 0.12 , and 0.38 ± 0.20 , respectively, with the uncertainty represented by the standard deviation. Multiplying the average ratio for each operation by the original

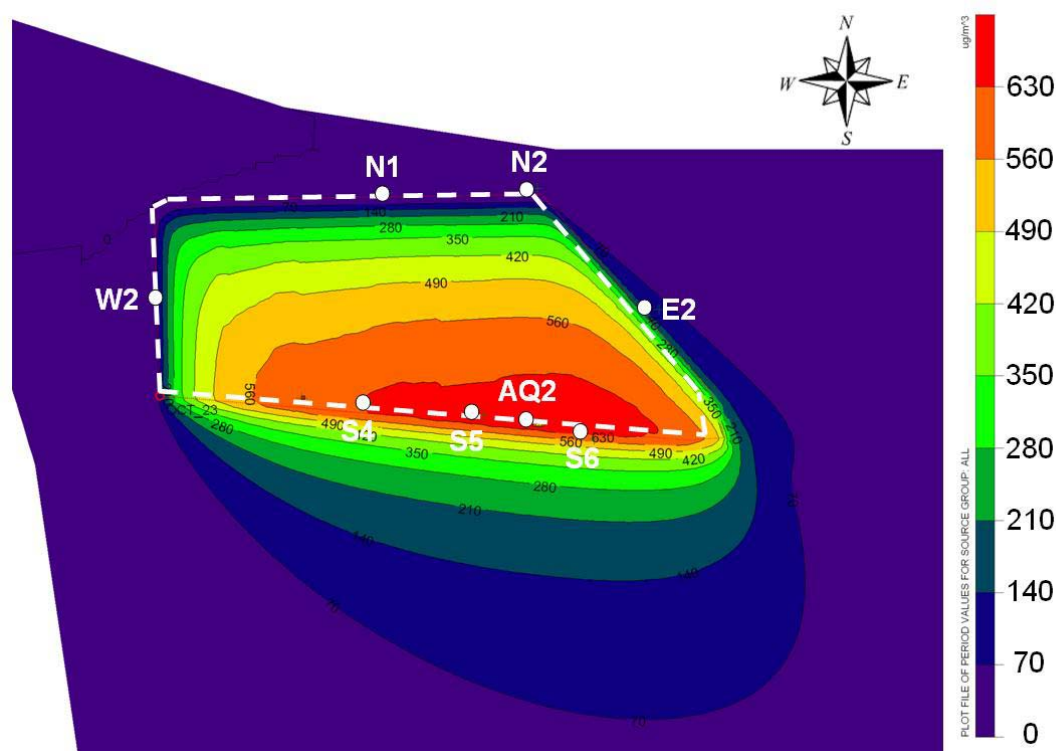


Figure 26. ISCST3 modeled results for a disc pass of the conventional tillage operations on October 23, 2008 with light north winds. The area of operations and sampler locations are denoted in white.

“seed” emission rate yielded the emission rates presented in Figure 27. $PM_{2.5}$ emission rates ranged from 0.23 to 5.3 $\mu\text{g s}^{-1} \text{m}^{-2}$, PM_{10} emission rates ranged from 2.4 to 9.6 $\mu\text{g s}^{-1} \text{m}^{-2}$, and TSP emission rates ranged from 11.8 to 30.6 $\mu\text{g s}^{-1} \text{m}^{-2}$.

TSP emission rates for disc pass 2A and for the land plane operations were not calculated in this manner due to the upwind TSP samples reporting higher concentrations than the downwind samples, with just one TSP sample per day for upwind and downwind. The more conservative TSP emission rate for other discing operations (1.68 $\text{E-5 g s}^{-1} \text{m}^{-2}$) was assigned to Disc pass 2A for use in subsequent calculations. For the land plane operation, no supporting data were available, and to be conservative the PM_{10} emission rate was also assigned as the TSP emission rate. Figure 27 shows the emission rates determined, or assigned, for each operation. As can be derived from Figure 27, TSP emission rates are roughly four times those for PM_{10} , and the PM_{10} emission rates are roughly 8 times those determined for $PM_{2.5}$.

The emission rates were then normalized by the time of operations, converting to units of mass emitted per unit area. During the sample runs there were times when either multiple tractors were operating, or the tractors were stopped due to equipment malfunction or for a lunch break. To accurately characterize the emissions, the emission rates in units of mass per area were further multiplied by the ratio of sample time to tractor time in order to represent the mass of emissions per unit area each tractor contributed (see Table 19). This then allowed comparison to literature and allowed the emissions for each of the days to be summed and to compare the conventional and combined tillage practices.

The mass of PM emitted per unit area of the individual operations was then summed to provide total mass emitted from the combined and conventional tillage operations. Combined operations produced a total ($\pm 1\sigma$) of 0.04 ± 0.06 (0.15 ± 0.24), 0.11 ± 0.04 (0.44 ± 0.17), and 0.36 (1.44) g m^{-2} (kg acre^{-1}) of $\text{PM}_{2.5}$, PM_{10} , TSP, respectively, while the conventional tillage operations produced a total of 0.12 ± 0.52 (0.47 ± 2.10), 0.28 ± 0.06 (1.11 ± 0.23), and 0.85 (3.43) g m^{-2} (kg acre^{-1}) of $\text{PM}_{2.5}$, PM_{10} , TSP, respectively, as shown in Figure 28. These results suggest that the combined operations produced about 40% as much PM_{10} and TSP as the conventional operations and 30 percent of the $\text{PM}_{2.5}$.

Concentrations modeled using AERMOD ranged from 0.0 to $421 \mu\text{g m}^{-3}$, as with the ISCST3 runs the higher concentrations typically modeled at lower elevations on the southern edge of the tillage sites depending on the wind direction which shifted slightly

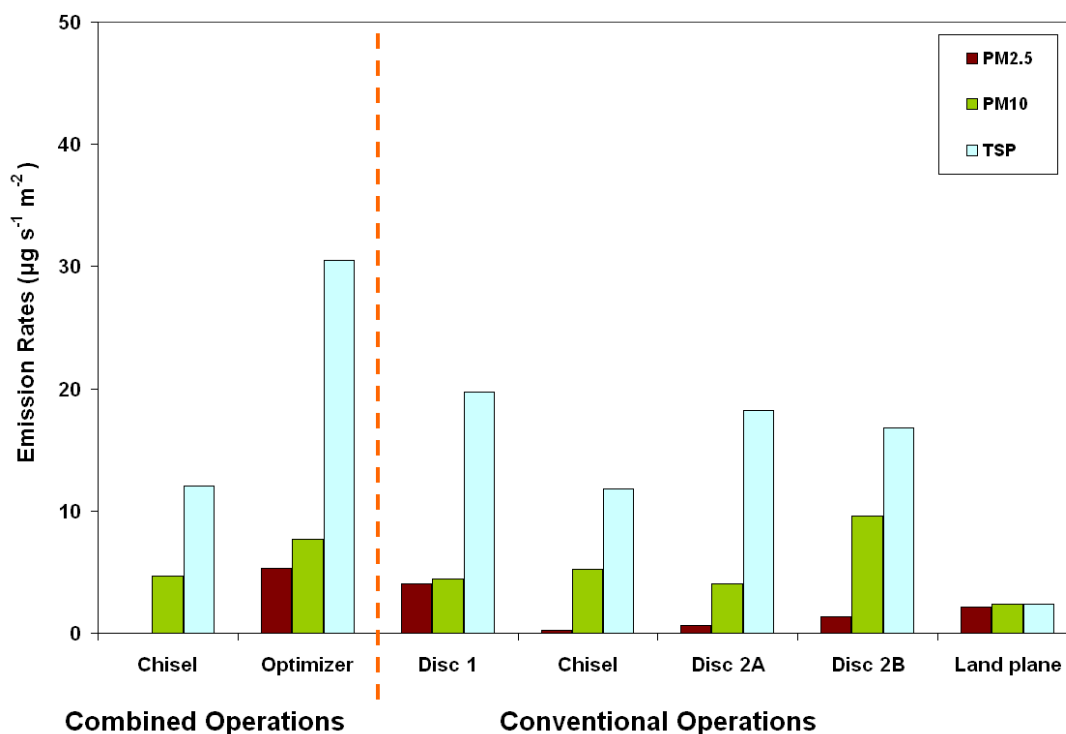


Figure 27. ISCST3 emission rates for each operation

over the course of the study. Figure 29 shows an example of AERMOD modeled concentrations for the same disc pass shown in Figure 26. As can be seen, the concentration contours produced by the two models are quite similar, although the absolute concentrations for the October 23 disc pass predicted by AERMOD are about 59% of those predicted by ISCST3.

Table 19. Emission rates for each operation determined by inverse modeling using ISCST3

Date	Operation	PM _{2.5} g m ⁻²	PM ₁₀ g m ⁻²	TSP g m ⁻²
19-Oct	Chisel	-	0.06	0.15
20-Oct	Optimizer	0.04	0.05	0.21
23-Oct	Disc 1	0.07	0.08	0.34
25-Oct	Chisel	0.00	0.05	0.12
26-Oct	Disc 2A	0.02	0.13	0.54
27-Oct	Disc 2B	0.01	0.10	0.18
29-Oct	Land plane	0.03	0.03	0.03

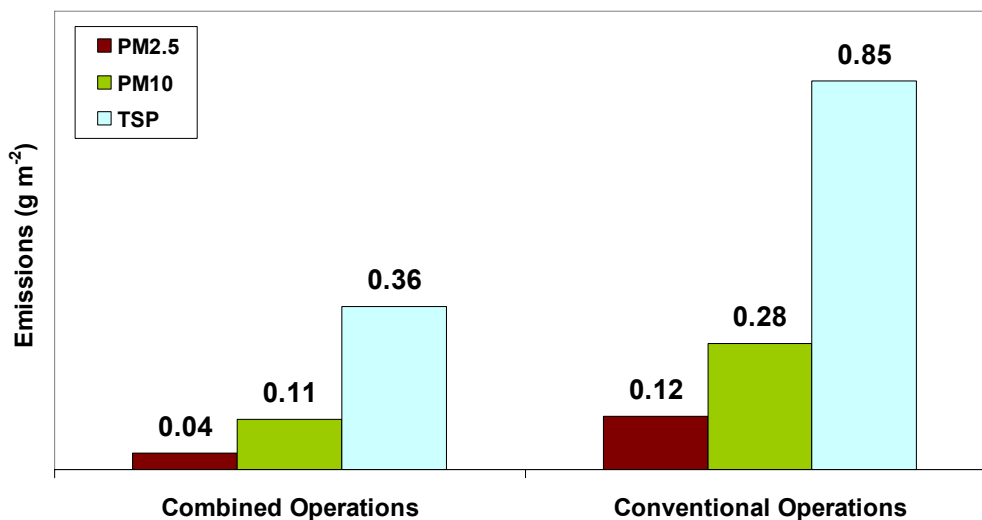


Figure 28. PM emissions (g m⁻²) of combined and conventional tillage operations for PM_{2.5}, PM₁₀, and TSP determined using ISCST3.

As with the previous model, AERMOD emission rates were determined using the inverse modeling techniques. The plume edge was again defined as 10% of the maximum modeled concentration and only the ratios calculated for the sample locations impacted by the plume were used. The average measured-to-modeled ratios during the study for $PM_{2.5}$, PM_{10} , and TSP were 0.059 ± 0.111 , 0.16 ± 0.20 , and 0.65 ± 0.29 , respectively, with the uncertainty represented by one standard deviation. The average ratio for each operation was multiplied by the original “seed” emission rate yielding the emission rates shown in Figure 30. $PM_{2.5}$ emission rates ranged from 0.30 to $6.1 \mu g s^{-1} m^{-2}$, PM_{10} emission rates ranged from 1.9 to $8.8 \mu g s^{-1} m^{-2}$, and TSP emission rates ranged from 9.4 to $46.5 \mu g s^{-1} m^{-2}$.

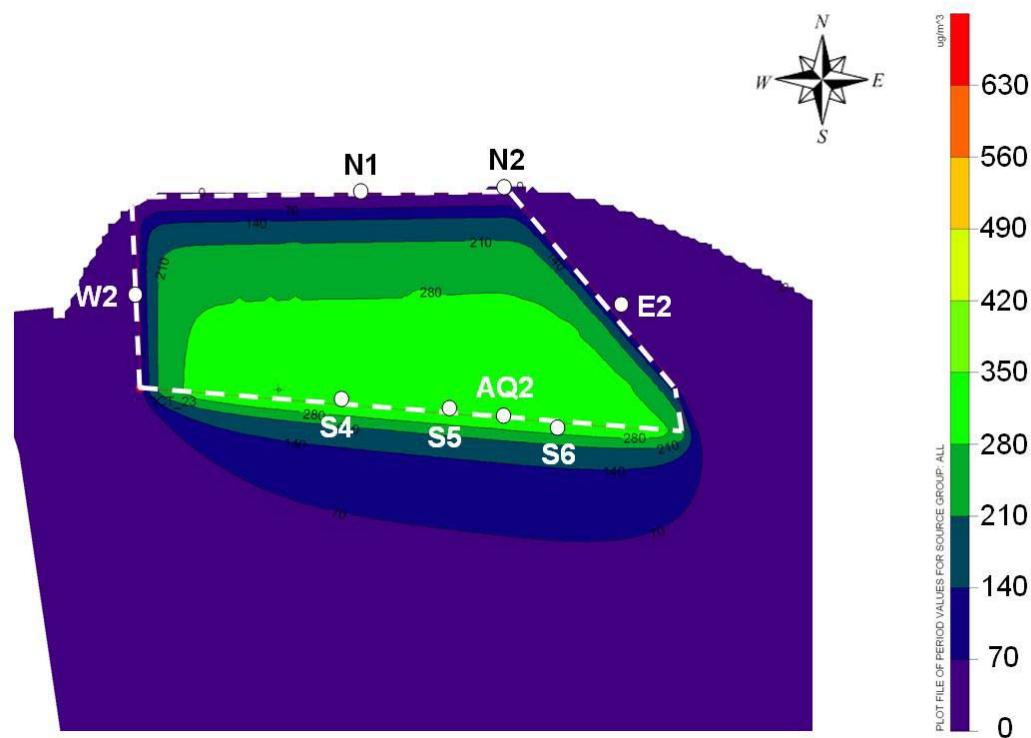


Figure 29. AERMOD modeled results for a disc pass of the conventional tillage operations on October 23, 2007 with light north winds. The area of operations and sampler locations are denoted in white.

TSP emission rates for disc pass 2A and for the land plane operations were not calculated for reasons described in the previous section, but were similarly estimated for use in subsequent calculations. Figure 30 shows the emission rates determined, or assigned, for each operation. As illustrated by Figure 30, TSP emission rates were found to be roughly four times those for PM_{10} and the PM_{10} emission rates were roughly nine times those determined for $PM_{2.5}$.

As with the ISCST3 emission rates, to compare combined and conventional operations, the AERMOD emission rates of individual operations were normalized by the operation time and multiplied by the ratio of sample time to tractor time, shown in Table 20. The mass of PM emitted by the individual operations were then summed to provide total mass emitted from the combined and conventional tillage operations. Combined operations produced a total ($\pm 1\sigma$) of 0.04 ± 0.07 (0.17 ± 0.27), 0.16 ± 0.06 (0.66 ± 0.25), and 0.51 (2.1) $g\ m^{-2}$ ($kg\ acre^{-1}$) of $PM_{2.5}$, PM_{10} , TSP, respectively, while the conventional tillage operations produced a total of 0.04 ± 0.06 (0.18 ± 0.26), 0.29 ± 0.06 (1.2 ± 0.24), and 1.3 (5.1) $g\ m^{-2}$ ($kg\ acre^{-1}$) of $PM_{2.5}$, PM_{10} , TSP, respectively, as shown in Figure 31. These results suggest that, for total mass, the combined operations produced 95% as much $PM_{2.5}$, 57% as much PM_{10} , and 41% as much TSP as the conventional operations.

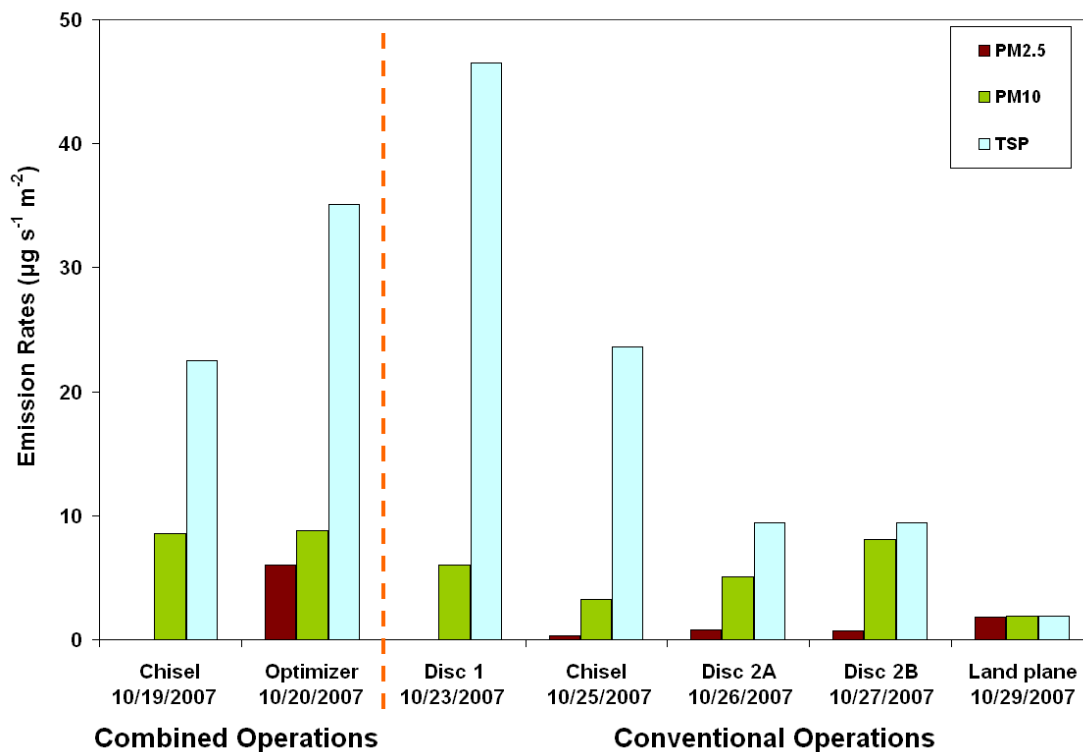


Figure 30. Emission rates for each operation determined by inverse modeling using AERMOD.

Table 20. Emission rates for each operation determined by inverse modeling using AERMOD

Date	Operation	PM _{2.5} g m ⁻²	PM ₁₀ g m ⁻²	TSP g m ⁻²
19-Oct	Chisel	-	0.10	0.27
20-Oct	Optimizer	0.04	0.06	0.24
23-Oct	Disc 1	-	0.10	0.80
25-Oct	Chisel	0.00	0.03	0.24
26-Oct	Disc 2A	0.03	0.16	0.30
27-Oct	Disc 2B	0.01	0.08	0.10
29-Oct	Land plane	0.02	0.03	0.03

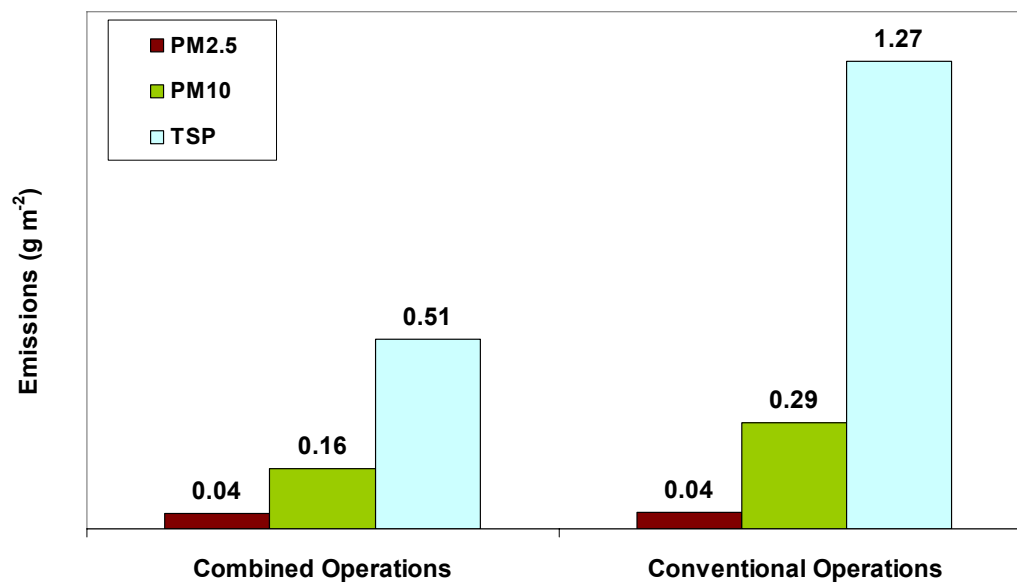


Figure 31. PM emissions (g m^{-2}) of combined and conventional tillage operations for $\text{PM}_{2.5}$, PM_{10} , and TSP determined using AERMOD.

SUMMARY AND CONCLUSIONS

In this study, inverse modeling techniques, described herein, along with the U. S. EPA approved dispersion models ISCST3 and AERMOD were used to determine emission rates from almond harvest, cotton gin, and land tilling agricultural processes. This methodology proved to be a reasonable and seemingly valid approach for determining particulate emissions from each process examined.

Almond Harvest Conclusions

The harvesting operations of an almond orchard, measuring nearly 230 m by 700 m and containing approximately 3850 almond trees, were studied from late September into October in 2006. Three processes were examined as part of the almond harvest: shaking, sweeping, and pickup. The overall emission rates ($\pm 1\sigma$) determined using ISCST3 for each of these operations were, see Figure 32, 3.4 kg of $\text{PM}_{10} \text{ ha}^{-1}$ for shaking; $0.81 \pm 0.76 \text{ kg of } \text{PM}_{2.5} \text{ ha}^{-1}$, $4.8 \pm 3.7 \text{ kg of } \text{PM}_{10} \text{ ha}^{-1}$, and $7.5 \pm 5.1 \text{ kg of TSP ha}^{-1}$ for sweeping, and $1.7 \pm 1.5 \text{ kg of } \text{PM}_{2.5} \text{ ha}^{-1}$, $6.1 \pm 1.9 \text{ kg of } \text{PM}_{10} \text{ ha}^{-1}$, and $10.3 \pm 3.8 \text{ kg of TSP ha}^{-1}$ for pickup. The overall emission rates determined using AERMOD for each operation were 4.4 kg of $\text{PM}_{10} \text{ ha}^{-1}$ for shaking, $1.3 \pm 1.5 \text{ kg of } \text{PM}_{2.5} \text{ ha}^{-1}$, $8.3 \pm 9.4 \text{ kg of } \text{PM}_{10} \text{ ha}^{-1}$, and $27.0 \pm 41.2 \text{ kg of TSP ha}^{-1}$ for sweeping, and $2.7 \pm 1.3 \text{ kg of } \text{PM}_{2.5} \text{ ha}^{-1}$, $15.7 \pm 14.1 \text{ kg of } \text{PM}_{10} \text{ ha}^{-1}$, and $42.3 \pm 20.7 \text{ kg of TSP ha}^{-1}$ for pickup. The PM_{10} emission rates determined in this study can be compared to those provided by CARB (2003). The CARB PM_{10} emission rate for shaking was 0.415 kg ha^{-1} , while the PM_{10} emission rates determined in this study for shaking were 3.4 kg ha^{-1} using ISCST3, and 4.4 kg ha^{-1} using AERMOD. Both rates determined in this study are an order of

magnitude higher than those provided by CARB; however, this difference is not implausible due to variability of equipment and ground cover from orchard to orchard. CARB reported an emission rate of 4.15 kg ha^{-1} for PM_{10} during sweeping operations. The PM_{10} emission rates for sweeping determined in this study were $4.8 \pm 3.7 \text{ kg ha}^{-1}$ using ISCST3 and $8.3 \pm 9.4 \text{ kg ha}^{-1}$ using AERMOD, which compare reasonably well with the CARB emission rate. The CARB PM_{10} emission rate for pickup was 41.2 kg ha^{-1} , while for this study the PM_{10} emission rates for pickup were $6.1 \pm 1.9 \text{ kg ha}^{-1}$ using ISCST3 and 15.7 ± 14.1 using AERMOD. Again, due to variance between orchard operations, equipment and ground cover these emission rates seem to be plausible. A graphical comparison of the studied-derived emission rates and the CARB recommended rates are shown in Figure 32.

The emission rates determined using AERMOD were typically greater than those determined using ISCST3 because lower concentrations were modeled by AERMOD for

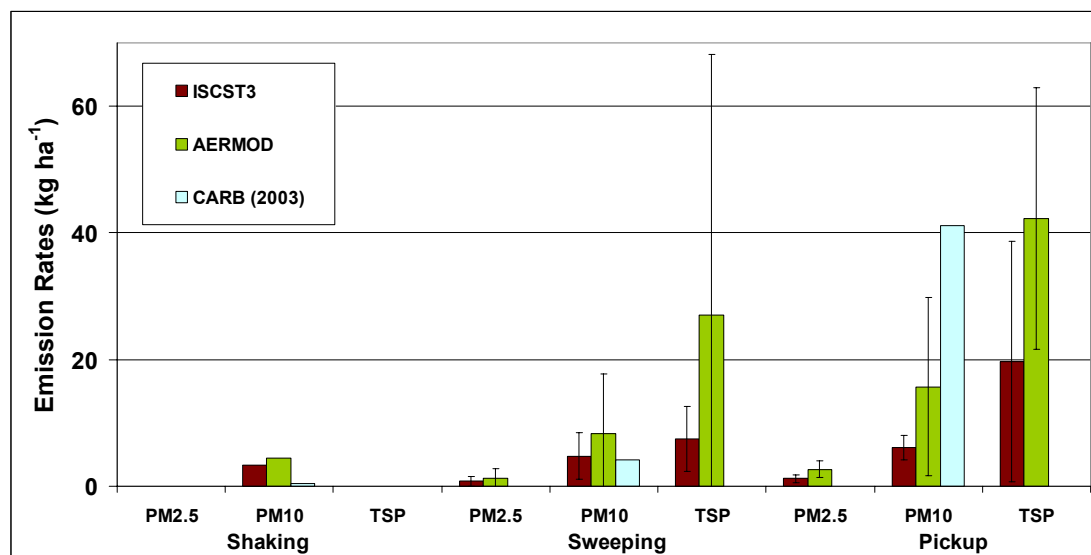


Figure 32. Summary of ISCST3, AERMOD, and CARB (2003) emission rates from the various processes of an almond harvest. Error is represented by the standard deviation.

a given seed emission rate, likely a result of AERMOD predicting more dispersion, and resultantly lower concentrations. Higher emission rates are then needed to match the measured concentrations. Ratios of the AERMOD determined emission rates to the ISCST3 determined emission rates can be found in Table 21. On October 1 the AERMOD determined emission rates are nearly half those determined using ISCST3. The same is true for the PM_{2.5} emission rates on October 9. For all other dates the AERMOD determined emission rates exceed those determined using ISCST3. Inverse modeling emission rates determined using AERMOD for shaking were 1.3 times those determined using ISCST3. Emission rates determined using AERMOD were from 0.51 to 3.6 times those determined using ISCST3. The ratio of AERMOD to ISCST3 emission rates averaged 1.4 with a standard deviation of 0.74.

As discussed earlier, good agreement was found between the filter-based samplers and the optical particle counters and ISCST3 model derived concentrations for the almond orchard at the 2 m height, but the agreement is weakened with the inclusion of point sampler data taken at 9 m. AERMOD, conversely, seemed better equipped to model non-buoyant pollutants released at ground-level. To further support this claim, an

Table 21. Ratio of AERMOD determined emission rates to ISCST3 determined emission rates

Date	Operation	AERMOD/ISCST3		
		PM _{2.5}	PM ₁₀	TSP
9/26/2006	shaking	-	1.3	-
10/1/2006	sweeping	0.5	0.5	0.5
10/2/2006 am	pickup	1.4	1.4	3.6
10/2/2006 pm	pickup	-	-	-
10/3/2006	mock sweeping	-	-	-
10/9/2006	mock sweeping	0.51	1.4	1.0
10/10/2006 am	pickup	1.1	1.5	1.3
10/10/2006 pm	pickup	1.6	1.8	2.2
10/11/2006	mock sweeping	1.6	1.9	2.0

examination of emission rates determined at 2 m and at 9 m can be made. If the models were accurately predicting concentrations at both heights the emission rate derived would not change with height, assuming the filter-based samplers have made accurate concentration measurements, and a ratio of the emission rate at 9 m to that at 2 m would equal one. For the almond harvest study the ISCST3 ratio of the 9 m emission rate to the 2 m emission rate averaged 3.0 ± 1.8 , and ranged from 1.6 to 8.0. To compare, the ratio of 9 m emission rates to 2 m emission rates for AERMOD averaged 1.7 ± 0.85 , and ranged from 0.74 to 3.5. An examination of the emission rates at 2 m only, however, gave no improvement in the AERMOD to ISCST3 emission rates ratio with the average being 1.8 ± 1.1 . One possible reason for a discrepancy in the emission rate determination using ISCST3 at increased elevation is the ambiguity associated with assigning a stability class, at least from a novice perspective. Whereas AERMOD calculates the stability function based on measured temperature, insolation, wind speed, and other meteorological parameters, ISCST3 uses an assigned, discrete, stability class. Stability class is determined by looking at a myriad of meteorological data and choosing the most appropriate stability class, which is not always cut and dry. The discontinuity of the stability classes for ISCST3 can limit modeling results.

Cotton Gin Conclusions

PM concentrations were measured at a cotton gin from December 11 to December 14, 2006 in order to determine emission rates for comparison between AERMOD and ISCST3 models, used for an inverse modeling calculation of emission rates, and for comparison with the cotton gin AP-42 emission factors and the emissions data for the specified gin. The models for PM_{10} and TSP were setup to run based on information

provided in the AP-42 emission factors summary, while the models for PM_{2.5} were setup to run based on the emissions data found on the CARB website. The total PM₁₀ emission rate found using the emission factors was 13.1 g s⁻¹ and that for TSP was 39.0 g s⁻¹. The CARB emissions data, obtained through stack testing procedures, specified that 0.24 g s⁻¹ of PM_{2.5}, 0.86 g s⁻¹ of PM₁₀, and 1.76 g s⁻¹ of TSP were being emitted. The cotton gin was permitted to emit 1.37 lb bale⁻¹ of PM₁₀. Direct PM₁₀ emission rate measurements were also taken at the cyclones on December 12, 13, and 14. These measurements showed 1.32 lb bale⁻¹ of PM₁₀ being emitted. Assuming a processing rate of 18 bales hour⁻¹ (found by taking the number of bales produced per day, ~ 360, and dividing that by the number of hours worked per day, ~ 20) this is equivalent to a permitted emission rate for PM₁₀ of 3.1 g s⁻¹ and an actual PM₁₀ emission rate of 3.0 g s⁻¹.

Overall emission rates determined using inverse modeling techniques with ISCST3 ($\pm 1\sigma$) were 1.7 ± 1.4 g s⁻¹ for PM_{2.5}, 14.3 ± 17.0 g s⁻¹ for PM₁₀, and 27.9 ± 41.1 g s⁻¹ for TSP. Overall emission rates determined using AERMOD were 0.9 ± 0.9 g s⁻¹ for PM_{2.5}, 10.5 ± 18.8 g s⁻¹ for PM₁₀, and 43.0 ± 79.9 g s⁻¹ for TSP. These emission rates were compared to the gin's emission data and the emission rates determined using the AP-42 emission factors for cotton ginning, the results are shown in Figure 33.

While these modeled rates, with one exception (TSP using AERMOD), are below the emission rates determined using the AP-42 emissions summary, they are all an order of magnitude greater than the reported emissions data. Unusually high PM₁₀ and TSP emission rates were determined using both ISCST3 and AERMOD for December 11, an order of magnitude higher than those determined on all other days of the study. These high emission rates could be due to a difference in plant operations, but there is currently

no evidence to support this claim. Lidar data could be used to verify the high emission rates for this day. Due to the anomaly in the data and the fact that emissions were not directly measured on December 11, average emission rates for PM_{2.5}, PM₁₀ and TSP were also determined for the remaining dates and were found to be $2.0 \pm 1.5 \text{ g s}^{-1}$ for PM_{2.5}, $5.8 \pm 2.9 \text{ g s}^{-1}$ for PM₁₀, and 7.4 ± 3.7 for TSP using ISCST3, and using AERMOD the average emission rates were $0.86 \pm 1.1 \text{ g s}^{-1}$ for PM_{2.5}, $1.1 \pm 0.07 \text{ g s}^{-1}$ for PM₁₀, and $3.1 \pm 2.6 \text{ g s}^{-1}$ for TSP. The AERMOD determined emission rate for PM₁₀ was within 20% of the emissions data for PM₁₀, and the AERMOD determined emission rate for TSP was nearly twice the emissions data for TSP. ISCST3 determined emission rates for PM₁₀ and TSP were both roughly 15 times their respective emissions data. For PM_{2.5} no anomaly was seen on December 11, and the AERMOD determined emission rate was 3.5 times the emissions data, while the ISCST3 determined emission rate was nearly 7 times

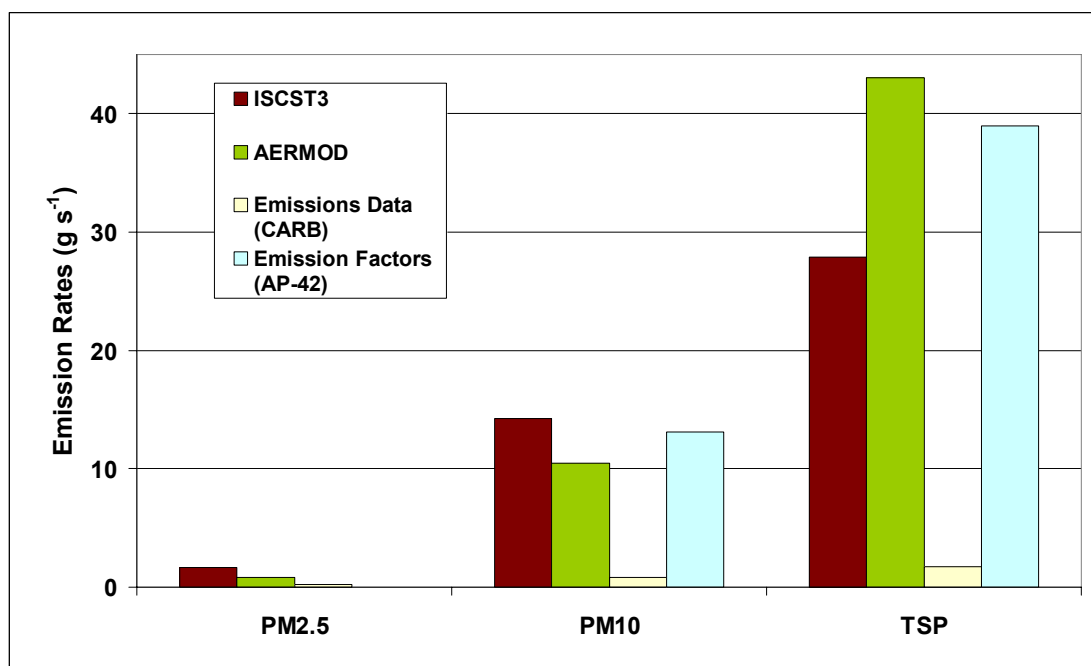


Figure 33. Average of the daily emission rates determined by of ISCST3, AERMOD, Emissions Data, and Emission Factors for the cotton gin.

the emissions data. The average of the PM₁₀ emission rates for dates with in-stack emissions measurements from the cyclones, $5.8 \pm 2.9 \text{ g s}^{-1}$ for ISCST3 and 1.1 ± 0.1 for AERMOD, compare well to the permitted, 3.1 g s^{-1} , and actual, 3.0 g s^{-1} , emission rates as shown in Figure 34. This being the case, although the samplers were not directly impacted by the gin plume the model derived PM₁₀ emission rates were similar to the permitted and in-stack measured values.

Tillage Conclusions

Tillage operations were studied from October 19 to October 29, 2007. Two fields were studied, in one field (62.9 acres) conventional tillage operations were examined and in the other (128.1 acres) a combined tillage practice was examined. The combined tillage operations included a chisel pass and a pass with an optimizer. The

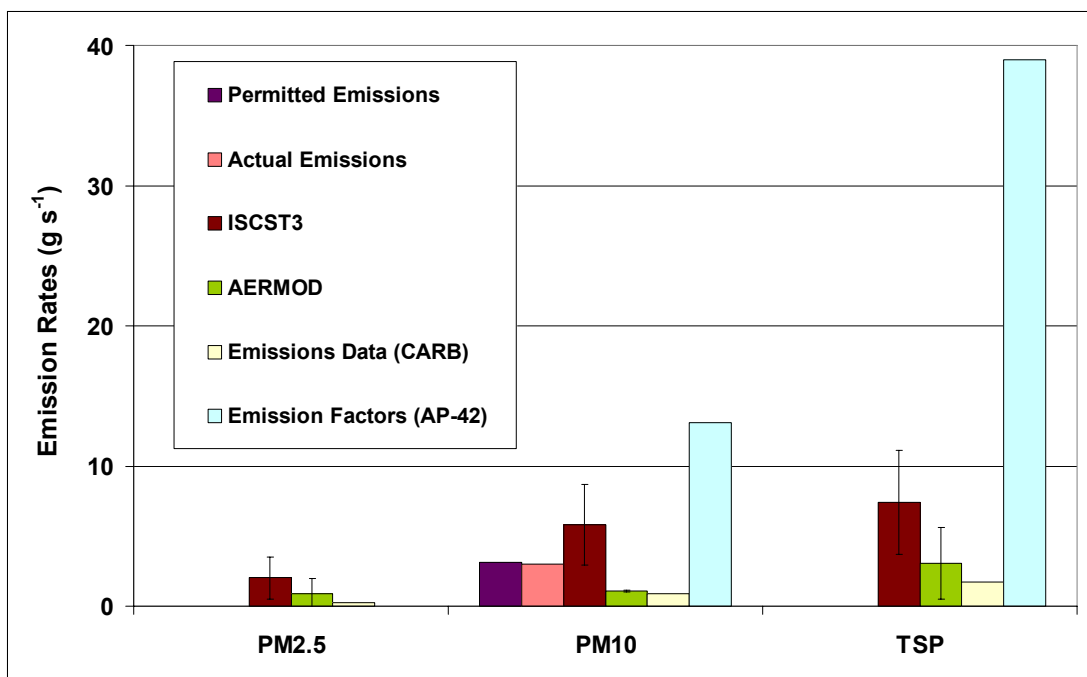


Figure 34. Average emission rates from the cotton gin for December 12 – 14, 2006. Error is represented by the standard deviation.

conventional tillage operations included a first disc pass, chisel pass, a second disc pass and a land plane pass. Table 19 shows the emission rates determined using ISCST3 for each of these operations and Table 20 presents the emission rates for each operation determined using AERMOD. Using the ISCST3 emission rates and normalizing by operation time the combined operations produced a total ($\pm 1\sigma$) of 0.04 ± 0.06 (0.15 ± 0.24), 0.11 ± 0.04 (0.44 ± 0.17), and 0.36 (1.44) g m^{-2} (kg acre^{-1}) of $\text{PM}_{2.5}$, PM_{10} , TSP, respectively, while the conventional tillage operations produced a total of 0.12 ± 0.52 (0.47 ± 2.10), 0.28 ± 0.06 (1.11 ± 0.23), and 0.85 (3.43) g m^{-2} (kg acre^{-1}) of $\text{PM}_{2.5}$, PM_{10} , TSP, respectively, as shown in Figure 35. AERMOD emission rates normalized by operation time yielded mass totals for combined operations produced a total ($\pm 1\sigma$) of 0.04 ± 0.07 (0.17 ± 0.27), 0.16 ± 0.06 (0.66 ± 0.25), and 0.51 (2.1) g m^{-2} (kg acre^{-1}) of $\text{PM}_{2.5}$, PM_{10} , TSP, respectively, while the conventional tillage operations produced a total of 0.04 ± 0.06 (0.18 ± 0.26), 0.29 ± 0.06 (1.2 ± 0.24), and 1.3 (5.1) g m^{-2} (kg acre^{-1}) of $\text{PM}_{2.5}$, PM_{10} , TSP, respectively, also shown in Figure 35.

The ratios comparing emission rates determined using AERMOD to those determined using ISCST3 are presented in Table 22. Emission rates determined using AERMOD were from 0.6 to 1.9 times those determined using ISCST3. The ratio of AERMOD to ISCST3 emission rates averaged 1.2 with a standard deviation of 0.53. It is interesting to note that on the October 20th Optimizer run AERMOD and ISCST3 predicted emission rates within 10% of each other for all size fractionations. The meteorology during this sample run was also unique with consistent strong (6.7 m s^{-1}) winds; this is likely the reason for this agreement between the two models.

Normalizing these mass emissions by acreage allows them to be compared with

the AP-42 emissions estimate for tillage. Soil samples taken from the tillage site during the study were analyzed and found to contain 36% silt. With this information, emissions estimates for each tractor pass were calculated for each particle size using Equation 2. The estimated PM_{2.5} emission rate for each tractor pass was 0.050 kg acre⁻¹, the estimated PM₁₀ emission rate for each tractor pass was 0.25 kg acre⁻¹, and the estimated TSP emission rate for each tractor pass was 1.18 kg acre⁻¹. Figure 35 shows a comparison of the emission rates determined using ISCST3 and AERMOD with the AP-42 emission estimates. .

ISCST3 PM_{2.5} emission rates were typically 170% of the AP-42 PM_{2.5} emissions estimates, while those for PM₁₀ and TSP were 88% and 59% of the AP-42 emissions estimates. The AERMOD PM_{2.5} emission rate for the combined operations was 168% greater than the AP-42 estimated PM_{2.5} emission rate; however, the PM_{2.5} emission rate for the conventional operations was 71% of the AP-42 estimate. AERMOD emission rates for PM₁₀ were 133% and 92% of those estimated with the AP-42 emission factor for the combined and conventional operations, respectively. TSP emission rates determined using AERMOD were both 87% of those estimated by the AP-42 emission factors. The

Table 22. Comparison of ISCST3 and AERMOD determined emission rates

Date	Operation	AERMOD/ISCST3		
		PM _{2.5}	PM ₁₀	TSP
19-Oct	Chisel	-	1.8	1.9
20-Oct	Optimizer	1.1	1.1	1.1
23-Oct	Disc 1	-	1.4	2.4
25-Oct	Chisel	1.3	0.6	2.0
26-Oct	Disc 2A	1.3	1.3	0.6
27-Oct	Disc 2B	0.6	0.8	0.6
29-Oct	Land plane	0.9	0.8	0.8

emission rates determined using ISCST3 and AERMOD both compared very well with those estimated by the AP-42 emissions factor algorithm.

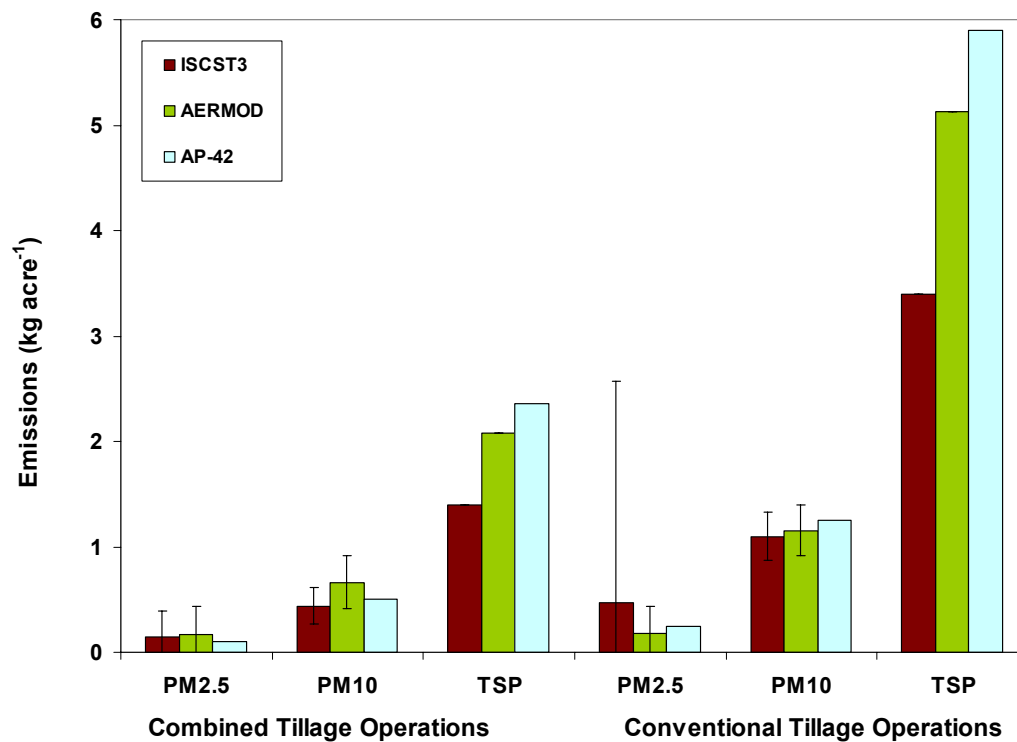


Figure 35. Comparison of ISCST3, AERMOD emission rates and AP-42 emission estimates for the tillage operations. Error is represented by the standard deviation.

ENGINEERING SIGNIFICANCE

A reliable method for determining emission factors from complex area sources, such as agricultural facilities, including multi-source and large-scale operations, is needed for effective regulation and assessment. Given the non-homogeneous nature of such emissions and site-specific meteorological conditions, an accurate characterization of the PM emissions from a facility would require an unreasonably large number of point samplers at multiple elevations in precise, often difficult-to-access, locations. The feasibility and cost of making these types of measurements to determine emission factors for various types of facilities and to enforce any emission-limiting regulations is likely impractical. A reliable means for measuring emission factors from multi-source and large facilities is needed. The inverse modeling approach described within this manuscript was successfully applied to the determination of size-fractionated particulate emission rates from almond harvesting, cotton ginning, and conventional vs. combined tillage operations. Additionally, the emission rates derived herein for these operations can be used by the agricultural and regulatory communities for future air quality management decisions.

Within the overall study, of which this work was a part, two methods were examined, an inverse modeling approach described herein using U.S. EPA approved models ISCST3 and AERMOD and the use of a lidar particulate mapping system coupled with a mass balance approach. Ultimately, with the results of this study, an appropriate technique can be chosen based on cost, feasibility, effectiveness and reliability on a case-by-case basis. AERMOD should be the model of choice because it incorporates more recent knowledge of atmospheric physics than does ISCST3. Due to this, it seems to

better predict concentrations at higher elevations, has a more robust and accurate characterization of the atmosphere, and it calculates stability based on measured meteorological inputs, and, therefore, is not prone to an inexperienced user assigning an inappropriate stability class.

FUTURE WORK

At this stage of analysis, lidar measured concentration fields seem to correlate well with the models. Analysis is being continued to examine this in greater detail for all studies described herein. Lidar derived emission rates will also be determined and compared to those calculated by inverse modeling. Lidar produced concentration fields can also be used as an infinite number of receptor points to compare with the models, which could potentially increase the confidence in the emission rates being determined. Additional campaigns are being completed and planned to further develop emission rates for a variety of agricultural operations, including a dairy and additional tillage studies. Increased information on agricultural emission rates will be of use to the agricultural and regulatory communities when implementing and enforcing regulation and when evaluating conservation practices.

REFERENCES

- Aneja, V. P., W. H. Schlesinger, D. Niyogi, G. Jennings, W. Gilliam, R. E. Knighton, C. S. Duke, J. Blunden, and S. Krishnan. 2006. Emerging national research needs for agricultural air quality. *EOS. American Geophysical Union* 87(3): 25-29.
- Arya, S. P. 1998. *Air pollution meteorology and dispersion*. Oxford University Press, Oxford. 134 p.
- Bingham, G., J. Hatfield, J. Prueger, T. Wilkerson, V. Zavyalov, R. Pfeiffer, L. Hipps, R. Martin, P. Silva, and W. Eichinger. 2006. An integrated approach to measuring emissions from confined animal feeding operations at the whole facility scale, pp. 88-89. In: Viney P.A. *et al.* (Eds.). *Proceedings: Workshop on Agricultural Air Quality: State of the Science*. Department of Communication Services, North Carolina State University, Raleigh, NC.
- Bunton, B., P. O'Shaughnessy, S. Fitzsimmons, J. Gering, S. Hoff, M. Lyngbye, P. S. Thorne, J. Wasson, and M. Werner. 2006. Monitoring and modeling of emissions from concentrated animal feeding operations: Overview of methods. *Environmental Health Perspectives* v.115(2): 303-307. Accessed: January 2007. Available: <http://www.pubmedcentral.nih.gov/articlerender.fcgi?artid=1817704>.
- Buser, M. D. 2004. Errors associated with particulate matter measurements on rural sources: appropriate basis for regulating cotton gins. Ph.D. Dissertation, Department of Biological and Agricultural Engineering, Texas A&M University, College Station, Texas. 12 p.
- Buser, M. D., C. B. Parnell, R. E. Lacey, B. W. Shaw, and B. W. Auvermann. 2001. Inherent biases of PM₁₀ and PM_{2.5} samplers based on the interaction of particle size and sampler performance characteristics. *Transactions of the ASABE* 01-1167.
- California Air Resources Board (CARB). 2003. *Agricultural Harvest Operations*. Accessed: January, 2008. Available: <http://www.arb.ca.gov/ei/areasrc/fullpdf/full7-5.pdf>.
- California Irrigation Management Information System (CIMIS). 2008. Hourly data. Department of Water Resources. Office of Water Use Efficiency. California. Accessed: March 2008. Available: <http://www.cimis.water.ca.gov/cimis/frontHourlyReport.do>.
- Capareda, S. C., C. B. Parnell, B. W. Shaw, and J. D. Wanjura. 2005. Particle size distribution analyses of agricultural dusts and report of true PM₁₀ concentrations. *Transactions of the ASABE* 054044.

- Coates, W. 1996. Particulates generated by five cotton tillage systems. *Transactions of the ASABE* 39(5):1593-1598.
- Code of Federal Regulations (CFR). 2007. Title 40 Part 50.6, Part 50.7. Accessed: March 2007. Available: http://ecfr.gpoaccess.gov/cgi/t/text/text-idx?c=ecfr&sid=6229d01b19ddc67fc224f911eccea51e&tpl=/ecfrbrowse/Title40/40cfr50_main_02.tpl
- Colls, J. 2002. *Air pollution*. Second edition. Spon Press, New York. 118 p.
- Cooper, D. C., and F. C. Alley. 2002. *Air pollution control: A design approach*. Waveland Press Inc., Prospect Heights, Illinois. 608 p.
- Cooper D. I., W. E. Eichinger, J. Archuleta, L. Hipps, J. Kao, M. Y. Leclerc, C. M. Neale, and J. Prueger. 2003. Spatial source-area analysis of three-dimensional moisture fields from lidar, eddy covariance, and a footprint model. *Agricultural and Forest Meteorology* 114: 213-234.
- Dockery, D. W., F. E. Speizer, D. O. Stram, J. H. Ware, J. D. Spengler, and B. G. Ferris, Jr. 1989. Effects of inhaled particles on respiratory health of children. *American Review of Respiratory Disease* 139: 587-594.
- E.H. Pechan and Associates. 2004. Documentation for the onroad National Emissions Inventory (NEI) for base years 1970-2002. Report prepared for the Office of Air Quality Planning and Standards, Emission Factor and Inventory Group, U.S. Environmental Protection Agency, Research Triangle Park, NC, by E.H. Pechan & Associates, Springfield, VA, January.
- Earth Tech. 2001. Final Technical Work Paper for Air Quality and Odor Impacts. Prepared for the Generic Environmental Impact Statement on Animal Agriculture. St. Paul, MN:Environmental Quality Board. Accessed: January 2008. Available: http://www.eqb.state.mn.us/geis/TWP_AirQuality.pdf .
- Faulkner, W. B., J. M. Lange, J. J. Powell, B. W. Shaw, and C. B. Parnell. 2007. Sampler placement to determine emission factors from ground level area sources. *Atmospheric Environment* 41(35): 7672-7678.
- Flocchini, R.G., C. B. Parnell, T. A. Cassel, S. C. Capareda, J. D. Wanjura, P. Wakabayashi, and K. Nabaglo. 2005. Improvement of PM10 Emission Factors for Almond Harvesting. Report to the Almond Board. March 2005. California Almond Board, Sacramento, CA. Accessed: January 2008. Available: <http://www.almondboard.com/Programs/AirQualityDetail.cfm?ItemNumber=4072>.

- Gaffney, P., and H. Yu. 2003. Computing agricultural PM₁₀ fugitive dust emissions using process specific emission rates and GIS. EPA Annual Emission Inventory Conference. San Diego CA, April 2003. California Air Resource Board, Planning and Technical Support Division. Accessed: January 2008. Available: <http://www.epa.gov/ttn/chief/conference/ei12/fugdust/yu.pdf>.
- Galvin, G., C. Henry, D. Parker, R. Ormerod, P. D'Abreton, and M. Rhoades. 2006. Efficacy of a Lagrangian and a Gaussian model for back calculating emission rates from feedyard area sources. In: Viney, P.A. et al. (Eds.). Proceedings: Workshop on Agricultural Air Quality: State of the Science. Department of Communication Services, Campus Box 7603, North Carolina State University, Raleigh, NC 27695-7603, USA.
- Gassman PW, and A. Bouzاهر. 1995. Livestock pollution: lessons from the European Union. In: K. Steele (Ed.). Animal waste and the land-water interface. FL:Lewis Publishers, Boca Raton, Florida.
- Goodrich, L. B., S. Capareda, J. Powell, C. Krauter, and M. Beene. 2007. Quantification of almond sweeping emission reductions through changes in a sweeper operation. 2007 ASABE Annual Meeting. 074104. American Society of Agricultural and Biological Engineers, St. Joseph, Michigan.
- Haupt, S. E., G. S. Young, and C. T. Allen. 2006. Validation of a receptor-dispersion model coupled with a genetic algorithm using synthetic data. *Journal of Applied Meteorology and Climatology* 45(3): 476-490.
- Holmen B. A., W. E. Eichinger, and R. G. Flocchini. 1998. Application of elastic lidar to PM₁₀ emissions from agricultural nonpoint sources. *Environmental Science & Technology* 32(20): 3068-3076.
- Holmen, B. A., A. T. James, L. L. Ashbaugh, and R. G. Flocchini. 2001a. Lidar-assisted measurement of PM10 emissions from agricultural tillage in California's San Joaquin Valley – Part I: lidar. *Atmospheric Environment* 35(2001): 3251-3264.
- Holmen, B. A., A. T. James, L. L. Ashbaugh, and R. G. Flocchini. 2001b. Lidar-assisted measurement of PM10 emissions from agricultural tillage in California's San Joaquin Valley – Part II: emission factors. *Atmospheric Environment* 35(2001): 3265-3277.
- Jacobson, M. Z. 2002. Atmospheric pollution: History, science and regulation. Cambridge University Press, New York. 118 p.
- Jerez, S. B., Y. Zhang, J. W. McClure, A. J. Heber, L. D. Jacobson, S. J. Hoff, J. A. Koziel, J. M. Sweeten, and D. Beasley. 2005. Aerial pollutant concentration and emission rate measurements from a swine farrowing building in Illinois. AWMA Paper No. 1026; 98th Annual AWMA Conference: Minneapolis, Minnesota.

- Keddie A.W.C. 1980. Dispersion of odors. In: Valentine FHH, North AA (Eds.). *Odour control: A concise guide*. Stevenage, Hertfordshire, UK:Warren Springs Laboratory, Department of Industry.
- Kovalev V. A., and W. E. Eichinger. 2004. *Elastic lidar: theory, practice, and analysis methods*. Hoboken: John Wiley and Sons, Inc. 103 p.
- Liang, Y., H. Xin, A. Tanaka, S. H. Lee, H. Li, E. F. Wheeler, R. S. Gates, J. S. Zajackowski, P. Topper, and K. D. Casey. 2003. Ammonia emissions from U.S. poultry houses: Part II – layer houses. In: H. Keener (Ed.). *Air pollution from agricultural operations III, Proceedings from the 12-15 October 2003 Conference*, American Society of Agricultural Engineers.
- Ludwig, G. 2007. Simple steps can reduce almond harvest dust. Western Farm Press. Penton Media Inc. Accessed: January 2008. Available: http://westernfarmpress.com/mag/farming_simple_steps_reduce/
- Lundquist, D. 1993. Written communication from Darin Lundquist, Central California Almond Growers Association, to Dallas Safriet, U. S. EPA. Accessed: January 2008. Available: http://www.epa.gov/ttn/chief/old/ap42/ch09/s1021/reference/ref05_c09s1021_1995.pdf
- Martin R. S., K. D. Moore, and V. S. Doshi. 2008. Determination of particle and gas-phase ammonia emissions from a deep-pit swine operation using arrayed field measurements and inverse Gaussian plume modeling. In progress.
- Menut L., C. Flamant, J. Pelon, and P. Flamant. 1999. Urban boundary-layer height determination from lidar measurements over the Paris area. *Applied Optics* 38: 945-954.
- Mihelcic, J. R. 1999. *Fundamentals of environmental engineering*. John Wiley & Sons, Inc., New York. 335 p.
- Mount, G.H., B. Rumburg, J. Havig, B. Lamb, H. Westberg, D. Yonge, K. Johnson, and R. Kincaid. 2002. The measurement of atmospheric ammonia at a dairy using differential optical absorption spectroscopy in the midultraviolet. *Atmospheric Environment* 36: 1799-1810.
- National Agricultural Statistics Service (NASS). 2008. Cotton ginnings. Accessed: January 2008. Available: <http://usda.mannlib.cornell.edu/usda/current/CottGinn/CottGinn-01-11-2008.pdf>
- National Research Council of the National Academies (NRC). 2003. *Air emissions from animal feeding operations: current knowledge, future needs*. National Academic Press, Washington, D.C. pp. 8-13, 75.

- Paine, R. J., R. F. Lee, R. Brode, R. B. Wilson, A. J. Cimorelli, S. G. Perry, J. C. Weil, A. Venkatram, and W. D. Peters. 1998. Model evaluation results for AERMOD. Research Triangle Park, NC: U.S. Environmental Protection Agency, Office of Air Quality Planning and Standards Emissions, Monitoring, Analysis Division. Accessed: March 2008. Available: <http://www.epa.gov/scram001/7thconf/aermod/evalrep.pdf>
- Palmquist, R. B., F. M. Roka, and T. Vukina. 1997. Hog operations, environmental effects, and residential property values. *Land Economics* 73(1):114-124.
- Parnell, S. E., B. J. Lesikar, J. M. Sweeten, and B. T. Weinheimer. 1993. Dispersion modeling for prediction of emission factors. American Society of Agricultural Engineers. Meeting Paper, Winter 1993. (93-4545/93-4579), 18 p.
- Parnell, S. E., B. J. Lesikar, J. M. Sweeten, and R. E. Lacey. 1994. Determination of an emission factor for cattle feedyards by applying dispersion modeling. American Society of Agricultural Engineers. Meeting Paper, Summer 1994. (94-4042/94-4082). 15 p.
- Penfold, B. M., D. C. Sullivan, S. B. Reid, and L. R. Chinkin. 2002. Development of agricultural dust emission inventories for the Central States Regional Air Planning Association. Accessed: December 2007. Available: <http://www.epa.gov/ttn/chief/conference/ei14/session7/reid.pdf>
- Pope, C.A., 1991. Respiratory hospital admissions associated with PM10 pollution in Utah, Salt Lake, and Cache valleys. *Archives of Environmental Health* 46: 89-97.
- Price, J.E., R. E. Lacey, B. W. Shaw, N. A. Cole, R. Todd, S. Capareda, and C. B. Parnell. 2004. A comparison of ammonia emission rates from an agricultural area source using dispersion modeling: Gaussian versus backward-Lagrangian stochastic. Paper 044199, presented at the 2004 American Society of Agricultural Engineers Annual International Meeting, Ottawa, Ontario, Canada, August 1-4, 2004. Contact Information: American Society of Agricultural and Biological Engineers, 2950 Niles Road, St. Joseph, MI 49085, USA.
- Redwine, J.S., R. E. Lacey, S. Mukhtar, and J. B. Carey. 2002. Concentration and emissions of ammonia and particulate matter in tunnel-ventilated broiler houses under summer conditions in Texas. *Transactions of the ASAE* 45: 1101-1109.
- Rege, M. A., and R. W. Tock. 1996. Estimation of point-source emissions of hydrogen sulfide and ammonia using a modified Pasquill-Gifford approach. *Atmospheric Environment* 30(18):3181-3195.
- Turner, D. B. 1970. Workbook of atmospheric dispersion estimates. U.S. Environmental Protection Agency, Washington, DC.

- USDA-AAQTF. 2007. Task Force Mission. USDA Natural Resources Conservation Service. Accessed: January 2008. Available: <http://www.airquality.nrcs.usda.gov/AAQTF/>
- U. S. EPA. 1985. Compilation of air pollutant emission factors (AP-42): Chapter 9. Research Triangle Park, N.C. EPA.
- U. S. EPA. 1995. User's Guide for the Industrial Source Complex (ISC3) Dispersion Models. Research Triangle Park, NC:U.S. Environmental Protection Agency, Office of Air Quality Planning and Standards Emissions, Monitoring, Analysis Division. Accessed: January 2008. Available: <http://www.epa.gov/scram001/userg/regmod/isc3v2.pdf>
- U. S. EPA. 1998. Guideline on Air Quality Models. Appendix W. U.S. Code of Federal Regulations, 40 CFR Part 51 Accessed: December 2007. Available: http://www.epa.gov/scram001/guidance/guide/appw_98.pdf
- U. S. EPA. 2002. National Emissions Inventory (NEI) Air pollutant emissions trends data. Research Park, North Carolina.
- U. S. EPA. 2003a. Fugitive Dust from Agriculture Tilling. Research Park, North Carolina. Accessed: January 11, 2008. Available: <http://www.epa.gov/ttn/chief/eiip/techreport/volume09/agtilling.pdf>
- U. S. EPA. 2003b. Particle pollution and your health. EPA-452/F-03-001. Office of Air and Radiation. Research Park, North Carolina. Accessed: March 1, 2007. Available: <http://cfpub.epa.gov/airnow/index.cfm?action=particle.airborne#1>.
- U. S. EPA. 2004. National emissions inventory: Ammonia emissions from animal husbandry operations, Draft Report, January 30, 2004.
- U. S. EPA. 2005. Revision to the Guideline on Air Quality Models: Adoption of a Preferred General Purpose (Flat and Complex Terrain) Dispersion Model and Other Revisions; Final Rule. 40 CFR Part 51. Washington, DC: U.S. Environmental Protection Agency. Accessed: January 2008. Available: http://www.epa.gov/ttn/scram/guidance/guide/appw_05.pdf
- U. S. EPA. 2006a. Animal feeding operations air agreement. Accessed: January 2008. Available: <http://yosemite.epa.gov/opa/admpress.nsf/a8f952395381d3968525701c005e65b5/a3b628e23af32f68852571d200618474!OpenDocument>
- U. S. EPA. 2006b. Particulate matter, health and environment. Accessed: March 2007. Available: <http://epa.gov/pm/health.html>.

- U. S. EPA. 2008. Health and Environment. Accessed: August 2008. Available: <http://www.epa.gov/PM/health.html>.
- Venkatram, A. 1999. Using a dispersion model to estimate emission rates of particulate matter from paved roads. *Atmospheric Environment* 33(7): 1093.
- Wakelyn, P. J., D. W. Thompson, and B. M. Norman. 2005. Why cotton ginning is considered agriculture. *Cotton Gin & Oil Mill Press* 106(8): 5-9.
- Wanjura, J. D., M. D. Buser, C. B. Parnell, B. W. Shaw, and R. E. Lacey. 2005. A simulated approach to estimating PM₁₀ and PM_{2.5} concentrations downwind from cotton gins. *Transactions of the ASAE* 48(5):1919-1925.
- Wilkerson, T. D., G. E. Bingham, V. V. Zavyalov, J. A. Swasey, J. J. Hancock, B. G. Crowther, S. S. Cornelsen, C. Marchant, J. N. Cutts, D. C. Huish, C. L. Earl, J. M. Andersen, and M. L. Cox. 2006. AGLITE: A multi-wavelength lidar for measuring emitted aerosol concentrations and fluxes and air motion from agricultural facilities. *Proceedings of SPIE, the International Society for Optical Engineering* 6409: 64090.
- Zavyalov, V. V., C. Marchant, G. E. Bingham, T. D. Wilkerson, J. Swasey, C. Rogers, D. Ahlstrom, and P. Timothy. 2006. Retrieval of physical properties of particulate emission from animal feeding operations using three-wavelength elastic lidar measurements. *Proceedings of SPIE, the International Society for Optical Engineering* 6299: 62990.

APPENDICES

Appendix A: Almond Orchard Field Experiment Notes

Orchard Equipment:

- Shaker: Make - Orchard Rite, Model - "The Bullet" Sideshaker
- Sweeper: Make - Weiss McNair, Model - HS30 (> 20 years old)
- Harvester: Make - Flory, Model - LD 80, PTO driven (2006 model)

N Met Tower: 5 cup anemometers

Sonic Tower: 3 sonic anemometers

S Met Tower: 5 cup anemometers + met station

9/26/06 Shaking

Description: shaking of Carmel and Monterey variety trees in whole orchard moving from W to E (in increasing row #s in each section)

- moved along rows in serpentine shape shaking one tree at a time

- Rows shaken:

Sections 2 & 3: 3, 5, 9, 11, 15, 17, 21, 23, 27, 29, 33, 35, 39, 41, 45, 47, 53

Section 1: 3, 6, 9, 12, 15, 18, 21, 24, 27, 30, 33, 36, 39, 42, 45, 48, 51, 54, 57, 60

Operation start: ~ 07:00

Instrumentation:

Sampling array concentrated on south side of the orchard

- LiDAR located next to AQ Trailer

- OPCs began collecting data at ~ 07:15

- Airmetrics: started at ~ 07:30

Notes: Stopped 4321, 4329, and 4326 at 09:40 when shaking of Sections 2 & 3 was complete. Stopped 3769 @ 16:00

All Airmetrics checked out okay after the truck hit the AQ trailer and the samplers were knocked over.

10/1/06 Sweeping of Sections 2 & 3

Description: Swept Sections 2 & 3.

Operation began @ 9:15 and the finish time is unrecorded time

- 2 aisles to sweep per row of trees: 1) sweep against row shaken w/ blower active, 2) return in same aisle with sweeping other side w/out blower, 3) wait for rakers to finish underneath row shaken, 4) sweep against row shaken w/out blower, and 5) return in same aisle sweeping the other side

- Tree rows swept (swept aisle on each side of row): 3, 5, 9, 11, 15, 17, 21, 23, 27, 29, 33, 35, 39, 41, 45, 47, 53

Instrumentation:

Samplers returned to south side of orchard and set to measure from Sections 2 & 3. Winds from the north in the morning, switching to E and SE near midday.

- LiDAR located next to AQ Trailer

- Tethersonde launched from Balloon S location

- OPCs collected data (receiver and computer returned to AQ Trailer permanently)
- Airmetrics started at 8:30 and sampled background levels for 45 minutes before sweeping began, possibly compromising data collected, and they were stopped shortly after wind direction changed to E and SE

Notes: Met data for first 30 minutes of shaking operation lost due to loss of connection between met station and console inside AQ Trailer

- Dr. Wilkerson's sample plates were deployed from ~ 9:18 to 13:50 as follows:
 - #1 located 17 m inside orchard in a row not swept
 - #2 located due S from 1, 17 m from edge of orchard
 - #3 located 17 m S of #2

10/2/06 Harvest of Section 1

Description: Pickup of Monterey variety in morning and Carmel variety in the afternoon.

Morning operation began at 7:00 and ended at 11:15 and moved from W to E

- Harvesting involves picking up the nuts, separating the leaves, twigs, and dirt, and loading a trailer behind the harvester. Only one pass is required per aisle.
- Rows harvested (one pass on the two adjoining aisles): 6, 12, 18, 24, 30, 36, 42, 48, 54

Afternoon operation began at 11:50 and ended at 14:00

- Rows harvested (one pass on the two adjoining aisles): 3, 9, 15, 21, 27, 33, 39, 45, 51

Instrumentation:

Sampling array set on both the north and south sides of Section 1 in case of change in wind direction as occurred on 10/1/06, with more on the south side of the orchard.

- LiDAR located in SW corner of property
- Tethersonde launched from Balloon S location
- OPCs from the south side of the orchard and U1 collected data, but an OPC was not placed at the N11 location on the north side of the orchard because of interference
- OPCs were started between 7:15 and 8:00
- Airmetrics started between 7:15 and 8:00 for morning period and stopped from 11:15 – 11:25. Afternoon sampling started from 11:50 - 12:00 and stopped from 14:10 – 14:20. The filter heads were swapped out between sample periods.

Notes: The orchard to the northeast of this facility (east of U1) was sweeping and harvesting throughout the day, and was creating a visually much larger vertical and horizontal plume. The samples collected on the north side of Section 1 were impacted and visually darker than those collected to the south of Section 1.

10/3/06 Mock Sweeping

Operation: Mock sweeping in Section 1 in aisles w/out almonds.

- swept every other row beginning from row 51 and moving W: 1) moved from N to S w/ blower engaged and 2) moved from S to N in same aisle w/out blower
- Rows swept (aisle to E swept): 23, 25, 27, 29, 31, 33, 35, 37, 39, 41, 43, 45, 47, 49, 51

Started sweeping at 15:20 and stopped sweeping at 17:10

Instrumentation:

Sampling array set up on both the north and south sides of the orchard to account for the E and SE winds. Background location (SA1) was established further south than sampling line on the south side of the orchard to avoid being impacted from sweeping operation.

- LiDAR located in SW corner of property
- Tethersonde was launched from the Balloon S location
- OPCs on south side of orchard and Cow were logging data, no other OPCs placed on north side of orchard (lack of communication with the receiver/laptop at the AQ trailer)
- Airmetrics started between 15:15 and 15:25 and stopped between 17:10 and 17:20
- Dr. Wilkerson's samples were placed on north side of orchard and were deployed from ~ 15:30 to 17:20 as follows:

#4 located 17 m inside orchard in a row not swept

#5 located due N from 4, 17 m from edge of orchard

#6 located 17 m N of #5

#7 located 17 m N of #6

Samplers were not directly hit because sweeping did not reach this far W, but all were downwind of the sweeping operation

- Sampling array was set up as follows:

Notes: Met data at trailer lost due to operator error.

10/9/06 Mock Sweeping of Sections 2 & 3

Description: Swept Sections 2 & 3 from E to W and back

Operation began at 13:25 and stopped at 15:35

- 2 passes per aisle with blower constantly engaged
- Tree rows swept in order (swept aisle to the E): 50, 48, 43, 42, 36, 30, 24, 18, 12, 6, 1, W side of 1, 7, 13
- at 14:50, asked operator to start from W end and move to the E, re-sweeping if necessary (as per Gail Bingham) – rows swept from 14:50-15:35 in order: W side of 1, 1, 7, 12, 6, 19
- sweeping occurred between aisles w/ almonds, therefore dust, leaves, etc. were blown back onto the windrows

Instrumentation:

Sampling array set up on the south side of the orchard and set to measure from Sections 2 & 3. Strong winds (15 min avgs 8-15 m/s) from the north throughout the test period

- LiDAR located in SW corner of property

- Tethersonde was not launched due to unexpected ability to collect data after set up
 - OPCs collected data
 - Airmetrics started at 13:20 and stopped between 15:35 and 15:52
- Notes: At 15:30, noticed a pickup operation in progress in the orchard kitty-corner to the NW corner of this orchard. There was a visible plume moving SE (toward this orchard), but the length of operation was unknown and the impact on point samplers is unknown

10/10/06 Harvest of Sections 2 & 3

Operation: Pickup of Monterey variety in morning and Carmel variety in the afternoon.

Morning operation began at 8:00 and ended at 11:05

- Harvesting involves picking up the nuts, separating the leaves, twigs, and dirt, and loading a trailer behind the harvester. Only one pass is required per aisle.
- Rows harvested in order (one pass on the two adjoining aisles): 5, 11, 17, 23, 29, 35, 41, 47, 53 (moved from W to E)

Afternoon operation began at 12:45 and ended at 15:05

- Rows harvested in order (one pass on the two adjoining aisles): 3, 9, 15, 21, 27, 33, 39, 45 (moved from E to W)
- These windrows were conditioned (picked up like harvesting and put back down in windrow after removal of dust, leaves, twigs, etc.) twice to facilitate drying. According to Stan Cutter, one pass of conditioning cleans the windrows well. However, the mock sweeping operation of 10/09/06 blew dust, leaves, etc. back onto the windrows. Stan Cutter estimated the windrows were at about 80% of the pre-conditioned state as far as dust goes.

Instrumentation:

& 3. Strong winds (15 min avgs 8-15 m/s) from the north throughout the test period

- LiDAR located in SW corner of property
 - Tethersonde was not launched due to high winds
 - OPCs collected data
 - Airmetrics started at 8:00 for morning period and stopped from 11:05 – 11:20.
- Afternoon sampling started from 12:40 - 12:50 and stopped from 15:15 – 15:25. The filter heads were swapped out between sample periods.

Notes: High winds (15 min avgs 8 – 15 m/s) throughout test periods lifting visible dust plumes from free soil surface, extent of sample interference unknown

10/11/06 Mock sweeping in Section 1

Operation: Mock sweeping in Section 1

Began at 11:00 and ended at 15:20

- Sweeping operation carried out in the following steps: 1) sweep w/ blower from N to S, 2), return in same aisle sweeping w/out blower, 3) skip one aisle and repeat steps 1 & 2, 4) when finished steps 1 & 2 on every other row in section return to other end, 5) sweep w/out blower on both sides of aisle, 6) skip one aisle

and repeat step 5 until finished with orchard (every aisle will have been swept in this method, assuming just 2 varieties spaced every other row)

- Steps 1 & 2 above performed on aisles to E of row #s (in order) from 11:00-13:10: 1, 3, 5, 7, 9, 11, 13, 15, 17, 19, 21, 23, 25, 27, 29, 31, 33, 35, 37, 39, 41, 43, 45, 47, 49, 51, 53, 55, 57, 59

- Step 5 performed on aisles to E of row #s (in order) from 13:10 – 15:20: 2, 4, 6, 8, 10, 12, 14, 16, 18, 20, 22, 24, 26, 28, 30, 32, 34, 36, 38, 40, 42, 44, 46, 48, 50, 52, 54, 56, 58, 60

Instrumentation:

Sampling array was concentrated on the south side of Section 1 in the same setup as used on 10/9 and 10/10 for Sections 2 & 3, except there was not a tower placed at D11.

- LiDAR located in the SW corner of the property

- Tethersonde was launched from location south of orchard

- OPCs collected data in the layout described below

- Airmetrics started at 11:00 and were stopped between 15:25 and 15:35

Appendix B: Cotton Gin Specifications and Emissions Data

Table 23. Exhaust specifications for the cotton gin

16 STAND - 20 BALE PER HOUR ROLLER GIN FAN DISCHARGE PIPING				
Roller Gin System	CFM	Pipe dia. (in)	Velocity (fpm)	Collectors
Unloading System	17,777	27	4,471	4 - 40"
#1 Burner Fan	18,054	27	4,541	
#1A Incline Cleaner	8,022	18	4,540	2 - 38"
#1B Incline Cleaner	8,022	18	4,540	2 - 38"
#2A Incline Cleaner	9,027	19	4,585	
#2A Burner Fan	8,888	19	4,514	2 - 40"
#2B Incline Cleaner	9,027	19	4,585	
#2B Burner Fan	8,888	19	4,514	2 - 40"
#3A Incline Cleaner	8,888	19	4,514	
#3A Burner Fan	8,888	19	4,514	2 - 40"
#3B Incline Cleaner	8,888	19	4,514	
#3B Burner Fan	8,888	19	4,514	2 - 40"
#1 A & B Stick Machines	8,022	18	4,540	2 - 38"
#2 A & B Stick Machines	9,800	20	4,492	2 - 42"
"A" Overflow and seed reclaimmer	8,022	18	4,540	2 - 38"
"B" Overflow and seed reclaimmer	8,022	18	4,540	2 - 38"
Feeder Dust	8,022	18	4,540	2 - 38"
#1 A Lint cleaner condensor	16,200	26	4,394	2 - 54"
#1 B Lint cleaner condensor	16,200	26	4,394	2 - 54"
"A" Lummus Guardian lint cleaner condensor pull	11,755	22	4,453	2 - 46"
"B" Lummus Guardian lint cleaner condensor pull	11,755	22	4,453	2 - 46"
"A" lint cleaner trash	10,755	21	4,471	2 - 44"
"B" lint cleaner trash	10,755	21	4,471	2 - 44"
Battery Condensor	28,800	34	4,568	2 - 72"
Robber fan for condensor collectors	11,755	22	4,453	2 - 46"
Seed Blower	1,745	8	4,999	seed bunker

Table 24. Emissions data for the cotton gin

Emissions Data

	Pollutant	Emissions	Unit
Data from 2005 Download CSV file	TOG	0.1	Tons/Yr
	ROG	0.1	Tons/Yr
	CO	0.4	Tons/Yr
	NOX	1.8	Tons/Yr
	SOX	0.1	Tons/Yr
	PM	18.7	Tons/Yr
	PM10	9.2	Tons/Yr
	PM2.5	2.6	Tons/Yr

1.7557 g/s
 0.8638 g/s
 0.24411 g/s

Handwritten:
 $\frac{3}{5} \times \frac{2}{4} = \frac{6}{20} = \frac{3}{10}$

The emission inventory data provided here may have been developed over several years and is the most recent information available at ARB for this inventory year. Many facilities are only required to update their toxic emission data if there has been an increase in emissions. Therefore, the toxic emission data presented here should generally be viewed as maximum emission values which may have decreased since this information was reported. If you have questions regarding data updates, please contact the local air district. Note: If this facility has diesel-fueled internal combustion engines, then a portion of the PM10 shown is considered to be diesel exhaust PM10.

[\[Start a new search\]](#) [\[Report an Error\]](#)

Handwritten: PM₁₀

[ARB Homepage](#)

A department of the California Environmental Protection Agency

Handwritten:
 PM_{2.5}
 2.6 tons/year
 2358680 grams/year

Handwritten:
 @ Mono
 6.22 hrs/day

Handwritten:
 0.244778 grams/second
 0.005828 grams/second/cycle time

Appendix C: Tillage Instrumentation

Table 25. Summary of instruments located at each site for tillage study of field PA-47

Instrument Location	Description
S1	1 - 10 meter tower 2 - OPC's @ 2 and 9 meters 4 - MiniVols: PM ₁₀ and PM _{2.5} @ 2 and 9 meters
S Met 1	1 - 15 meter tower 5 - cup anemometers 1 - wind vane @ 15 meters. 6 - temp/RH sensors 2 - Campbell Scientific dataloggers 1 - Sonic Anemometer 1 - energy balance system
S2	1 - 10 meter tower 2 - OPC's @ 2 and 9 meters 6 - MiniVols: TSP, PM ₁₀ , PM _{2.5} , and PM ₁ @ 9 meters; PM ₁₀ and PM _{2.5} @ 2 meters
S3	1 - 10 meter tower 1 - OPC @ 9 meters 4 - MiniVols: PM ₁₀ and PM _{2.5} @ 9 m; PM ₁₀ and PM _{2.5} @ 2 meters
E1	1 - 10 meter tower 1 - OPC @ 9 meters 2 - MiniVols: PM ₁₀ and PM _{2.5} @ 9 meters 1 - sonic anemometer 1 - Campbell Scientific datalogger
N1	1 - 10 meter tower 2 - OPC's @ 2 and 9 meters 6 - MiniVols: TSP, PM ₁₀ , PM _{2.5} , and PM ₁ @ 9 meters; PM ₁₀ and PM _{2.5} @ 2 meters
N2	2 - MiniVols: PM ₁₀ and PM _{2.5} @ 2 meters
NMet	1 - 15 meter tower 5 - cup anemometers 1 - wind vane @ 15 meters 6 - temp/RH sensors 2 - Campbell Scientific dataloggers 1 - sonic anemometer
U1	1 - OPC @ 9 meters 2 - MiniVols: PM ₁₀ and PM _{2.5} @ 9 meters
W1	2 - MiniVols: PM ₁₀ and PM _{2.5} at 9 meters (PM _{2.5} stopped working on 10/20) 1 - sonic anemometer 1 - Campbell Scientific datalogger

Tethersonde	1 - tethersonde data collection instrument 1 - MadgeTech Pressure, Humidity Temperature sensor
Lidar 1	1 - Lidar data collection system 1 - Davis met station for lidar operator's reference
AQ1	1 - OPC 2 - MiniVols: PM _{2.5} and PM ₁₀ 1 - Davis met station 1 - OC/EC Analyzer 1 - Aerosol Mass Spectrometer (AMS) 1 - radio and laptop for OPC Data collection

Table 26. Summary of instruments located at each site for tillage study of field PA-46

Instrument Location	Description
S4	1 - 10 meter tower 2 - OPC's @ 2 and 9 meters 4 - MiniVols: PM ₁₀ and PM _{2.5} @ 2 and 9 meters
S Met 2	1 - 15 meter tower 5 - cup anemometers 1 - wind vane @ 15 meters. 6 - temp/RH sensors 2 - Campbell Scientific dataloggers 1 - Sonic Anemometer 1 - energy balance system
S5	1 - 10 meter tower 2 - OPC's @ 2 and 9 meters 6 - MiniVols: TSP, PM ₁₀ , PM _{2.5} , and PM ₁ @ 9 meters; PM ₁₀ and PM _{2.5} @ 2 meters
S6	1 - 10 meter tower 1 - OPC @ 9 meters 4 - MiniVols: PM ₁₀ and PM _{2.5} @ 9 m; PM ₁₀ and PM _{2.5} @ 2 meters
E2	1 - 10 meter tower 1 - OPC @ 9 meters 2 - MiniVols: PM ₁₀ and PM _{2.5} @ 9 meters 1 - sonic anemometer 1 - Campbell Scientific datalogger
N1	1 - 10 meter tower 2 - OPC's @ 2 and 9 meters 6 - MiniVols: TSP, PM ₁₀ , PM _{2.5} , and PM ₁ @ 9 meters; PM ₁₀ and PM _{2.5} @ 2 meters
N2	2 - MiniVols: PM ₁₀ and PM _{2.5} @ 2 meters
NMet	1 - 15 meter tower 5 - cup anemometers 1 - wind vane @ 15 meters

	6 - temp/RH sensors 2 - Campbell Scientific dataloggers 1 - sonic anemometer
U2	1 - OPC @ 9 meters 2 - MiniVols: PM ₁₀ and PM _{2.5} @ 9 meters
W2	2 - MiniVols: PM ₁₀ and PM _{2.5} at 9 meters (PM _{2.5} stopped working on 10/20) 1 - sonic anemometer 1 - Campbell Scientific datalogger
Tethersonde	1 - tethersonde data collection instrument 1 - MadgeTech PRHT sensor
Lidar 2	1 - Lidar data collection system 1 - Davis met station for lidar operator's reference
AQ2	1 - OPC 2 - MiniVols: PM _{2.5} and PM ₁₀ 1 - Davis met station 1 - OC/EC Analyzer 1 - AMS 1 - radio and laptop for OPC Data collection
Tr1*	2 - MiniVols: PM ₁₀ and PM _{2.5} @ 2 meters (* temporary location for sampling on 10/27 due to the area of the field being worked being largely to the west of most downwind towers)